AD-A115 394 FOREIGN TECHNOLOGY DIV WRIGHT-PATTERSON AFB OH F/G 9/5
ANTENNAS.(U)
MAY 82
UNCLASSIFIED FTD-ID(RS)T-1170-81 NL

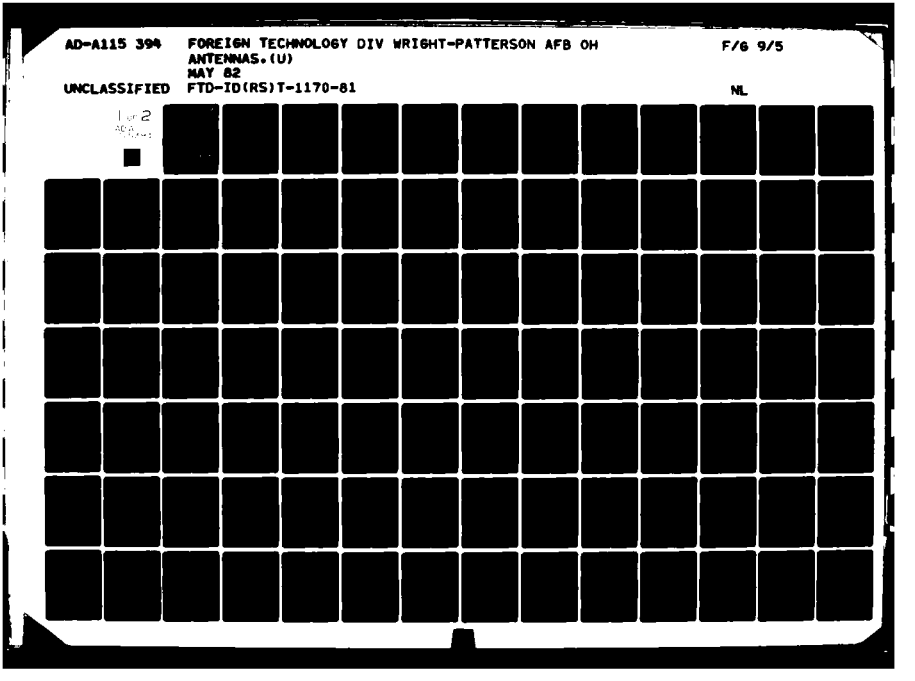

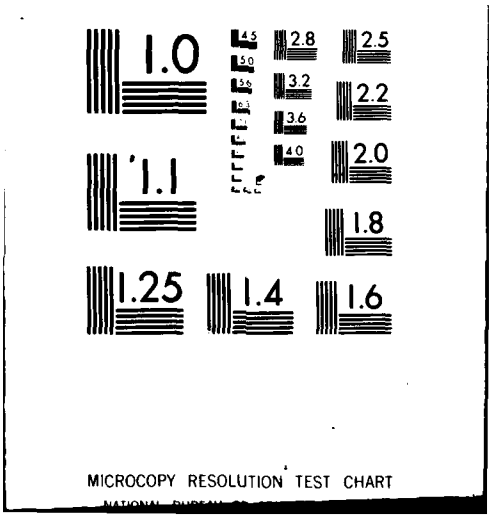
1.0
1.1
1.25
1.4
1.6
1.8
2.0
2.2
2.5
2.8
3.2
3.6
4.0
MICROCOPY RESOLUTION TEST CHART

FTD-ID(RS)T-1170-81

AD A115394

FOREIGN TECHNOLOGY DIVISION

ANTENNAS

Approved for public release;
distribution unlimited.

EDITED TRANSLATION

FTD-ID(RS)T-1170-81 13 May 1982

MICROFICHE NR: FTD-82-C-000604

ANTENNAS

English pages: 172

Source: Antenny, Nr. 1, 1966, pp. 1-152

Country of origin: USSR
Translated by: LEO KANNER ASSOCIATES
F33657-81-D-0264
Requester: USAMICOM

PREPARED BY:

TRANSLATION DIVISION
FOREIGN TECHNOLOGY DIVISION
WP-AFB, OHIO.

TABLE OF CONTENTS

Foreword

Antenna and waveguide technology plays a large role in contemporary radio engineering and is rapidly developing hand in hand with it. Specialists are interested in the systematic acquisition of information on the development of one or another of the many trends in antenna technology, in results of recent theoretical and experimental studies in the area of antennas, and in adjacent scientific and technological fields, as well as in the discussions surrounding questions of interest to them. In addition, inasmuch as at the present articles on the questions to be indicated here are published in various journals, their concentration in one print medium is also to be desired.

The Antenna Section of the Scientific-Technological Society for Radio Engineering and Electronic Communications im. A. S. Popova, together with the "Svyaz'" Publishers, has begun to issue a series of regular publications of works of the Section in the form of collections of articles under the title, "Antennas." The present collection is the first issue. The editorial board hopes that the regular publication of articles and works of the Section, articles reflecting the present level in antenna technology and fields native to that subject, will be useful for a large portion of radio specialists.

Success in initiating an Antenna Section and in a publishing venture would be unthinkable without the active creative participation of members of the Society in this endeavor. This participation may be expressed, not only in the publication of articles, but also in reviews of articles submitted for publication. In connection with this, the editorial board would like to express its gratitude to G. A. Fvstropov, V. D. Kuznetsov, and A. K. Stolyarov, who took part, together with members of the editorial board, in reviewing the articles submitted for publication in the first collection.

The editorial board will be grateful to readers for their critical commentaries and suggestions concerning the nature of these collections and the materials published in them.

Reader commentaries, as well as materials for subsequent collections should be directed to the editors of "Svyaz'" Publishers of the "Antennas" collections (Moscow Central, Chistoprudnyy Boulevard, 2).

Editorial Board

U. S. BOARD ON GEOGRAPHIC NAMES TRANSLITERATION SYSTEM

Block	Italic	Transliteration	Block	Italic	Transliteration
А а	*А а*	A, a	Р р	*Р р*	R, r
Б б	*Б б*	B, b	С с	*С с*	S, s
В в	*В в*	V, v	Т т	*Т т*	T, t
Г г	*Г г*	G, g	У у	*У у*	U, u
Д д	*Д д*	D, d	Ф ф	*Ф ф*	F, f
Е е	*Е е*	Ye, ye; E, e*	Х х	*Х х*	Kh, kh
Ж ж	*Ж ж*	Zh, zh	Ц ц	*Ц ц*	Ts, ts
З з	*З з*	Z, z	Ч ч	*Ч ч*	Ch, ch
И и	*И и*	I, i	Ш ш	*Ш ш*	Sh, sh
Й й	*Й й*	Y, y	Щ щ	*Щ щ*	Shch, shch
К к	*К к*	K, k	Ъ ъ	*Ъ ъ*	"
Л л	*Л л*	L, l	Ы ы	*Ы ы*	Y, y
М м	*М м*	M, m	Ь ь	*Ь ь*	'
Н н	*Н н*	N, n	Э э	*Э э*	E, e
О о	*О о*	O, o	Ю ю	*Ю ю*	Yu, yu
П п	*П п*	P, p	Я я	*Я я*	Ya, ya

*ye initially, after vowels, and after ъ, ь; e elsewhere.
When written as ё in Russian, transliterate as yë or ë.

RUSSIAN AND ENGLISH TRIGONOMETRIC FUNCTIONS

Russian	English	Russian	English	Russian	English
sin	sin	sh	sinh	arc sh	$\sinh^{-1}$
cos	cos	ch	cosh	arc ch	$\cosh^{-1}$
tg	tan	th	tanh	arc th	$\tanh^{-1}$
ctg	cot	cth	coth	arc cth	$\coth^{-1}$
sec	sec	sch	sech	arc sch	sech^{-1}
cosec	csc	csch	csch	arc csch	csch^{-1}

Russian	English
rot	curl
lg	log

GRAPHICS DISCLAIMER

All figures, graphics, tables, equations, etc. merged into this translation were extracted from the best quality copy available.

PROBLEMS IN THE DESIGN AND METHODS FOR CALCULATING THE PARAMETERS OF VERY LOW FREQUENCY AND LOW FREQUENCY ANTENNAS

B. V. Braude, E. G. Aleksandrova

Examined here are problems in the rational design of base-station antennas of the capacitor (volumetric) kind. It is demonstrated that the basic electrical features of these kinds of systems are determined only by the volume occupied by the antenna system and do not depend on its configuration; the criterion for the selection of the configuration may be the system cost. Here, a method for calculating the basic parameters (capacitance, operational height, and loss resistance) in the antenna grounding system.

Introduction

The necessity for creating communication systems with enhanced reliability and effective range has once again attracted the attention of specialists to the range of low frequency and very low frequency waves; these waves possess not only the capability of being propagated at great distances with relatively small attenuation, but also assure stable functioning under conditions of ionospheric disturbance.

In creating a radio station using the low frequency (LF) and very low frequency (VLF) ranges,[1] the predominating problem is the choice of a radiating system that must have the required electrical parameters, reliability, and lowest possible cost.

It has been impossible up to now to predicate the antenna dimensions for antennas working in this wave range, although as a rule, as with the antenna dimensions of antennas in other wave ranges, the dimensions are roughly dependent on wave length. It is known only, however, that these antenna dimensions are small in comparison to wave length.

Despite the fact that the electrodynamic model of this kind of system is quite simple, the creation of LF and VLF antenna systems is connected with great difficulties, first of all, because of the enormous margins of reactive power in

[1] We are concerned here with frequency ranges of 150-50 kHz (the conventional long waves) and 50-10 kHz (conventional very long waves).

them, and secondly, because of the necessity for modern systems to function across wide frequency ranges.

It should be remarked that up to the present time the only criterion for /5
evaluating the effectiveness of antennas of the type indicated here has not been made use of: problems in rational design have been approached by means of a method of sampling, but the choice of optimal system dimensions has been dependent on the designer's experience.

General Design Principles

In designing LF and VLF antennas, it is necessary to take into account that it is the operational conditions in the long wave portion of the frequency range, where the antenna and its elements for tuning form a simple oscillatory circuit, that will be the most troublesome.

The effectiveness of fixed or base-station antennas, which may be called volumetric type antennas, is characterized by their Q-factors, by which is understood the ratio of reactive power reserve in the antenna to its emissive or radiating power. For antennas whose dimensions are small in comparison with wave length, radiation resistance can be computed according to Rudenberg's formula, and the computation of reactance is based on taking the antenna to be in the shape of a flat capacitor, without taking into account edge effect influences. This latter does not lead to any appreciable error, because the allowable error is compensated for by a drop in capacitance, caused by the wire structure of the curtain array.

The antenna Q-factor is calculated as the ratio of its reactance to its radiation resistance, written in the form:

$$Q_A = \frac{3\lambda^3}{8\pi^2 v}, \qquad (1)$$

where λ is wave length; $v=Sh$, the volume occupied by the antenna; S is the surface area occupied by the antenna; h is the height of the antenna curtain array suspension, which may be taken equal to the antenna operational height.

The antenna efficiency coefficient is determined by the following expression, first introduced by A. A. Pistol'kors [1]:

$$\frac{\quad}{\quad}.$$

where Q_η is the Q-factor of the adjustment elements taking into account antenna losses.

The antenna circuit Q-factor and the antenna bandwidth are expressed as:

$$\left.\begin{aligned} Q_{AK} &= Q_A \eta \\ 2F &= \frac{f}{Q_{AK}} \end{aligned}\right\}. \qquad (3)$$

Here, f is the carrier frequency.

When a power P is fed to an antenna circuit, it is easy to derive the following expression for the voltage on the antenna:[1]

$$U = \frac{1\sqrt{90P}}{2\pi}\frac{\lambda^2}{S}. \qquad (4)$$

Equations (1)-(4) make it possible to establish the following important conclusions: (1) The antenna circuit efficiency coefficient and its bandwidth at given wavelengths and adjustment element Q-factors are determined only by the volume occupied by the antenna system, and does not depend on the configuration of this volume. In other words, an antenna may take up a small surface area, but it must be suspended on high masts, and if the antenna is suspended on low masts, it must take up a large surface area. (2) The antenna voltage at given wavelengths and volumes is determined by the radiation power, and it increases in the height of the masts used for suspending the antenna curtain.

It is expedient and necessary to use the cost of an antenna as a criterion for finding its optimal volumetric configuration; the cost is basically determined by the weight of the metallic parts used for supporting the antenna curtain. The weight of metal parts, in its turn, is proportional to the load on the masts and the number of masts.

Let the load on the masts be determined by wind pressure on the antenna curtain array. Then, the load on one mast is expressed thusly:

$$T \approx \frac{d\,l^2}{p}. \qquad (5)$$

[1]Formulas (1) and (4) are also derived in [19].

where l is the span length, p is the conductor sag, and d is the diameter of the conductors in the antenna array.

Assuming that the span length and the conductor sag are proportional to the mast height H, and the number of masts in the system is $N = \frac{S}{l^2}$, we derive the following expression for the total weight G of the metal work:

$$G \approx \frac{dS}{H}. \qquad (6)$$

This expression was first derived by Yu. A. Savitskiy.

As the conductor diameters of the antenna curtain array are proportional to the voltage as determined by equation (4), we have:

$$G = K \frac{\lambda^2 \sqrt{P_\Sigma}}{H}. \qquad (7)$$

where K is the coefficient of proportionality. To find the coefficient of proportionality, it is sufficient to calculate any concrete antenna system.[1]

From equation (7), which determines in the final analysis the cost of the antenna, it follows that the antenna cost is proportional to the square of the wavelength and the square root of the radiational power. Further, it follows from this equation that antenna cost is reduced with an increase in mast height. It is necessary to remember, however, that together with an increase in mast height, the surface area occupied by the antenna, as well as the number of antennas, must be decreased. An increase in mast height is connected at the same time with a proportional increase in antenna voltage.

In this way, it is advisable to use higher masts in designing LF and VLF antennas, if the mast height is not restricted by any kinds of special conditions.

The antenna volume required for assuring determined features and characteristics can be realized in various ways. This may be by means of a system made from one or several gamma-shaped, T-shaped, or umbrella antennas working in parallel, whose feed is realized according to the simple parallel circuit suggested by I. G. Freyman [2], or according to the circuit of Aleksandersen [3-5]. The slot radiator

---

[1] According to a communication from G. Z. Ayzenberg, for some types of antennas, the value of H in formula (7) should be more correctly substituted by H^n (n<1). The value of n depends on the concrete type of antenna system being used.

schemes with extended horizontal portions, suggested by G. Z. Ayzenberg and studied by B. S. Nadenenko [6], can also be used.

In using slots that are disconnected or open on the ends, these kinds of vibrations are of considerable interest also for the wave ranges under consideration here. A similar system was used in creating the "valley" antenna [7], according to which the horizontal curtain is suspended between mountain ridges.[1]

The layouts for the antenna types indicated above are shown in Figs. 1-4.

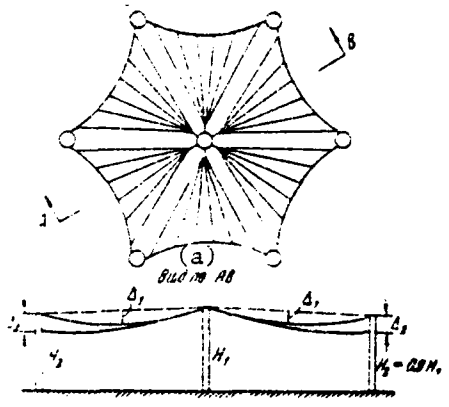

Fig. 1. Antenna system with horizontal portion in the shape of a convex polygon.
Key: (a) view along AB

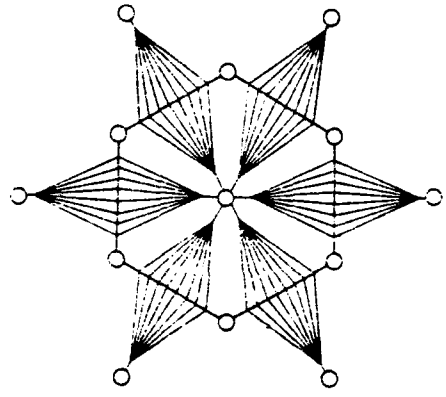

Fig. 2. Antenna system with horizontal portion in the shape of a six-pointed star.

The choice of the number of individual constituent elements making up the antenna system volume necessary for assuring the required electrical characteristics is determined basically by the range of waves over which the antenna must function, as well as by its slewability and reliability. Normally, the number of system elements is chosen in such a way that their natural resonance frequency is equal to, or almost equal to, the highest range frequency. In this case, the necessity for using expensive capacitors for adjusting the antenna disappears, and antenna adjusting is carried out only by means of inductors. The existence of several elements also lowers the ground losses and enhances station slewability as a whole.

[1]The efficiency coefficient for this kind of antenna turned out to be low due to the negligible conductivity of the mountain rock in the area where the antenna was set up. As slight conductivity in rock is characteristic for almost all mountain regions, the effectiveness of "valley" antennas is low as a rule.

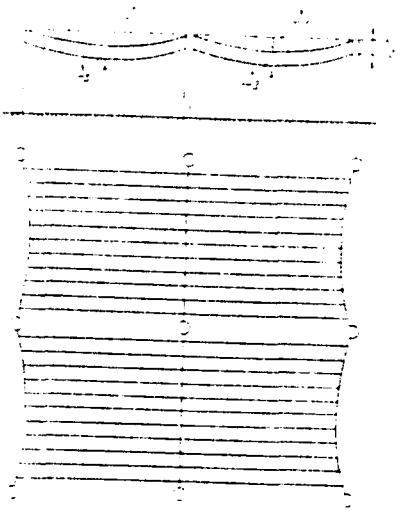

Fig. 3. Antenna system with horizontal portion in the shape of a rectangular screen.

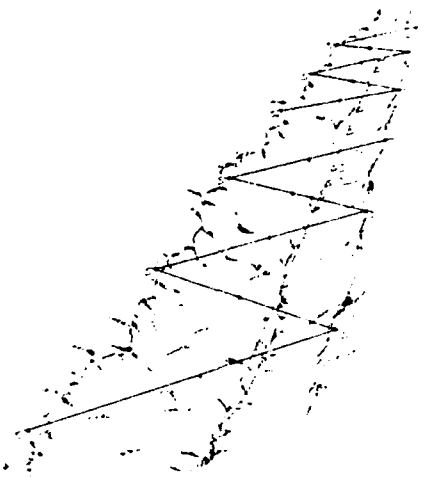

Fig. 4. "Valley" antenna.

An important place in designing antennas is occupied by the problem of selecting maximum voltage values. For conductors with diameters on the order of 25 mm, the maximum allowable voltage at which corona losses do not exceed /8 allowable values, is about 200 effective kV. This voltage is also used in modern large-scale VLF radio stations. It is characteristic that the transition to higher voltages does not lower the cost of antenna equipment, because conductors with larger diameters must be used in this, and as a consequence, the metal construction weight increases [see formula (6)]. In addition, with an increase in voltage, the insulation problem for the antenna curtain becomes more complex, especially with regard to the antenna feed, and for this reason using voltages higher than 200 effective kV is not possible at present.

The most complex problem in creating LF, and especially VLF, antennas is de- /9 riving high values for the coefficient of efficiency. As may be seen from the ratios cited above, this value depends as a rule on the selection of antenna volume, which determines its Q-factor, Q_A, and the Q-factors of the adjustment elements, taking into account ground losses $Q_п$. Keeping in mind that the margins of reactive power in extended inductors and in the antenna system are identical, it is possible to choose a surface area for an antenna and the grounding equipment taking the condition of the equality of losses in the ground and in the extension

inductors as a starting point. For this, it is necessary to decrease by two times the Q-factor for the adjustment elements cited above and to be entered in expression (2), in comparison with the natural inductor Q-value. It is natural that in each concrete case ground losses and losses in the extension inductors can occur in other relationships and according to other ratios. However, the demands made on the adjustment elements and the grounding systems should be regulated by means of a predetermined method.

It should be noted that the use of Litz wire with a large cross section makes it possible to derive at the present time a natural Q-factor for the extension inductors of about 1,500. Taking the cited Q-factor of an inductor to be equal to 750, from formulas (1) and (2) it is easy to conclude that for the creation, for example, of an antenna with an efficiency coefficient on the order of 50% for a wave of 30 km, its volume must be approximately equal to 1.35 km^3. For this, the overall extent of the conductors in the grounding system, depending on the conductivity of the soil, may amount to 1,000 to 3,000 km.

The Method for Calculating Basic Parameters

The Calculation of Static Capacitance and the Natural Resonance Wave

The most widely used method in calculating the capacitance of antenna systems is the method derived by How; however, for greatly extended wire curtains, it turns out to be very cumbersome. The considerable success achieved recently in the area of the theory of wire curtains (mostly, thanks to the work of M. I. Kontorovich [8, 9]), makes it possible to substantially simplify the methods for calculating antenna capacitances.

The individual elements of an antenna made from a series of conductors are substituted by thin, solid metallic surfaces, whose dimensions and shapes correspond to the wire portions of the antenna. If the distance between conductors in the net is smaller than twice the height of their suspension over the ground, then it is possible to demonstrate that the differences in potentials of the wire net and the solid metallic surface with the same dimensions can be determined basically by the difference between the potentials of one conductor and a solid plate whose width is equal to the distance between the conductors in the system. The

capacitance of the wire curtain relative to the ground is expressed in the following manner:

$$C = \frac{1}{\frac{1}{C_0} - \frac{2}{l} \ln \frac{d}{2\pi r}}, \qquad (8)$$

where C_0 is the capacitance of the solid metallic surface having the shape of a wire curtain, and l, d, and r are respectively the overall length of all conductors in the curtain, the distance between the conductors, and the radius of the cross sectional area of the conductors expressed in centimeters.

The capacitance of the solid metallic surface with a surface area $S=\pi R^2[cm^2]$, disposed parallel to the ground surface at a height of h [cm], is determined according to the following formula:

$$C_0 = \frac{R^2}{4h} - \frac{R}{2\pi}\left(1 - \ln \frac{8\pi R}{n}\right). \qquad (9)$$

This last formula may be used both for curtains in the shape of a disk, as well as for curtains in the shape of convex polygons. With a curtain rectangular form, it is necessary that the dimensions of its sides differ from each other by not more than three to four times. For the six-pointed star in Fig. 2, the radius of the described circle, equal to R_0, should be taken as $R=0.825 \cdot R_0$ in formula (9).[1]

The expressions cited above make it possible to easily calculate the capacitance of the horizontal portion of an antenna. The antenna downlead capacitance for the antennas being considered here is, as a rule, quite negligible in comparison with the capacitance of the horizontal portion. However, its value is necessary for calculating the antenna feed impedance. It is possible to show that the influence of the charges of a greatly extended horizontal antenna portion reduces the downlead capacitance by twofold in comparison with the value calculated taking into account the influence of the horizontal portion. In this way, the antenna downlead capacitance for umbrella antennas is:

[1]The height of the antenna curtain is determined in the following manner:

- for umbrella antennas:

$h = H - \frac{2}{3}(H_1 - H_2 + f_1 + \frac{2}{3} f_2)$; for rectangular curtains: $h = H - \frac{2}{3} f_1$

Here, f_1 and f_2 are the conductor sags for the curtains (see Figs. 1-3). The formulas have been derived with the presumption that the antenna wires are twisted according to a parabolic principle.

$$C = \frac{\quad}{1 - \frac{\quad}{r_0}}$$

where h_c is the downlead length, cm, and r_0 is the cross sectional area radius of a cylindrical downlead. If a downlead is made of n conductors with a radius of r, disposed in a circle with radius R, then $r_0 = R\sqrt[n]{\frac{nr}{R}}$.

For slot antennas, the downlead capacitance is determined by the expression:

$$C_0 = \frac{1}{\frac{4\ln 4}{\pi d} - \frac{4}{\pi h_c}\ln\frac{d}{2\pi r}}. \qquad (11)$$

The natural wavelength of the antenna in a first approximation is written in the form:

$$\lambda_0 = 2\pi h_c \sqrt{\frac{C_0 - C_n}{C_n}}. \qquad (12)$$

where C_n is the capacitance of the antenna's horizontal portion. This formula is derived with the assumption that the antenna inductance is determined by its downlead. It is necessary to use long-line theory for the precise determination of an antenna's natural wavelength and its reactive capacitance.

Calculation of the Operational Antenna Height Taking into Account the Horizontal Curtain Suspension and the Counterphase Excitation of the Supporting Metal Mass

In determining the operational height for LF and VLF antennas, it is necessary to take into account the distribution of capacitance throughout the whole system between its horizontal and vertical parts, as well as the influence of the wire suspension of the horizontal parts and the currents excited in the supporting structures of the antennas. /1

If we assume that the shape of the conductors forming the antenna is parabolic, and the wire suspension sag is significantly less than its total length, then for T-shaped and slot antennas the operational height is determined by the expression:

$$h_д = [H - (\Delta_1 - \Delta_2)]\left(1 - \frac{C_n}{2C_\Sigma}\right) - \frac{1}{3}(\Delta_1 - \Delta_2)\left(1 - \frac{C_n}{C_\Sigma}\right)^{1/2} \qquad (13)$$

where Δ_1 and Δ_2 are the suspension sags in the horizontal curtain in two mutually perpendicular surfaces, $C_A=C_h+C_r$, the antenna available capacitance.

For an umbrella antenna with an upper part in the form of a cone with a large angle at the apex:

$$h_1 \approx H_1\left(1-\frac{C_0}{2C_1}\right)-\frac{2}{3}\left[H_1-H_2-\frac{2}{3}\Delta_2-\Delta_1\right]\left(1-\frac{C_0}{C_1}\right), \quad (14)$$

where H_1 is the central mast height, H_2 is the height of periphery masts (normally $H_2\approx 0.9\ H_1$), Δ_1 is the vertical suspension sag of the radial wires, and Δ_2 is the vertical suspension sag of the periphery wire ropes between the peripheral masts.

In practical applications of antenna equipment, it is a variant of the system's construction, according to which the masts and the guy-wires supporting them, are grounded. The mast with guy-wires in this case forms a nonhomogeneous line, whose driving capacitance decreases according to an increase in the distance from the ground to the cross section under consideration. The dependency of the driving capacitance C_1 on the mast height may be approximated by an equation of the form:

$$C_1 = C_{10}\left(1-\frac{x}{H}\right)^n. \quad (15)$$

where C_{10} is the driving capacitance of the mast with guy-wires in its foundation, H is the mast height, and x is the distance from the mast foundation to the cross sectional area under consideration. The degree indicator n cannot be precisely calculated; however, for masts with three surfaces of guy-wires, disposed at a 45° angle to the mast column, the value of n, as calculations have shown, can be taken equal to 2. For grounded masts with insulated guy-wires, n should be taken equal to 0.

Taking a grounded mast as a receiving antenna, around which an electrical field with voltage E is distributed,[2] and using the reciprocity principle, it is possible to demonstrate that the distribution of charge excited by the antenna field in a

[1]This formula and the subsequent ones were derived under the assumption that the heights of the grounding supports are small in comparison with the wavelength. The natural wavelength of the grounded masts with their guy-wires is about 3.5·H. For this reason, the cited formulas may be used if the working wavelength is greater than 7·H.

[2]For antennas with a greatly extended horizontal portion, it is possible to take E as a constant magnitude.

cross section of the mast, is expressed by the relationship:

$$\frac{I_z}{I_0} = \left(1 - \frac{z}{H}\right)^{n-1} + (n-1)\frac{z}{H}\left(1 - \frac{z}{H}\right)^{n-2}, \qquad (14)$$

where $k_0 = \frac{\omega}{c}\sqrt{\frac{2(n-1)}{n-2}}$, $\omega = \frac{\pi}{\lambda}$ is the wave number, and $C = \frac{C_0 H}{n-1}$ is the available capacitance in the mast with guy-wires, which can be determined by means of integrating (15).

As model measurements have shown, the available capacitance of mast with guy-wires depends basically on the dimensions of the guy-wires. For masts with three to five tiers of guy-wires disposed in three layers at an angle of 45° to the mast column, the capacitance C_n may be found according to the following semi-empirical formula:

$$C_n \approx \frac{4H}{2\ln\frac{H}{3r}}, \qquad (15)$$

where r is the radius of the guy-wire cross section. All dimensions are expressed in centimeters.

The operational mast height, with respect to the current in its foundation, is determined by integrating expression (16), and amounting to:

$$l_д = \frac{2}{n-3} H. \qquad (16)$$

In this way, all necessary data for calculating the operational antenna height taking into account the currents excited by the antenna in the grounded masts are determined.

With a voltage U on the antenna, the current in its foundation is:

$$I_A = U\frac{i\omega C_A}{30}. \qquad (17)$$

If the operational antenna height is equal to $h_д$ without taking into account the influence of the mast, the resulting operational height $h'_д$ can be found from

---

[1]For grounded masts with insulated guy-wires,

$$C_n = \frac{H}{2\left(\ln\frac{H}{r_{cp}} - 1\right)},$$

where r_{cp} is the equivalent radius of the mast column cross section.

the following relationship:

$$I_A' = I_A - \sum_{i=1}^{N} I_{A_i} \qquad (21)$$

where N is the number of grounded masts in the antenna system.

Substituting the value of I_A from formula (19), I_0 from formula (16), and I_{A_i} from formula (18) into this, we get:

$$\frac{h_A'}{h_A} = 1 - \frac{\dots}{\dots} \left(\frac{1}{N} \sum_{i=1}^{N} \frac{\dots}{\dots} \right). \qquad (22)$$

It should be noted that grounded masts in an antenna system also increase the system's capacitance; this may be found from the following expression:

$$\frac{C_A'}{C_A} = 1 - \frac{N C_n}{\dots C_A} \left(\frac{1}{N} \sum_{i=1}^{N} \frac{HE_i}{U} \right)^2. \qquad (22)$$

where C_A' is the antenna capacitance taking into account the influence of grounded masts.

If of the overall number of grounded masts N, N_1 masts are peripheral masts, and N_2 masts are disposed on the interior of the antenna curtain, then for the peripheral masts $HE_i = 0.56\ U$, and for the internal masts $HE_i = 0.75\ U$. These relationships are derived with the assumption that the peripheral masts are disposed at a distance on the order of $0.1 \cdot H$ from the antenna curtain, and that the capacitance of the wire antenna curtain is about 0.75 of the capacitance of the same kind of curtain, but one made from a solid metal surface.

On the basis of what has been outlined above, we have:

$$\frac{1}{N} \sum_{i=1}^{N} \frac{HE_i}{U} = \frac{0.56 N_1 + 0.75 N_2}{N_1 - N_2}. \qquad (23)$$

For the antenna systems illustrated in Figs. 1 to 3, $h = 0.75 \cdot H$; $h_A' = 0.9\ h = 0.675 \cdot H$; $C'_A = 1.03\ C_A$. For this situation, the distance between masts is taken to be equal to twice the height, and the suspension sag of the wires in the antenna curtain is about $0.15 \cdot H$; the downlead capacitance is about 5% of the capacitance of the horizontal portion.

Calculating the Antenna Dielectric Strength

As the distance between the conductor wires in the kinds of antennas under consideration here are, as a rule, many times greater than the conductor wire diameters, the average voltage gradient along the conductor wires of the horizontal portion of the antenna can be expressed as:

$$E_{\left(\frac{cp}{cp}\right)} = \frac{2U_{(cp)}C_{r(cp)}}{r_{(cp)}l_{r(cp)}}, \qquad (24)$$

where l_r is the overall length of all conductor wires in the horizontal portion.

The average voltage gradient on the conductor wires in the vertical portion of the antenna can also be determined according to formula (24), if the index r is substituted by h and equations (10) or (11) are used.

In addition to the dielectric strength of the basic mass of conducting wires determined by equation (24), it is necessary to calculate the dielectric strength of the peripheral conductor wires of the antenna and those parts of it which are disposed near the ground or near the metal grounded supports. Thus, the well-known expression following may be used for the voltage gradient of peripheral conductor wires in the horizontal portion:

$$E = \frac{U}{r \ln \frac{2h}{r}}.$$

If a peripheral conducting wire is located near the grounded mast, the gradient can be calculated in the following manner [18]:

$$E = \frac{U}{3r \ln \frac{R}{\sqrt{2rr_{cp}}}}$$

where R is the distance from the conducting wire to the mast, and r_{cp} is the average radius of the mast cross section.

In assessing the dielectric strength of the periphery conducting wires, it is necessary to take the greatest of the values derived.

For a downlead composed of n conducting wires disposed around a grounded mast, the voltage gradient should be determined according to the following formula:

$$E = \frac{U}{\pi r \ln\left[\frac{2h}{R}\sqrt{1+\left(\frac{2h}{R}\right)^2}\right]}$$

where R is the distance from the downlead conducting wires to the mast axis.

It is possible to use formula (27) also when n=1; in this case, it is suitable for calculating the gradient on the downlead conducting wires of slot antennas that are disposed near grounded masts.

The voltage gradient on conducting wires of a distributor feeder for slot antennas is expressed thusly:

$$E = \frac{U}{\pi r \ln\left[\frac{2h}{R}\sqrt{1+\left(\frac{2h}{R}\right)^2}\right]}$$

where R is the area of the circle over which n feeder conducting wires are disposed.

In evaluating an antenna's dielectric strength, it must be taken into consideration that the breakdown voltage gradient for air is, under normal atmospheric conditions, about 21.2 $\frac{\text{eff. kV}}{\text{cm}}$. The voltage gradient at which corona losses begin in moist air is about 10 $\frac{\text{eff. kV}}{\text{cm}}$. For this reason, in antenna designing, a working voltage is chosen in such a way that the maximum voltage gradient on the conducting wires will be less than the value indicated above.

Antenna insulations must be fitted with electrostatic protection accessories for the creation of uniform field distribution across the porcelain insulators. The voltage gradient on the construction elements in the accessories may be calculated according to the formulas cited in [18]. The gradient across the porcelain should not exceed 0.7 $\frac{\text{eff. kV}}{\text{cm}}$ $\left(1 \frac{\text{kV ampl.}}{\text{cm}}\right)$.

Calculating the Resistance to Grounding Losses

The theory of groundings for LF antennas across the period of the first four decades in the development of radio engineering was the least developed area in radiation theory. The methods used and applied for calculating groundings did not reflect any galvanic physical substance to radiation processes and the distribution

of electromagnetic energy, and they yielded only the most approximate and preliminary data on losses in the ground.

A substantial shift in grounding theory took place in 1935 with the method of Brown [10], which he developed for calculating currents in a ground excited by an antenna field. The Brown theory made it possible to determine the direction and magnitude of currents flowing in the ground, and in this way, it yielded a basis for a more rational construction of grounding systems. The detailed data of Brown, Louis, and Epstein [10] that appeared subsequently in 1937 concerning the distribution of currents in a ground with the presence of a grounding constituted from radially distributed conducting wires, occasioned a considerable simplification and facilitation in investigations concerning this problem. However, Brown's assumptions and allowances did not make it possible to determine the absolute magnitude of losses.

The basic idea underlining his theory consists in the following. It is assumed that a ground is an ideal conductor, and from the equation $i=\frac{c}{4\pi}\cdot H$, where H is determined according to the theory of the distribution of electromagnetic waves for a vertical radiator, the surface current density in the ground may be found.

It is further assumed that with a finite, but ground of sufficiently high conductivity, the earth current will remain practically the same (subsequently, this was experimentally confirmed for relatively small distances from an antenna).

In this way, knowing the conductivity of the ground and the current magnitude, it is possible to calculate losses in each volume element of ground surface. However, when these losses are integrated across the whole ground surface taking into account the finite depth of current penetration into the earth, it turns out that the expression for losses goes to infinity.

This result is completely explicable if it be taken into account that the overall current induced in an ideally conducting ground, at an infinite distance from the antenna, goes to a finite magnitude. On the strength of these reasons, Brown, Louis, and Epstein were forced, in their comparisons of various grounding systems, to limit the summing of losses to the limits of the grounding systems considered.

Somewhat earlier, in 193[illegible], M. S. Newman proposed a method of dividing an electromagnetic field of antennas into component inductions and radiations; this method made it possible to avoid the complications cited above and to find an absolute value for the losses. The components of the field current in the ground excited by the induction field and the radiation field, as with the field components themselves, are shifted through a phase of 90°. On the strength of this, ground losses caused by these currents can be algebraically summed. The component radiation current, equal to zero in the antenna foundation, increases with the distance and approaches a constant limit at infinity. The component induction current, equal in the foundation to the antenna field current, drops off with distance and goes to zero at infinity.

Ground losses from the first current component determine the nature of the attenuation of electromagnetic waves in their dissemination and are dependent basically on the soil parameters. The grounding arrangement has no substantial influence on these losses, as it occupies a comparatively small area near the antenna with minimal values for the radiation current component.

The second field component is connected directly with the antenna current /1 and determined by the Biot-Savart Law. Ground losses caused by this component are usually called "grounding losses." The metallization of the ground near an antenna sharply reduces these losses. Integrating them across the whole surface from the foundation of the antenna to infinity, taking into account only the second field component, it is possible to derive an expression for calculating resistance to ground losses.

In 1944, M. I. Kontorovich and N. S. Beschastnov suggested a method for calculating ground losses [12] based on the calculation of antenna capacitance by means of the mirror reflection of the antenna and its counterpoise in the ground, and possessing arbitrary parameters.[1] In 1946, S. I. Nadenenko [11] suggested summing the ground losses from the field current in the half-wave radius, for calculating ground resistance, beginning with the assumption that the induction fields beyond the limits of this zone are no longer great.

[1]With the existence of finite soil conductivity, the antenna capacitance turns out to be complex, and for this its imaginary component makes it possible to calculate the antenna resistance caused by ground losses.

In the same year, on the basis of the Hansen and Beckerley theory [13], a precise method for calculating the antenna impedance was developed, with a precision up to a given current distribution in the antenna and a given grounding [14]. In particular, it was demonstrated that if the antenna dimensions and the grounding dimensions are small in comparison with the wavelength in the soil, the results of a precise calculational method will agree with the results of M. I. Kontorovich's and N. S. Beschastnov's approximative method. At the same time, the resistance to ground losses turns out to be not dependent on frequency (for the case when the displacement currents in the soil are small in comparison with the conduction currents).

If, however, the antenna dimensions and the grounding dimensions are large in comparison with the wavelength in the soil (which does not exclude the possibility of their being small in comparison with the wavelength in the air), then the resistance to ground losses is proportional to the $\sqrt{f}$ (where f is frequency), that is, the nature of this phenomenon is conditioned by the skin-effect phenomenon, all of which vindicates the Brown method of calculation. In addition to this, as it emerges from the precise method of calculation, ground losses which lower the antenna efficiency coefficient are caused only by its induction fields. This is the basis of M. S. Newman's idea explained above.

In 1954 and 1958, Wait and Pope suggested a method for determining the antenna feed impedance, taking into account the finite conductivity of the ground; the method was based on using the Lorenz lemma. The essence of this method consists in the following. The antenna feed impedance, taking into account the finite conductivity of the ground, is taken as the sum of antenna feed impedance assuming ideal ground conductivity and of a small accessory impedance taking into account its finite conductivity. This latter is expressed as the ratio of induced emf as a result of the finite conductivity to the current in the antenna foundation. In agreement with the Lorenz lemma, the induced emf is determined as the integral of the current distribution function for an ideally conducting ground, integrated across the whole ground surface (with the ideally conductive ground normalized for a current in the antenna base), and multiplied by the tangential value of the electrical field at the ground surface arising with its finite conductivity. The tangential field value at the ground surface is found by means of multiplying the current in the ground (assuming that its conductivity is ideal)

by the surface impedance of the actual ground surface. Beyond the limits of the grounding, this latter may be determined only by means of soil parameters according to skin-effect formulas, and within the grounding limits, as the parallel joining of the actual ground impedance and the metallic wire mesh.

It is necessary to note that the accessory and antenna impedance, calculated according to the Wait method, turns out to be finite as a result of the finite ground conductivity, and this makes this method quite convenient for practical applications.

In a series of works concerned with the design of grounding systems, only the loss components depending on frequency have been taken into account. At the same time, calculations have demonstrated that losses in the grounding zone with a large number of conducting wires increase, as a rule, with increases in soil conductivity and decrease with decreases in soil conductivity. From this, it has been concluded that it is advisable to set up antennas in a place where soil conductivity in the grounding zone is small, and beyond the limits of this zone, where it is great [5]. However, the use of the expressions for ground surface impedance is justified only in the case when the antenna and grounding dimensions are great in comparison to the wavelength in the soil. In calculations for antennas working in a range of very low frequencies, however, where the distances between the grounding conducting wires are, as a rule, less than the wavelengths in the soil, it is necessary to take into account, in addition, the supplementary resistance to ground losses, which does not depend on frequency and has the character of resistance in the grounding electrode wires for a direct current grounding electrode [12, 14, 17]. Because this resistance is inversely proportional to soil conductivity, an antenna site with high soil conductivity both in the grounding zone as well as beyond its limits must be selected.

In those cases, when for any of a number of reasons, soil conductivity in the grounding zone is small, it is necessary to select a number of grounding conducting wires, such that the specific gravity of the supplementary ground losses, caused by the grounding wire structure, is sufficiently small, and such that the influence of conductivity variations in the upper soil level under varying meteorological conditions would have no influence on antenna parameters.

On the basis of what has been explained above, it is possible to derive the following relatively simple expressions for calculating the resistance to ground losses in LF and VLF antennas with greatly developed horizontal parts:

$$R_3 = \sqrt{[illegible]} \left[\frac{1}{2} \ln \left(1 + \frac{[illegible]}{[illegible]} \right) - \frac{1}{2} \ln (1 + b + [illegible]) - [illegible] \, \mathrm{arctg} \, [illegible] \right] + \frac{1}{4 \pi \sigma} \frac{[illegible]}{n} \left(\ln \frac{[illegible]}{n r_3} - 1 \right), \qquad (29)$$

where:

$$b = \frac{2 \pi [illegible]}{n} \sqrt{120 \sigma [illegible]} \ln \frac{[illegible]}{n r_3}.$$

For the case when b<<1, the formula is simplified, and the following form is arrived at:

$$R_3 = \sqrt{[illegible]} \left[\frac{1}{2} \ln \left(1 + \frac{[illegible]}{[illegible]} \right) + \frac{120 \pi^2 [illegible]}{[illegible]} \ln^2 \frac{[illegible]}{n r_3} \right] + \frac{1}{[illegible]} \frac{[illegible]}{n} \left(\ln \frac{[illegible]}{n r_3} - 1 \right), \qquad (30)$$

where:

$h_д$ -- antenna operational height, m;

ρ -- grounding radius, m;

n -- number of conductors in the radial grounding;

r_3 -- radius of grounding conductor cross sectional area, m; /1

σ -- soil conductance, S/m;

λ -- wavelength, m;

b -- ratio of reactive impedance of the wire grid to active impedance of the ground surface.

Because the depth of current penetration into the ground, in accordance with skin-effect theory, is several tens of meters for VLF waves, in calculating the first member in expressions (29) and (30), the value of σ may be taken to be independent of meteorological factors. The second component of the losses does not depend on frequency and is determined by the value of σ at depths equal approximately to the distance between the grounding conductors. For this reason, it is advisable, when this is being computed, to take the smallest value of σ for a given locale for frozen soil or dry weather.

Calculating the Antenna Efficiency Coefficient

As Hansen and Beckerley demonstrated [13], the radiation resistance of an

antenna located on semiconducting soil is always less than the radiation resistance of an antenna located on an ideally conducting, unbounded flat surface. This is determined by the following expression [14]:

$$R_{\Sigma} \ldots$$ [illegible]

where: $x = 1 \ldots$ [illegible]

$R_{\Sigma 0}$ is the antenna radiation resistance determined according to the Rudenberg formula; $\beta = 60 \cdot \lambda\sigma$, the imaginary component of the soil dielectric permittivity constant, which is assumed to be much greater than the material component.

The antenna efficiency coefficient, from the point of view of the field voltage of the ground wave created by it is:

[illegible]

where R_{Π} is the antenna ground loss resistance in its adjustment elements as well.

With a grounding system that has been well constructed, the value of η can be larger than unity; this has been observed several times in measurements done on actual antenna equipment. This kind of result is not absurd, insofar as the value of η in this determination is the coefficient of antenna gain.

Special Features in Calculations for Multi-Element Antennas /2

If an antenna system is composed of several, for instance, p elements, then in calculations for the whole system it is necessary to begin with the overall surface area of the horizontal curtains and to use expression (9). The capacitance of one element is a simple division of available capacitance by p. In this way, the reciprocal and mutual influences between the antenna system elements will be accounted for in computing the reactive component of its feed impedance. The radiation resistance of each element is computed according to the Rudenberg formula with the addition of all impedances from the other elements to be inserted. The inserted impedance from one element for the case when the distance between elements is $d \leq 0.25\lambda$, is determined according to the following simple formula:

$$\frac{R_{12}}{R_{11}} \approx 1 - \frac{k^2 d^2}{5}. \qquad (33)$$

Here, R_{1} is the radiation resistance of one element computed according to the Rudenberg formula.

If the overall surface area of the grounding system is equal to S, then with a number of radial grounding electrodes p, each of which consists of n conducting wires, the loss resistance with respect to the overall current in all the downleads in the antenna system is calculated according to the following formulas:

$$R_{\text{з}} = \sqrt{\frac{\omega\mu}{2\gamma}}\left[\frac{1}{2}\ln\left(1+\frac{b^2}{\pi^2}\right)+\frac{1}{2b}\ln\left(1+b^2+\frac{b^4}{2}\right)-\right.$$
$$\left.-\frac{1}{b}\operatorname{arctg}\frac{b}{2+b^2}\right]+\frac{1}{4\pi\gamma}\frac{\pi}{np}\ln\frac{\pi}{nr_0}-1\Big), \qquad (34)$$

where: $b=\frac{2\pi h}{n^2}\sqrt{120\pi\gamma}\ln\frac{\pi}{nr_0}$.

For the case where $b\ll 1$:

$$R_{\text{з}} = \sqrt{\frac{\omega\mu}{2\gamma}}\left[\frac{1}{2}\ln\left(1+\frac{b^2}{\pi^2}\right)+\frac{120\pi^2h^2}{n^4p^2}\ln^2\frac{\pi}{nr_0}\right]+$$
$$+\frac{1}{4\pi\gamma}\frac{\pi}{np}\ln\frac{\pi}{nr_0}-1\Big), \qquad (35)$$

Here, it is accepted that: $r_0=\sqrt{\frac{S}{\pi}}\cdot 0.8$ $p=\sqrt{\frac{S}{\pi p}}\cdot\frac{1}{1.7}$.

In conclusion, it should be stressed that the grounded masts with guy-wires must also have radial groundings with a relatively small number of conducting wires, and they must be connected with the overall antenna grounding system. Losses in these groundings can be calculated according to the same formulas, if h is taken equal to $l_{\text{м}}$ in expression (18), and the current in the mast foundation is calculated according to formula (16).

BIBLIOGRAPHY

1. Pistol'kors, A. A. "Teoriya kol'tsevoy difraktsionnoy antenny" [The Theory of Ring Diffraction Antennas], Journal of Technological Physics, Vol. 14, No. 12, 1944.

2. Freyman, I. G. "O moshchnoy radioveshchatel'noy stantsii dlya SSSR" [On a Large-Scale Radio Broadcast Station for the USSR], Electronic Communications, No. 5, 1928.

3. Nevyazhskiy, I. Kh. "Razvitiye tekhniki radioperedayushchikh ustroystv" [The Development of Radio Broadcasting Equipment Technology], Electricity, No. 15, 1946.

4. Takass, A. F. "Naval Communication System Begins Final Test Stage," Electronic News, Vol. 6, No. 256, 1961.

5. Magneson, N. J. "Navy's Most Powerful Radio Facility," Journal of the Construction Division, IX, Vol. 83, No. CO2, 1962, pp. 57-82.

6. Nadenenko, S. S. "Srednevolnovaya radioveshchatel'naya antenna na nizkikh machtakh" [Medium Frequency Radio Broadcasting Antenna on Low Masts], Radio Technology, Vol. 12, No. 12, 1957.

7. Hobart, G. D. "Navy VLF Transmitter Will Radiate 1000 kW," Electronics, No. 12, December 1952, pp. 98-101.

8. Kontorovich, M. I. "Premeneniye metoda usredneniya poley k issledovaniyu nekotorykh elektricheskikh sistem" [Application of a Field Averaging Method for Studying Several Electrical Systems], Doctoral Dissertation, LPI [Leningrad Polytechnic Institute im. M. I. Kalinin], 1940.

9. _____. "Ob usrednënnykh granichnykh usloviyakh na poverkhnosti setki s kvadratnymi yacheykami" [Concerning Averaged Boundary Conditions on the Surface of a Grid Having Square Meshes], Radio Technology and Electronics, Vol. 8, No. 3, 1963.

10. Antennye ustroystva [Antenna Equipment]: Sb. perevodnykh statey pod redaktsiey S. I. Nadenenko [Collection of Translated Articles, ed. S. I. Nadenenko]. Svyaz'-izdat [State Publishing House of Literature on Communications and Radio], 1959.

11. Nadenenko, S. I. "Vybor razmerov sistemy zazemleniya antenn" [Selecting Dimensions for an Antenna Grounding System], Radio Technology, Vol. 2, No. 2, 1946.

12. Kontorovich, M. I., Beschastnov, N. S. "O poteryakh v zemle pri ispol'zovanii korpusa peredatchika v kachestve protivovesa" [On Ground Losses Using the Transmission Circuit as Counterpoise], Works of the VKAS [expansion unknown] im. S. M. Budënnogo, No. 8, 1944.

13. Hansen, W. W., Beckerley, T. G. "Concerning New Methods of Calculating Radiation Resistance, Either with or Without Ground," Proceedings of the IRE, Vol. 24, No. 12, 1936.

14. Braude, E. V. "Metod raschëta polnogo aktivnogo soprotevleniya antenny s uchëtom konechnoy provodimosti zemli" [A Calculation Method for Active Antenna Impedance Taking into Account Finite Ground Conductance], Radio Technology, Vol. 2, No. 5, 1946.

15. Wait, J. R., Pope, W. A. "The Characteristics of a Vertical Antenna with a Radial Conductor Ground System," Appl. Sci. Res., Vol. 4, 1954.

16. _____. "A Study of Earth Currents Near a VLF Monopole Antenna with a Radial Wire Ground System," Proceedings of the IRE, Vol. 46, No. 8, 1958.

17. ____. "On the Calculation of Transverse Current Loss in Buried Wire Systems," Appl. Sci. Res., Vol. 7-B, 1958.

18. Braude, E. V. "Gradienty napryazheniya v moshchnykh peredatchikakh" [Voltage Gradients in Large-Scale Transmitters], Radio Technology, Vol. 2, No. 2, 1946.

19. Wheeler, H. A. "Fundamental Relations in the Design of a VLF Transmitting Antenna," IRE Transactions on Antennas and Propagation, Vol. AP-6, No. 1, January 1958, pp. 120-122.

QUASI-OPTICAL TRANSMISSION LINES FOR MILLIMETRIC WAVES /1

R. B. Vaganov, B. Z. Katsenelenbaum

In this article, new kinds of transmission lines for millimetric and submillimetric waves are examined -- quasi-optical reflecting beam waveguide lines and reflecting beam waveguide lines with lenses.

In the range of decimetric and centimetric waves, the most universally used waveguide lines use, for the most part, rectangular waveguides with a wave of H_{10}. In the millimetric range, the cross section of a common single-wave waveguide is very small, and for this reason, losses in its side walls increase greatly. At λ=1 mm, it is extraordinarily difficult to make a single-wave, rectangular waveguide. Attenuation in this kind of waveguide is about 10 dB/m.

There are two basic ways for creating effective millimetric carriers. It is possible to apply broad (in comparison with λ), that is, multi-wave waveguides manufactured with great care, in order that the unavoidable transformation processes of the principal wave into higher order waves will be sufficiently small in them; or it is possible to create quasi-optical reflecting beam lines or reflecting beam lines employing lenses, consisting of a series of equidistant lenses or curved mirrors that conduct the wave bundle. The development of these kinds of lines began about five or six years ago ([1], [2], see also the overview in [3]).

In describing millimetric wave propagation in reflecting beam mirror or lens lines, it is convenient to use the notion of an elementary bundle. "Elementary bundle" is the name for a propagating electromagnetic wave occupying a region of space with an approximately cylindrical shape. The field of the bundle has a finite value at $r<r_s$, where r is the cylindrical coordinate, and r_s is the bundle parameter, falling away exponentially at $r>r_s$. Each bundle is characterized by a parameter r_s and two pole numbers indicating the dependency of the field voltage /2 on the azimuth angle ϑ and on the radius r. More precisely stated, the field voltage on the middle plane is:

$$U_{mq}(r,\vartheta) \sim e^{-\frac{r^2}{r_s^2}} \left(\frac{r}{r_s}\right)^m L_q^m\left(\frac{r^2}{r_s^2}\right) \cos m\vartheta,$$

and the surface of equivalent phases is flat. Here, L_q^m is a so-called Laguerre polynomial.

For a simpler bundle, m=0 The larger the index q of the L_q^m polynomial, the greater will be the effective bundle width, that is, the value of the ratio r/r_s at which the effective exponential field decrease in a radial direction.

The field distribution along the bundle axis (along the z axis) is determined by the Maxwell equations. According to the distance from the plane, z=const., for which expression (1) applies, the parameter r_s increases (that is, the bundle expands) and at the same time, the surface of equivalent phases becomes curved. At the same time, it takes on the form of a spherical section, whose center of curvature lies to the left of the central plane (Fig. 1). To the left of this plane, the surface of equivalent phases has the form of a concave sphere. All of Fig. 1 is symmetrical with respect to the central plane. The field amplitude at r=0 is shown by the broken line.

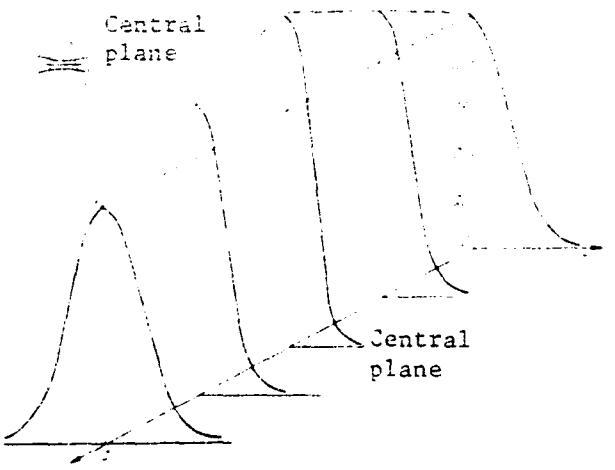

Fig. 1. An elementary bundle with indices m=0, q=0.

In this way, a bundle is a quite complex wave: that is, it converges to the left of the central plane, and diverges to the right of it, with respect to the field which is nonhomogeneous across a cross section. It is possible to imagine it as an aggregate of flat waves propagated in different directions, with these directions forming a small cone around the z-axis. A variation in the field structure of the bundle with the propagation of the bundle along the axis represents a typically diffractional effect, that is, an effect connected with

the finiteness of the wavelength. It is this diffraction that changes the radius of curvature of the bundle front, while in any arbitrary cross section, the size of the bundle remains finite, that is, the bundle is not contracted to a point. This size dimension r_s is proportional to $\sqrt{\lambda}$, which is typical for a series of diffraction phenomena, for instance, for the passage of a wave through the focus of an optical system. The analogy between this phenomenon and the nature of the bundle field near the central plane is quite far-reaching.

Bundles cannot exist by themselves; depending on the distance from the central plane, they become more and more dilated. In order to transform a diverging bundle into a converging one, lenses, mirrors, or systems of mirrors are used, and a series of these represents a quasi-optical line. If the surface of equivalent phases before it reaches a lens or mirror is convex, after the passage of the bundle through the lens or after it is reflected from a mirror, it becomes concave, and the amplitude field distribution in the plane perpendicular to the direction of bundle propagation does not change. The bundle is propagated further by means of the method described here.

Phase correction by successive lenses and mirrors completely regenerates the bundle. It becomes identical to the bundle as it passed through the preceding phase correction. In this way, the system of phase corrections guides the bundle and reiterates it as it passes through each correction phase.

Phase correction is a geometric concept. If the bundle field, as it approaches the correction phase, is characterized by a magnitude $u(x, y)$, then the field of the exiting bundle is characterized by a magnitude $u(x, y)e^{i\phi(x, y)}$. The function $\phi(x, y)$ is determined by the phase shift of a ray between the point with coordinates (x, y) as it enters the correction and the point with the same coordinates as it exits from it. This kind of calculation for phase correction has the same order of precision as geometrico-optical calculations in paraxial approximations. In this calculation, it is sufficient to account for the transformation in phase distribution; in geometric problems, a knowledge of the phase would be sufficient for determining the direction of the rays (as normal to the surfaces of equivalent phases), and it would not be necessary to account for wave refraction at the boundaries in an explicit form.

The notion of bundles with principally diffractional natures is used in quasi-optics to describe wave propagation in a free space. In this way, in order to represent the essence of processes in quasi-optical lines, it is necessary to take up both geometrico-optical (phase correction), as well as diffractional (wave bundle) concepts.

The processes of propagating electromagnetic waves in quasi-optical lines /1
may be viewed from another side as well. We shall describe a bundle in general as the natural wave of a system of identical, equidistant phase correctors. The field distribution of a natural wave across a cross sectional area is repeated with a precision to within a constant (complex) factor after it passes through the interval between lenses and passes through a lens. The constant factor determines the phase shift of the natural wave and its amplitude decrease. Field distribution after each lens is reiterated with a precision to within the phase shift, not dependent on the coordinates in the plane of the cross section. The elementary bundles described above are natural waves in a line composed of an infinite number of quadratic correctors, that is, correctors whose phase shift ϕ is proportional to the square of the radius r^2. The module of the complex factor in this case is equal to unity. Bundles with different indices (q, m) are propagated in a quasi-optical line with an infinite number of correctors independent of each other. The energy flux in any wave entering into the line is equal to the sum of energy fluxes of the natural waves. The variable r_s in expression (1) is proportional to the square root of the product of the distance L between correctors and the wavelength λ.

Natural waves (repeating bundles) also exist in systems with finite numbers /1
of correctors, that is, with correctors in absorption screens (Fig. 2). If the correctors are quadratic, the fields of the natural waves are similar to elementary bundles, with the exception however, that their energies decrease with propagation. This is connected with the fact that a portion of the energy exiting from a given lens does not in general reach a subsequent lens; this leads to the occurrence of radiational (they are sometimes called "diffractional") losses. For maintaining repeating bundles in these kinds of systems, in addition to phase correctors that adjust phase distribution according to the bundle cross section within the aperture limits, an important role is also played by absorption screens. These latter remove that portion of a bundle which does not correspond to the field as

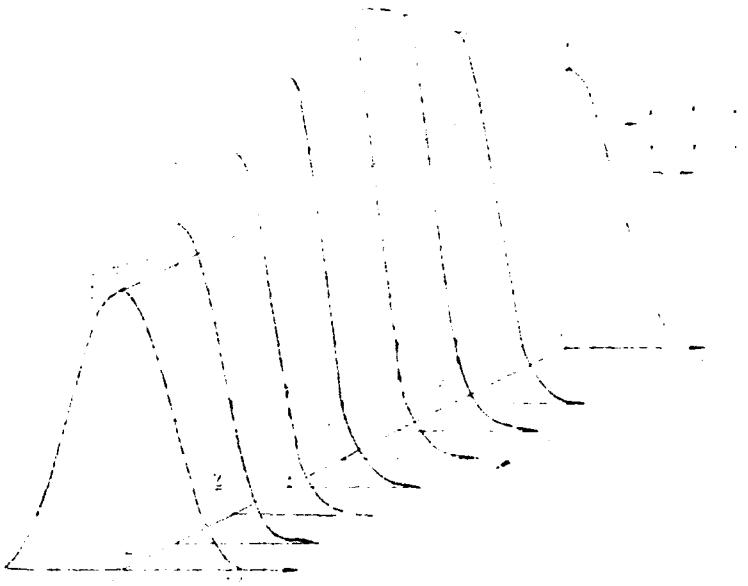

Fig. 2. Natural wave in a system of lenses in absorption screens.

it exits from a preceding correction phase.

For illustration's sake, field amplitude distributions in a quasi-optical line composed of restricted quadratic correctors are shown in Fig. 2. The variable $c=\frac{ka^2}{L}$, characterizing the radiational losses in the line, has been taken equal to 2π. This variable is a magnitude proportional to the square of the ratio of the lens radius a to the effective radius r_s of the bundle incident on the lens, which is proportional to $\sqrt{\lambda L}$. The larger value of this ratio, that is, the greater field concentrated near the axis, the fewer will be radiational losses. In the case under consideration here, the ratio $\frac{a}{r_s}$ is equal to 2.5, thus the losses are very small, and the field amplitudes with output from two neighboring lenses differ only slightly from each other. The field aperture distributions are reiterated: the portion of the bundle field at r>a is absorbed by the screen. The broken line shows the field amplitude at r=0. From a comparison of Fig. 1 and Fig. 2, it follows that with the existence of losses, the bundle is narrowest not midway between correction phases, but nearer the preceding correction phase.

A mathematical apparatus of integral equations is used for calculating radiational losses of a natural wave in systems with restricted correctors. The field for the output from one corrector is taken as an unknown function. According to

it, the input field into a subsequent correction phase may be determined from an approximative solution (according to the Huygens principle) of a Maxwell equation. The field as it exits from this latter corrector may be determined by multiplying by $e^{i\phi(x,y)}$. It should differ from the output field from the first corrector by only the constant factor. This leads to a homogeneous Fredholm integral equation of the second kind, which may be written in the following manner for the desired field:

$$\chi u(\xi, \eta) = e^{i\phi(\xi,\eta)} \int_S u(x, y) K(x, y, \xi, \eta) dx dy, \qquad (2)$$

where:

$$K = A \frac{e^{-ikr}}{r} e^{-i\frac{k}{2f}[(x-\xi)^2+(y-\eta)^2]} \quad \text{и} \quad A = \text{const.}$$

The value χ is an eigenvalue for this equation. It is equal to the change /2
in field as the bundle moves from corrector to corrector. Radiational losses are $1-|\chi|^2$. The bundle phase shift is determined by the argument of the eigenvalue χ, and the field distribution within the aperture limits is determined by the equation eigenfunction.

Depending on the type of phase correction $\phi(x, y)$, the form of the bundle (natural wave) also changes, as well as its radiational losses. There are many systems which may carry a wave with small radiational losses. Up to the present time, however, with no solutions for equation (2), it is impossible to determine whether or not a given system, specifying an aperture S and with a magnitude L and function ϕ, will assure small losses. In particular, all systems of quadratic correctors, whose focal lengths fall within the limits $L/4<f<\infty$, will carry a wave with allowable radiational losses. The dependency between these losses and the value $v=L/2f$ for some values of the variable c is shown in Fig. 3. It is apparent that the fewest losses occur in a system with confocal correctors ($v=1$). The curves are symmetrical with respect to the straight line $v=1$.

A common, thin dielectric lens is a phase corrector. In paraxial approximation, it carries out a quadratic correction, while the spherical, convex surface of the equivalent bundle phases is transformed into a concave spherical surface. The new radius of curvature is determined according to the "lens rule," well known in optical geometry.

For the calculation of lens systems in optical geometry, concepts of "point source" and "point image" are used. Each point in space for objects, according

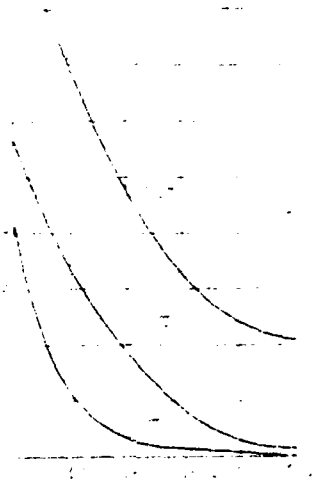

Fig. 3. Radiational losses in a system of quadratic lenses.

to simple notions of Gaussian optics, corresponds to a point in space for images. Real optical systems, systems possessing abberrations, are not included in these mechanisms, and this leads to image distortions. Systems with thin, quadratic lenses are closest of all to ideal systems without abberrations.

In quasi-optics, there are no geometrical requirements disallowing abberrations, at least in regular systems (equidistant, identical, coaxial correctors). In other words, it is not at all obligatory that a corrector transform a spherical front of an incident bundle into a spherical front of a bundle exiting from the corrector. Also possible, for example, are nonquadratic corrections. Lenses may /2 have the form of bodies of rotation, whose formative parts are straight line sections (that is, a corrector as a circular cone) or a broken polygonal line (for example, a corrector as a truncated cone).

The natural waves in a system consisting of nonquadratic lenses represent significantly more complex wave bundles than the elementary bundle described above. By way of example, shown in Fig. 4 is the amplitude distribution of the field of a natural wave with the smallest indices and having minimal radiational losses in a quasi-optical system which is a series of absorbing diaphragms ($\nu=0$). It may be seen from the figure that this wave is a wave bundle that is repeated at every subsequent aperture, while the bundle amplitude decreases.

In the lenses, which are small dielectric wafers of variable thickness, the phase correction is carried out as a result of differences in the optical paths

of the rays passing through various points in the lens. When there is a substantial lack of lens-correctors, the energy of the bundle is reflected off the surfaces and absorbed in the dielectric material.

The reflection factor is removed either by means of the application of an anti-reflecting coating [2], or by means of creating special lenses [4] of such a shape that if they are turned toward the axis of the bundle at the Bruster angle, the phase correction introduced by them is equal to the correction induced by normal spherical lenses, and reflection from the surfaces is removed. The output signal from a confocal line is shown in Fig. 5 (lens radius 8.4 cm, wavelength 8 mm, distance between lenses 175 cm), substituting a straight spherical lens made of plexiglass (refractive index n=1.6, focal distance 82.5 cm), with a Bruster lens inclined toward the system axis at various angles. If the incline angle is close to α_B=arc tg n, then with this kind of substitution, a substantial increase in signal due to reduction of lens surface reflection is observed.

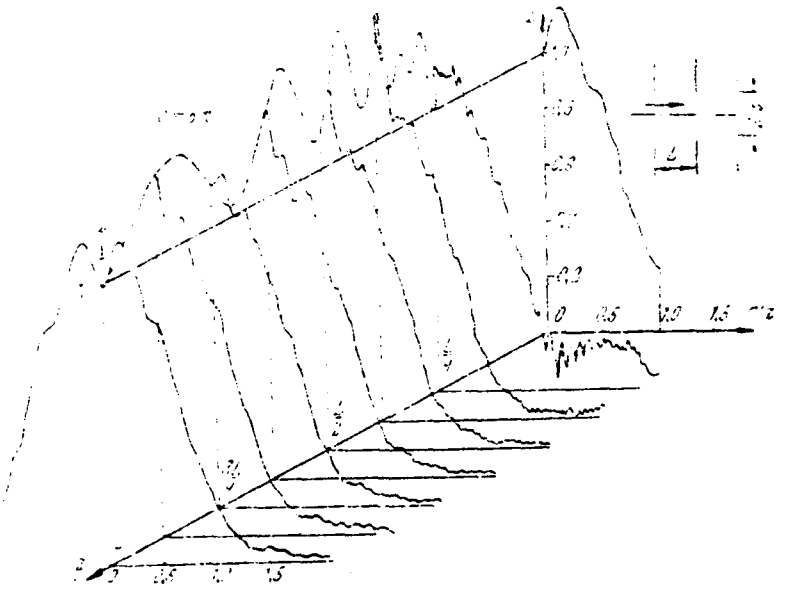

Fig. 4. The natural wave of a system of absorption screens.

It is not possible to do away with dielectric absorption; in addition, with a decrease in wavelength, the tangent of the loss angle in existing dielectrics increases. In connection with this, at present the use of focusing, reflecting mirrors, suggested in the cited works [5, 6], seems to be promising. Phase correction occurs as a result of the fact that rays reflected from various points

on the mirror describe different paths. Mirrors, in distinction to lenses, do not introduce dielectric losses. The losses caused by the finite conductivity of metal are small in comparison to dielectric losses.

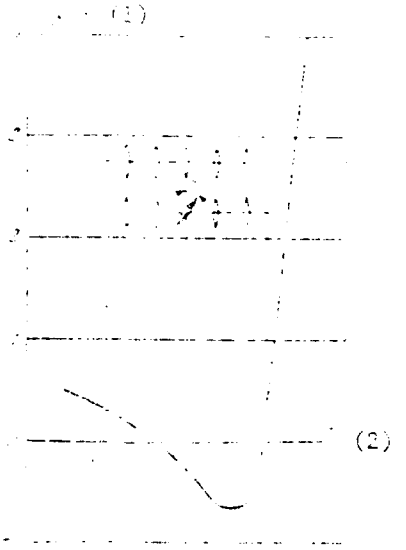

Fig. 5. Substituting a spherical lens by means of a nonreflecting lens (experimental).

Key: (1) dB; (2) a/ δ rad

Despite the fact that a mirror realizes a phase correction of the bundle in the plane not perpendicular to the bundle, nevertheless it is possible to construct mirrors which will carry bundles in a symmetrical fashion with respect to the axis. They must have the shape of a surface section of an ellipsoid body of rotation. A bundle in a system of mirror-ellipsoids is the same as in a system of quadratic lenses. However, simpler forms of mirrors (spherical sections) are also quite acceptable; these possess astigmatism in the optical geometrical sense. These kinds of correctors will conduct bundles of a somewhat more complex type than those pictured in Fig. 1. In the cross section of a bundle in a line with equivalent amplitudes, the shape will not be in the form of a circle but in the form of ellipses. The formation of a bundle is determined by the ratio between the radius of curvature of the mirror surface and the distance between mirrors. In particular, it is possible to construct a quasi-optical line, in which the amplitude distribution of the bundle field near the mirrors is symmetrical with respect to the axis [7].

A quasi-optical mirror line will be more compact if the mirrors are joined together in pairs (a periscope system, Fig. 6). If the distance $\bar{L}$ between mirrors in pairs is very much smaller than the radius of the mirror ρ, the phase correction of the double mirror system will be equal to the sum of corrections for the component mirrors.

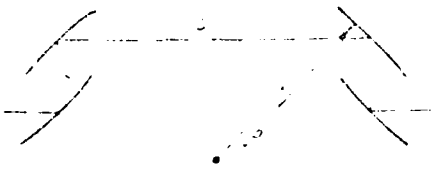

Fig. 6. A periscope system consisting of spherical mirrors.

For an energy evaluation of the line, it is necessary to determine the radiational losses, losses in the lens material or ohmic losses with reflection off of the mirrors, losses at the transmitting and receiving ends of the lines (the more substantial in general the balance of losses, the shorter is the line), and the losses in transformation of the wave types. Transformation takes place as a result of imprecisions in manufacture and justifying, as well as as a result of variations over time in the positionings of the lenses or mirrors.

In calculations for a line, it is necessary above all to sample the variable c which determines the radiational losses of the natural waves. It should not be small, in order that the losses in the principal wave are not great, and it must not be especially large, in order that the line's self-filtration mechanism not be too small; self-filtration is the eradication of higher order waves, arising as a result of excitations due to irregularities, from out of the line. In accordance with this, a value for the variable c is chosen between 1.6π and 2π for lines consisting of quadratic correctors.

With correctors of these sizes, radiational losses in the principal wave are an insignificant fraction of the overall losses. Losses due to excitation cannot be reduced appreciably beyond 1 dB. Losses to the correctors due to dielectric absorption and reflection off the surfaces are approximately 0.05 dB in matched lenses and 0.15 dB in unmatched lenses [2, 8]. Losses due to reflection off of aluminum mirrors amount to about 0.015 dB in a mirror line if the electric field vector in the bundle is perpendicular to the incidence plane, and about 0.02 dB if this vector lies in the incidence plane [9]. Transformation losses in a long line are, of course, most substantial, if line losses due to dielectric absorption or metal absorption are quite small.

Transformation losses must be analyzed according to the following system: one of the undisturbed natural waves in a system consisting of ideal correctors is incident on a deformed or displaced phase corrector. Displacement or deformation in the corrector disturbs the field phase front coming after it. A disturbed field can be expanded into a series of undisturbed natural waves, with the expansion coefficients as coefficients of connection between the waves and conditioned by the deformations or displacements in the correctors. As calculations have shown [10], for a lens line, lens displacement in the plane perpendicular to the axis has the greatest significance. For a mirror line, in addition, it is rotations in the mirrors that are dangerous. As demands on precision of aperture placement of the mirrors are very high, it is best to use periscope lines (Fig. 6), in which each corrector consists of two mirrors closely joined together.

If attenuation of a higher order wave arising as a result of irregularities is great in comparison with the degree of its excitation, a statistical analysis yields simple formulas for the mean additional losses in the principal wave at the corrector caused by lens displacement:

$$\text{[illegible]} \quad \text{dB}, \qquad (3)$$

with the rotation of individual mirrors,

$$\text{[illegible]} \quad \text{dB}, \qquad (4)$$

or with the rotation of periscope mirrors:

$$\text{[illegible]} \quad \text{dB}. \qquad (5)$$

In formulas (3-5), δ^2 is the mean square lens displacement in the plane perpendicular to the axis, and φ^2 is the mean square rotation of the mirrors (in radians). In accordance with these formulas, for instance for a confocal lens line with parameters L=30 cm and λ=1 mm, additional losses on the corrector are 0.1 dB with a mean squared lens displacement of $\sqrt{\delta^2}$=0.7 mm. In a mirror line with the same parameters, losses with a mean square deflection in a single mirror at an angle of $\sqrt{\varphi^2}$=4', are also 0.1 d3 on the mirror. In a periscope mirror line, where the distance between the centers of the double mirrors is $\bar{L}$=5 cm, the same losses will occur with an angle of incline in the double mirror system of $\sqrt{\varphi^2}$=76'. By way of illustration of the gain derived from substituting a single mirror by a

double mirror system, the results of calculations according to formulas (4) and (5) and the results of an experiment in the 8-millimetric wave range are shown in Fig. 7.

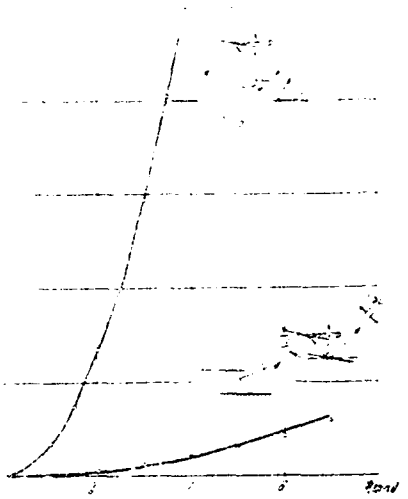

Fig. 7. Auxiliary losses in a line (L=82.5 cm, $\bar{L}$=10 cm, ν=1, λ=8 mm) for the rotation of a single mirror and a double mirror system.

From expression (3), it follows that, all other conditions being equal, losses due to transformation in a lens line are smaller as the lens focal distance f is greater. However, with increases in f (at given L and a), radiational losses in comparison with losses in a confocal system increase. For this reason, it is of great interest to find a value for f which will give the least number of overall losses (radiational losses plus transformation losses) at fixed a, L with mean square displacement values $\sqrt{\delta 2}$. The relationship between the optimal value for the variable ν=L/2f and the mean square lens displacement at various values of c is given. At δ=0, as may be expected, an optimum is achieved in a confocal system, that is, at f=L/2. In Fig. 9, overall losses in the principal wave in confocal lines and in lines with optimal variables are cited.

If the system self-filtration is small, or in other words, the lens width is great in comparison with the bundle width, then an investigation of deformation and displacement influences based on optical geometric analogies between a bundle and a ray are more effective. The movement of the center of the bundle in a line with displaced lenses obeys laws of paraxial optics. Under these conditions ($c \gg 2\gamma$), lens displacement merely causes a shift in the bundle as a whole with respect to the axis, and losses arise as a result of this only in the case when the bundle approaches near the edge of the lens or goes beyond it. At the same time,

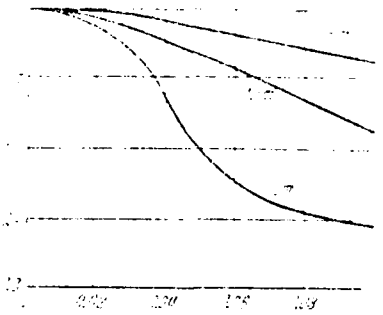

Fig. 8. Relationship between optimal value of γ and mean square lens displacement.

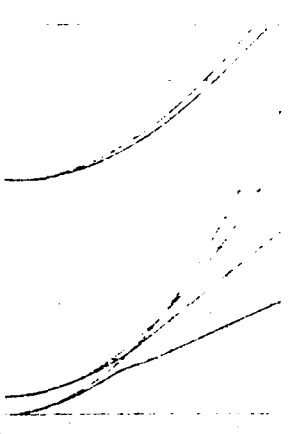

Fig. 9. Overall losses in the principal wave:

——— confocal system;

– – – system of optimal phase correctors.

it is possible to calculate the probability of projecting the bundle beyond the boundary of the line. This probability increases proportionally to the square root of the line. It will be the greatest when the focal length of the lenses is the smallest. For example, in a line consisting of 63 lenses with a mean square lens displacement equal to 0.7 mm, the possibility of projecting the bundle beyond the limits of a circle with a radius of 20 mm is equal to 0.01.

A more complete analysis, one that would make it possible to establish the probabilities for certain kinds of fixed losses in a given line, can be carried out by means of machine simulation of the process of bundle propagation in an ensemble line with an arbitrary displacement distribution.

Experiments on the transmission of millimetric and shorter waves, up to light waves, in open quasi-optical lines have only begun and are being carried out in several countries. In the theoretical aspect as well, there are many unclear problems that are being subjected to study, but a preliminary examination of these problems reveals promise in the ideas. It should be noted that in the case of lines which are not very long (lines that are only a few times greater than a^2/λ), lines made of nonhomogeneous correctors, which are possibly simpler to

adapt to receiving and transmitting terminals, are of great practical interest, and work is also being carried out in this direction.

BIBLIOGRAPHY

1. Gubo, Shvering. "Napravlennoe rasprostraneniye elektromagnitnykh volnovykh puchkov" [Directional Propagation of Electromagnetic Wave Bundles], Radio Electronics from Abroad, No. 11, 1961, p. 3.

2. Kristian, Gubo. "Eksperimental'noye issledovaniye luchevogo volnovoda dlya voln millimetrovogo diapazona" [Experimental Studies on a Beam Waveguide for Waves in the Millimetric Range], Radio Electronics from Abroad, No. 11, 1961, p. 16.

3. Katsenelenbaum, B. Z. "Kvaziopticheskiye metody formirovaniya i peredachi millimetrovykh voln" [Quasi-Optical Methods for Forming and Transmitting Millimetric Waves], Advances in the Physical Sciences, No. 1, Vol. 83, 1964, p. 81.

4. Shevchenko, V. V. "Opticheskaya liniya peredachi millimetrovykh i submillimetrovykh voln" [An Optical Transmission Line for Millimetric and Submillimetric Waves], Inventors Certificate, No. 171451 of 2 September 1963, Bulletin of Inventions, No. 8, 1962.

5. Katsenelenbaum, B. Z. "Peredacha millimetrovykh voln pre pomoshchi otrazheniy ot ryada fokusiruyushchikh zerkal" [The Transmission of Millimetric Waves Using Reflections from a Series of Focusing Mirrors], Radio Technology and Electronics, No. 9, Vol. 8, 1963, p. 1516, Bulletin of Inventions, No. 8, 1962.

6. Bondarenko, N. G., Talanov, V. I. "Nekotorye voprosy teorii kvaziopticheskikh sistem" [Several Problems in the Theory of Quasi-Optical Systems], Bulletin of Institutions of Higher Learning (Radio Physics), No. 2, Vol. 7, 1964, p. 313.

7. Vaganov, R. B., Dogadkin, A. B., Katsenelenbaum, B. Z. "Periskopicheskaya zerkal'naya liniya" [A Periscopic Mirror Line], Radio Technology and Electronics, No. 9, Vol. 10, 1965, p. 1672.

8. Valenzuela, G. R. "Millimeter: Transmission by Oversize and Shielded Beam Waveguides," IEEE Transactions, No. 5, Vol. MTT-11, 1963, p. 429.

9. Degenford, J. E., Sirkis, M. D., Steier, W. H. "The Reflecting Beam Waveguide," IEEE Internat. Conv. Rec., Part 2, 1964, p. 132.

10. Vaganov, R. B. "Poteri na preobrazovaniye v volny vysshikh tipov pri deformatsiyakh i smeshcheniyakh linz v konfokal'nom luchevode" [Losses Due to Transformation into Higher Order Type Waves in Lens Deformations and Displacements in a Confocal Light Guide], Radio Technology and Electronics, No. 11, Vol. 9, 1964, p. 1958.

THE DESIGN OF ANTENNA ARRAYS

E. G. Zelkin

One of the methods for an approximative synthesis of equidistant and nonequidistant antenna arrays is analyzed; linear and planar arrays are examined.

Introduction

Recently, great attention has been afforded to problems in the theory and practical applications of antenna arrays. The importance of investigations of these kinds of antennas is determined for the most part by the fact that they make it possible to control the radiation pattern diagram (directional pattern diagram, directivity diagram) across a wide range by means of varying the signal phase of each array element.

However, the advantages realized from applications of antenna arrays encounter substantial obstacles connected with the fact that in the formation of a narrow radiation pattern diagram, a large aperture is required, and consequently, also a large number of array elements. In fact, as is well known, for generating a narrow radiation pattern diagram that scans across a broad sector, with a small level of side lobes, it is necessary to arrange the elements in the array at a distance from each other not exceeding $\frac{\lambda}{2}$. If this condition is not fulfilled, with a beam deflection at a certain angle, quite significant side lobes arise with secondary peak values for the antenna array that are not always allowable. However, this kind of condition is practically never fulfilled, so that at the same time, the required number of elements in a planar array with a narrow radiation pattern diagram reaches several tens of thousands. The construction of these kinds of antennas becomes a decidedly complex task, and their costs are extraordinarily large. For this reason, the problem of developing controllable radiation pattern diagrams of a determined shape by means of antenna arrays with a restricted number of elements has become very important. Consequently, the basic task in designing antenna arrays is the creation of the required directivity diagrams with a minimum number of elements. The use of nonequidistant arrays, that is, arrays with nonuniform placement spans between the elements on the antenna

aperture, offer a great number of possibilities in this direction. These kinds of antenna arrays make it possible to create radiation pattern diagrams with a substantially low level of minor lobes.

The number of works that have been published dedicated to the study of the various problems in the theory of antenna arrays is quite large. Recently, a series of works has appeared showing studies carried out on nonequidistant antenna arrays. In some of them, attempts were made to develop methods for designing these kinds of arrays; however, there is to the present no general theory for the design of these kinds of nonequidistant antenna arrays.

The method for designing the kinds of antenna arrays analyzed in the present work makes it possible to determine relatively easily the placement of the antenna radiators, as well as the current magnitudes in the radiators that will assure the generation of radiation pattern diagrams sufficiently close to the required one.

We shall examine at first methods for deriving a determined radiation pattern diagram by means of equidistant arrays, and then we shall provide a solution for the same problem using nonequidistant arrays.

Planar Antenna Arrays with a Required Achievable Radiation Pattern Diagram

As is well known, the radiation pattern diagram of a system of discrete, singly polarized radiators, arbitrarily placed in a plane, is expressed by the following formula:

$$D(\Theta,\Psi) = \sum_{n=1}^{N} D_n(\Theta,\Psi)\, e^{\,j\frac{2\pi}{\lambda} d_n [\sin\Theta\cos(\Psi-\Psi_n)]}$$

where $D_n(\Theta,\Psi)$ is the radiation pattern diagram of an n-th radiator (the n-th element) of an array; N is the number of radiators; d_n is the distance of the n-th radiator up to an arbitrarily chosen point in the plane X, Y, taken as the zero point for the coordinates and called the center of the system (Fig. 1); Ψ_n is the angle between the direction towards the aiming point and the lines joining the center of the system with the center of the radiator; Θ,Ψ are the coordinate angles of the aiming point.

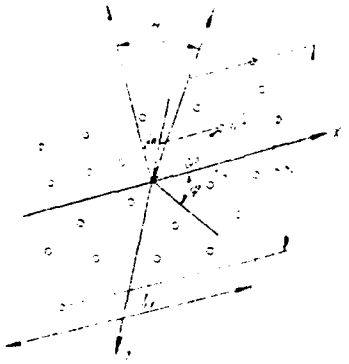

Fig. 1. Planar array of radiators. Coordinate system.

If the angular coordinate points of the placement of the n-th radiator are designated by Θ_n', ψ_n', then:

$$\cos\psi_n = \cos\Theta\cos\Theta_n' + \sin\Theta\sin\Theta_n'\cos\ldots$$

In the case under consideration here, the radiators are disposed in the same plane X, Y, and thus $\Theta_n'=\frac{\pi}{2}$. As a consequence, if we take $d_n \cos\psi_n'=x_n$, and $d_n \sin\psi_n'=y_n$, then:

$$D(\Theta,\psi)=\sum_{n=1}^{N} D_1(\Theta,\psi)\, e^{i\ldots} \qquad (2)$$

Formula (2) applies for any system of radiators, with an arbitrary shape, disposed in a plane. In this case, if the array is constituted of identical radiators with the same radiation pattern diagrams $D_1(\Theta,\psi)$, but differing from each other in current amplitude and current phase, then:

$$D(\Theta,\psi)=D_1(\Theta,\psi)\sum_{n=1}^{N} F_n e^{i\ldots} \qquad (3)$$

where $F_n=E_n e^{i\varphi_n}$ are the complex factors characterizing the amplitude and phase of an n-th radiator.

The functions $D(\Theta,\psi)$ and $D_1(\Theta,\psi)$ are taken to be known, and for that reason, the problem of designing a planar antenna array reduces to the determination from expression (3) [or (2)] of the unknown factors F_n and all the values of x_n and y_n. It is possible that this problem as well will not have a precise solution, because not every required diagram can be represented in the form of formula (3) [or (2)].

We shall examine a radiation pattern diagram in a certain plane ψ=const. At the same time, the value of $L_n(\psi)=x_n \cos\psi+y_n \sin\psi$ is also equal to a constant magnitude. It is not difficult to see that $L_n(\psi)$ is a projection of the distance from point zero, the zero point of the coordinate system, to the radiator center for a beam lying in plane X, Y and being projected from the zero point at an angle ψ. In this way, the radiation pattern diagram in the plane where $\psi=\psi_1$ is in agreement with a radiation pattern diagram of a linear array, whose radiators are placed on the X, Y plane along a straight line $\psi=\psi_1$ at the points $L_n(\psi)$:

$$D(\theta,\psi_1)=D_1(\theta,\psi_1)\sum_{n=1}^{N} e^{j\frac{2\pi}{\lambda}\sin\theta L_n(\psi_1)}. \qquad (4)$$

It follows from this that the conditions for achieving a radiation pattern diagram, as well as the methods for finding a solution to the realizable diagrams in planar arrays must be the same as for linear arrays. We transform expression (3), and we arrange the coordinate system in such a way that the abscissas of the two extreme points of the system are equal to $-\frac{l_1}{2}$ and $\frac{l_1}{2}$, and the ordinates of the two extreme points are equal to $-\frac{l_2}{2}$ and $\frac{l_2}{2}$ (Fig. 1). At the same time, we shall select a scale for the radiating system in such a way that the radiators are disposed in a square with sides equal to 2π. For this, we take $\frac{2\pi}{l_1}x_n=\nu_n$, and $\frac{2\pi}{l_2}y_n=\nu_n$. In addition, let $z_1=\frac{l_1}{\lambda}\sin\theta\cos\psi$, $z_2=\frac{l_2}{\lambda}\sin\theta\sin\psi$,

$\frac{D(\theta,\psi)}{D_1(\theta,\psi)}=R(z_1,z_2)$, and then:

$$R(z_1,z_2)=\sum_{n=1}^{N} F$$

The function $R(z_1,z_2)=\frac{D(\theta,\psi)}{D_1(\theta,\psi)}$ is called the array factor.

We shall fix one of the variables, for example z_2, and take $R(z_1,z_2)$ as a function of the same variable z_1:

$$R(z_1,z_2)=\sum_{n=1}^{N}$$

This expression is similar to the expression for the factor for a linear array of radiators. Fixing z_1 in exactly the same way, we get:

$$R(z_1,z_2)=\sum_{n=1}^{N}$$

Consequently, the function $R(z_1,z_2)$ must belong to whole, almost periodic, functions of a finite degree with indices $\sigma_1 \leq \pi$ and $\sigma_2 \leq \pi$ corresponding to each of the variables z_1 and z_2. We shall denote the class of these kinds of functions by B'_{σ_1,σ_2}.

If the array factor belongs to these functions, then the field distribution across the array that precisely reproduces it can be determined by using a double Fourier series:

$$f(x, y) = \sum_{n=-\infty}^{\infty} \sum_{m=-\infty}^{\infty} P(n, m) e^{-i(\ldots)}$$

where:

$$R(n, m) = \sum_{p=1}^{N} F_p e^{i(\ldots)}$$

In fact, changing the order of summation, we get:

$$f(x, y) = \sum_{p=1}^{N} F_p \sum_{n=-\infty}^{\infty} e^{-i n(x-\ldots)} \sum_{m=-\infty}^{\infty} e^{-i m(y-\ldots)}$$

$$= \sum_{p=1}^{N} F_p \delta(x-\ldots)\delta(y-\ldots)$$

Here, $\delta(y) = \sum_{n=-\infty}^{\infty} e^{-iny}$ is the periodic delta-function, equal to 0 for all y not equal to $\pm n\pi$ ($n=0, 1, 2\ldots$). At the points $y=\pm n\pi$, it goes to infinity, while $\int_{-\pi}^{\pi} \delta(y)dy = 1$. Consequently, $f(x, y)=f(x_p, y_p)=F_p\delta^2(0)$.

In this way, the function f(x, y), determinable by means of the double series (8), differs from the field distribution function across the array, which creates the determined array factor $R(z_1,z_2)$, only because of the presence of the factor $\delta^2(0)$. In what is to follow, this factor may be ignored.

If, however, the array factor does not belong to the class B'_{σ_1,σ_2}, then it is impossible to reproduce precisely. For its approximate calculation, it is necessary to approximate it preliminarily by means of a whole, almost periodic function of finite degree.

Insofar as the methods for solving the problems of designing a planar array are identical to methods for solving problems for linear arrays, we shall examine linear rays first of all.

Equidistant Linear Arrays

We shall take an odd number of radiators N=2n+1 and expand them along a straight line at equal distances from each other, equal to d. Then, taking $\varphi=0$, we may write expression (5) in the form:

$$R(u)=\sum_{p=-n}^{n} F_p e^{ipu}, \qquad (9)$$

where $u=hz=2\pi\frac{d}{\lambda}\sin\theta$, $h=\frac{2\pi}{\lambda}d$.

It is necessary to choose the coefficients of F_p and the number n in such a way that the right-hand member of formula (9) is the fixed function R(u) with any fixed degree of accuracy.

We shall search for a solution in the following form:

$$F_p=\frac{1}{2\pi}\sum_{m=-n}^{n} A_m e^{-ip\frac{2\pi m}{2n+1}}. \qquad (10)$$

Substituting this expression into formula (9), we find:

$$R(u)=\sum_{m=-n}^{n} A_m \frac{\sin(2n+1)\left(\frac{u}{2}-\frac{m\pi}{2n+1}\right)}{(2n+1)\sin\left(\frac{u}{2}-\frac{m\pi}{2n+1}\right)}. \qquad (11)$$

The right-hand member of the derived expression contains an interpolated trigonometric polynomial with equidistant interpolation nodes. It is not difficult to see that at the points $u=p\frac{2\pi}{2n+1}$, where p is a whole number:

$$\frac{\sin(2n+1)\left(\frac{u}{2}-\frac{m\pi}{2n+1}\right)}{(2n+1)\sin\left(\frac{u}{2}-\frac{m\pi}{2n+1}\right)}=\begin{cases}1 \text{ when } p=m\\ 0 \text{ when } p\neq m\end{cases}$$

Consequently:

$$A_m=R\left(m\frac{2\pi}{2n+1}\right).$$

The properties of the interpolated polynomial (11) have been studied quite well (see [1]). As is well known, if R(u) is a whole function, or a continuous, periodic function with a period of 2π, satisfying the Dini test, then the interpolational series (11) with a limitless increase in n will uniformly converge along the whole axis to the function R(u).

Consequently, if R(u) is an integral function or a continuous, period function satisfying the Dini test, then it may be represented approximately in the form of (11); at the same time:

$$F_1 = \frac{1}{2\pi} \sum_{-n}^{n} \dots$$

The degree of approximation of the assigned function of polynomial (11) depends on the number n, that is, on the number of radiators. The larger n, the more precisely the assigned radiation pattern diagram may be determined.

In this fashion, then, there are serious limitations to a fixed radiation pattern diagram. That is, it if is not an integral function and it does not satisfy the Dini test, then with an increase in n, the right-hand member of expression (11) will not converge to function R(u), and it is impossible to derive a good approximation of a derived radiation pattern daigram for a predetermined and fixed one. In this case, in order to improve the approximation, the fixed diagram should be approximated beforehand, as this is demonstrated in [2], with any arbitrary degree of accuracy by means of an intergral function of the form $U_m(z)P_k(z)$ $(k<2m)$, where $P_k(z)$ is a polynomial of degree k, $U_m(z)=\frac{\sin \pi z}{\pi z \prod_{p=1}^{m}\left(1-\frac{z^2}{p^2}\right)}$, after which this function should be represented approximately in the form of formula (11). Thus, series (11) will converge to the function R(u).

It should be remarked, however, that series (11) is a periodic function of the variable z with a period of 2n. For this reason, lobes equal to the magnitude of the major lobe (so-called secondary peaks) should arise across determined intervals in the variation of z in the diagram. If $2n>\frac{1}{\lambda}$, the secondary peak values will be found outside the area of actual angles.

Consequently, in order that the radiation pattern diagram have only one major lobe, the number of radiating elements in the array $N=2n+1$ should be not less than the number $\frac{1}{\lambda}$, that is, the distance between radiators should not exceed the wavelength, but with beam fluctuation, these minor lobes may arise. In this way, then, we reach the conclusion that the distance between radiators should be within the limits $\frac{\lambda}{2}\leq d<\lambda$. From this, the number of radiators in a linear, equidistant array should be of the order $2\frac{1}{\lambda}$.

Equidistant Planar Arrays

We shall examine now the case when radiators are disposed on a plane and form an orthogonal array. Let the number of radiators disposed along the same line be $N_1=2n+1$, and the number of radiators in the same column be $N_2=2m+1$. In this way, the number of elements in all in the array is $N=N_1N_2=(2n+1)(2m+1)$.

For this case, expression (5) may be written in the form:

$$R(u_1, u_2) = \sum_{p=-n}^{n} \sum_{q=-m}^{m} F_{p,q} e^{j(pu_1+qu_2)}. \qquad (14)$$

Let the distance between elements in each line be equal to d_1, and in each column, d_2. We shall introduce the following notations:

$$u_1=2\pi\frac{d_1}{\lambda}\sin\theta\cos\varphi,\quad u_2=2\pi\frac{d_2}{\lambda}\sin\theta\sin\varphi.$$

For this, $u_p z_1=pu_1$, $u_q z_2=qu_2$.

Consequently thus:

$$R'(u_1, u_2) = \sum_{p=-n}^{n} \sum_{q=-m}^{m} F_{p,q} e^{j(pu_1+qu_2)}. \qquad (15)$$

In the given case here, we shall search for a solution in the form:

$$F_{p,q} = \frac{1}{N} \sum_{k=0}^{2n} \sum_{l=0}^{2m} A_{k,l} e^{-j(kpu_1+lqu_2)}, \qquad (16)$$

where $u_1=\frac{2\pi}{2n+1}$, $u_2=\frac{2\pi}{2m+1}$.

Substituting expression (16) into (15), we get:

$$R'(u_1, u_2) = \sum_{k=0}^{2n} \sum_{l=0}^{2m} A_{k,l} \frac{\sin N_1\left(\frac{u_1}{2}-\frac{ku_1}{2}\right)\sin N_2\left(\frac{u_2}{2}-\frac{lu_2}{2}\right)}{N_1\sin\left(\frac{u_1}{2}-\frac{ku_1}{2}\right)N_2\sin\left(\frac{u_2}{2}-\frac{lu_2}{2}\right)}. \qquad (17)$$

If we take into account formula (12), it is not difficult to be convinced that $A_{k,l}=R'(ku_1, lu_2)$. Consequently:

$$F_{p,q} = \frac{1}{N} \sum_{k=0}^{2n} \sum_{l=0}^{2m} R'(ku_1, lu_2) e^{j(kpu_1+lqu_2)}.$$

If the array factor has the form:

then:

The interpolational polynomial (17) will converge to the function $R'(u_1, u_2)$ in the case when it satisfies the determined conditions which are analogous to the conditions for the linear array. The degree of approximation depends on the number of elements N_1 and N_2. The larger N_1 and N_2, the more precisely will the assigned function $R'(u_1, u_2)$ be assured, that is, all the deficiencies of a linear array are inherent to a planar array as well.

Nonequidistant Linear Arrays

Improving the approximation of a derived radiation pattern diagram to an assigned one is possible not only by means of increasing the number of radiators on a section $(-\pi, \pi)$, but also as a result of their more rational placement.

In fact, from the theory of interpolation it is well known that for purposes of improving the convergence of interpolational processes, the nodes should not be taken to be equidistant from each other, rather, they should be placed symmetrically with respect to the center of the interval, concentrating them toward its edges. Consequently, with one and the same n, better approximations will be derived with a nonequidistant array.

We shall go now to an investigation of nonequidistant arrays.

As was demonstrated in the cited work [2], functions of the class B'_σ, that is, functions representing a series of the type (6) or (7), can always be represented in the following form:

$$R(z) = R(0)\cos\pi z - \frac{z}{2\pi}\int_{-\sigma}^{\sigma} f_1(y)e^{-iyz}\,dy$$

where:

$$f_1(y) = \sum_{-\infty}^{\infty} \frac{R(n) - R(0)\cos n\pi}{-in} e^{-iny}$$

It is not difficult to note that if R(z) belongs to the class B'_σ, then $f_1(y)$ is a step function, and expression (19) may be rewritten in the form:

$$[illegible] = \frac{1}{2\pi} \sum [illegible]$$

The point at which function $f_1(y)$ has jumps are designated by S_K, and F_K is the magnitude of the jumps. In this case, the problem of synthesis may be solved exactly: the radiators must be placed at the points $y=S_K(-\pi \leq S_K \leq \pi)$. The current magnitudes in the edge radiators must be equal to $\frac{R(0)}{2} - \frac{1}{2\pi} f_1(\pi)$ and $\frac{R(0)}{2} + \frac{1}{2\pi} f_1(-\pi)$, and at the points $S_K(0<S_K<\pi)$ and F_K respectively.

We shall take a look at an example. Let $R(z)=\cos\frac{\pi z}{2}$. Then:

$$f_1(y) = \sum [illegible] \begin{cases} -\frac{\pi}{2} & \text{for } 0 < y < \pi \\ \frac{\pi}{2} & \text{for } -\pi < y < 0 \end{cases}$$

that is, $f_1(y)$ is a step function with jumps at the points π, 0, $-\pi$, with $f_1(\pi)=f_1(-\pi)=\frac{\pi}{2}$, $f_1(0)=\pi$. Consequently, the array factor $\cos\frac{\pi z}{2}$ is created by three point radiators disposed at the points $-\pi$, 0, π with current amplitudes equal to 1/4, 1/2, 1/4 respectively.

If R(z) is an integral function of finite degree, but does belong to functions of the class B'_σ, then the function $f_1(y)$ can have jumps, but in the intervals between jumps it will not be a constant and it will not be possible to represent it in the form of expression (21). The function $f_1(y)$ may be approximated with any degree of accuracy by means of a step function, and R(z) may be represented in the form of (21). For this, the right-hand member of formula (21) will approximately represent the assigned function R(z). The degree of approximation depends on the number of degrees and where they are placed. It is natural that the greater the number of degrees taken, the more precisely will function R(z) be represented by a function of class B'_σ. At the limit for an infinite number of degrees, we get a precise equivalence. It is possible to select the placement of the degrees in such a way such that the magnitudes of all the jumps of function $f_1(y)$ will be identical along the whole alternation interval y (from y=0 to $y=\pi$). For this, we derive an array with identical points in its elements; and this is easy to realize in practice and convenient for exploitation.

We shall give an evaluation of an approximation of a derived radiation pattern diagram to an assigned one.

A derived array factor may be represented in the form:

$$R'(z) = R'(0)\cos\pi z - \frac{iz}{2\pi}\int_{-1}^{1} F(y)e^{iyz}\,dy,$$

where F(y) is a jump function approximating the function $f_1(y)$. Taking formula (19) into account, it is possible to write:

$$R'(z) - R'(0)\cos\pi z = -\frac{iz}{2\pi}\int_{-1}^{1}[f_1(y) - F(y)]e^{iyz}\,dy.$$

Applying the Bunyakovskiy inequality to this equation, we get:

$$|R'(z) - R'(0)\cos\pi z| \leq \frac{|z|}{2\pi}\int_{-1}^{1}|f_1(y) - F(y)|\,dy \leq \frac{|z|}{2\pi}M,$$

where $M = |f_1(y) - F(y)|$ is the magnitude of the jump of function F(y). Consequently:

$$R'(z) = R'(0)\cos\pi z + \varepsilon(z), \qquad |\varepsilon(z)| \leq \frac{|z|}{2\pi}M.$$

This estimate is quite rough. As calculations show, in actuality, the derived approximation is significantly higher. However, this estimate shows that with small values for z, for instance, within the limits of the major lobe and several of its primary minor lobes, the approximation is quite high.

Another example. Let:

$$R(z) = \frac{\sin\frac{\pi z}{2}}{\frac{\pi z}{2}}\cdot\frac{1}{1-\left(\frac{az}{2}\right)^2},$$

where a is a certain variable.

As may be seen from this expression, R(z) is an intergral function of finite degree, restricted to the real axis, but not belonging to functions of the class $B_{\frac{1}{2}}^1$. It is possible to represent it in the form of a sum of two functions, one of which belongs to the class $B_{\frac{1}{2}}^1$, and the other to the class $W_{\frac{1}{2}}^1$. As a consequence, it is impossible to derive this radiation pattern diagram only by means of a system of point radiators. We shall attempt to do this in an approximation fashion. We shall find first the function $f_1(y)$:

$$f_1(y) = \sum_{-\infty}^{\infty}\frac{\left(\frac{2}{\pi}\right)^2\sin^2\frac{\pi}{2}n\left(\frac{1-a\pi^2}{a^2}\right)-\cos\pi n}{-1\pi}e^{-}$$

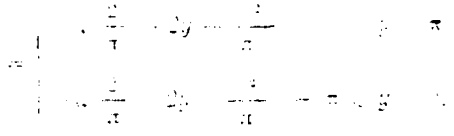

The curve of $f_1(y)$ is shown in Fig. 2. As may be seen from the figure, it has jumps at three points, $+\pi$, 0, and $-\pi$. However, in the intervals $(0, \pi)$ and $(-\pi, 0)$, it is not constant. We shall approximate $f_1(y)$ by means of a step function. We take the number of steps to be equal to 21 (10 steps on each side of

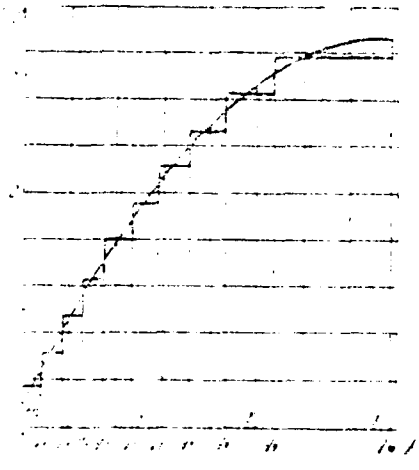

Fig. 2. An approximation of $f_1(y)$ by means of a step function.

the center of the array. We place them in such a manner that the magnitudes of all the jumps of the function are the same across the whole variation interval $f_1(y)$ from $f_1(0)$ to $f_1(\pi)$. At the point $y=0$, $f_1(y)=\frac{2}{\pi}a$, and at the points $y=\pi$, $f_1(y)$ has a maximum value equal to $\frac{2}{\pi}a+\pi$. As a consequence, the magnitude of the jumps must be equal to $\frac{f_1(\pi)-f_1(0)}{10}=\frac{\pi}{10}$. The points at which $f_1(y)$ have jumps are shown in the accompanying table.

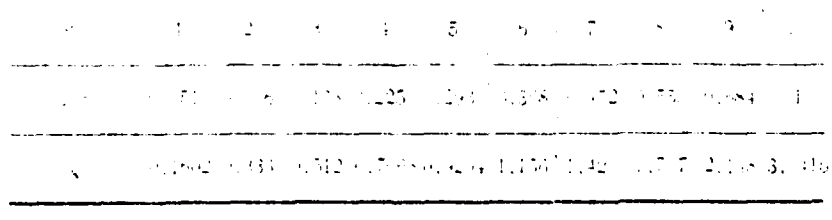

We take the magnitude of the jump of the function $f_1(y)$ at the point $y=0$ to be equal to $\frac{4a}{\pi}+\frac{\pi}{a}$, and at the points $y=\pm\pi$, to be equal to $\frac{\pi}{20}-\frac{2a}{\pi}$. At all the other points, the jumps will be the same in magnitude and equal to $\frac{\pi}{10}$. As a consequence:

Graphs of the assigned function R(z) (curve I) and the functions R*(u) approximating it (curve II) for a=0.01 are shown in Fig. 3. The diagrams are

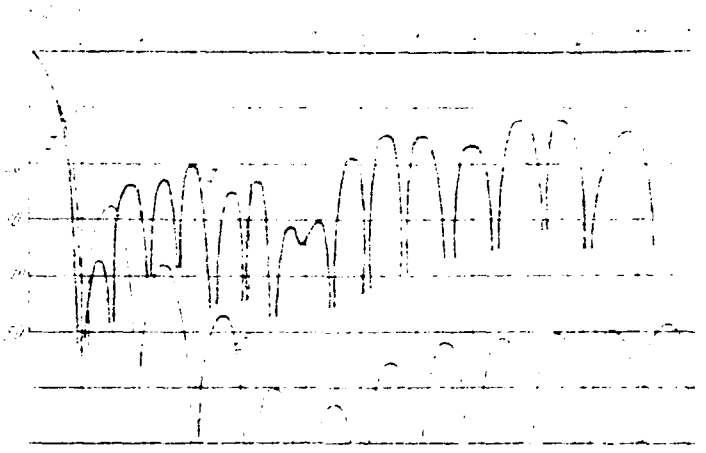

Fig. 3. Radiation pattern diagrams. I -- assigned; II -- derived.

constructed according to the field. As may be seen, a good approximation is derived for z not exceeding 4. The major lobe of the derived radiation pattern diagram is somewhat narrower than the major lobe of the assigned diagram, but the minor lobes are higher. The further minor lobes of the derived diagram are significantly higher than the corresponding minor lobes of the assigned diagram.

It should be noted that the approximation carried out here is not an optimal one. It is obvious that if the current amplitudes taken are not the same for all the array elements, but decrease from the central elements toward the edge elements, then it is possible to significantly reduce the minor lobes and approximate the derived diagram to the assigned diagram for larger values of z.

Nonequidistant Planar Arrays

The method for calculating nonequidistant linear arrays examined above can be extended also to planar, nonequidistant arrays.

In fact, it is easy to convince oneself that any function of class $B'_{\sigma,\sigma'}$ can be represented in the form:

$$R(z_1,z_2)=R_1(z_1,z_2)+R_2(z_1,z_2)+R_3(z_1,z_2)+$$

$$+\frac{1}{2\pi}\int_{-\infty}^{\infty}\int_{-\infty}^{\infty}f(x,y)\,e^{i(xz_1+yz_2)}\,dx\,dy,$$

where f(x, y) is a step function with the two variables x, y equal to: /4

$$f(x,y)=\int_{-\infty}^{\infty}\int_{-\infty}^{\infty}\frac{R(z_1,z_2)-R_1(z_1,z_2)-R_2(z_1,z_2)-R_3(z_1,z_2)}{z_1z_2}\times$$

$$\times e^{-i(xz_1+yz_2)}\,dz_1\,dz_2 \qquad (24)$$

Let, for example, $R(z_1,z_2)=\dots$ be a function

Calculating the integral of (24) for this function, we get:

$$f(x,y)=\begin{cases}\dots\\ \dots\end{cases}$$

If the function $R(z_1,z_2)$ is a sum of the form of formula (3), then $f(x, y)=F_n$ for corresponding values of x_n and y_n. If the function $R(z_1,z_2)$ does not belong to class B'_{σ_1,σ_2}, but it is an integral function of finite degree, restricted to the real axis, then f(x,y) will not be a step function; it may have jumps or steps, but in the interval between jumps its value will not be a constant. Consequently, in this case it is possible to provide an approximation of the assigned radiation pattern diagram by means of approximating f(x,y) as a step function.

If function $R(z_1,z_2)$ is fixed in the form of a function that cannot be represented in the form of expression (23), then it must be preliminarily approximated with any degree of accuracy, previously fixed, by means of a function of the form $U_{m,n}(z_1,z_2)\,P_{p,q}(z_1,z_2)$, belonging to functions of class $W_{\sigma,\sigma'}$, as this has been demonstrated in [2]. Then, using formula (24), it is necessary to determine a function f(x,y) which, in its turn, must be approximated by means of a step function. The degree of approximation of the function f(x,y) also determines the degree of approximation of the derived radiation pattern diagram to the assigned one.

BIBLIOGRAPHY

1. Akhiezer, N. I. Lektsii po teorii approksimatsii [Lectures on the Theory of Approximation]. Nauka, 1965.

2. Zelkin, E. G. Postroenive izluchayushchev sistemy po zadannoy diagramme napravlennosti [The Construction of a Radiating System According to an Assigned Radiation Pattern Diagram]. Gosenergoizdat [State Scientific and Technical Power-Engineering Publishing House], 1963.

ON THE THEORY OF MIXED PROBLEMS IN ANTENNA DESIGN AND SYNTHESIS /4

A.F. Bakanov, S.D. Krasnenitskiy

Several problems in the theory of radiation system design are examined. It is demonstrated that mixed problems in synthesis and design can be reduced to nonlinear integral equations.

The conditions for the existence of an exact solution to mixed synthesis and design problems are examined; methods for determining desired amplitude and phase distributions along a linear radiator are indicated, and it is proven that mixed problems in synthesis and design do not have unique solutions.

A unique method for calculating unknown current features in the antenna aperture is suggested for all types of mixed problems. Under some conditions assigned to the problem variables, it is proven that there is a solution and that there is convergence in the computation process.

Introduction

Normally, problems examined in the synthesis and design of radiation systems reduce to the determination of the current amplitude and phase distribution across the antenna aperture at a known vector (in the general case) radiation pattern diagram. However, it is often the case that a synthesis of only the amplitude or phase of radiation pattern diagrams is necessary, while the current amplitude or phase distribution along the antenna is assigned. In practice, these kinds of problems are encountered more and more often. A series of examples of these kinds of problems is examined in the cited work [2].

Problems, in which the amplitude or phase diagrams are fixed, as well as the current amplitude distribution and current phase distribution along the antenna, and in which it is necessary to determine the remaining two features in the diagram and in the current distribution, are called mixed problems in antenna synthesis and design. Individual questions in the theory of these kinds of problems have been investigated in a series of works [1, 2]. It is possible to distinguish the following types of mixed problems:

(1) to determine the current phase distribution along a radiator and the amplitude radiation pattern diagram realizing the fixed current amplitude

distribution along a radiator and the phase radiation pattern diagram;

(2) to determine the current amplitude distribution along a radiator and the phase radiation pattern diagram realizing a fixed amplitude radiation pattern /4
diagram and the current phase distribution along the radiator;

(3) to determine the amplitude radiation pattern diagram and the current amplitude distribution along a radiator realizing a fixed phase radiation pattern diagram and a current phase distribution along the radiator;

(4) to determine the phase radiation pattern diagram and current phase distribution along a radiator realizing a fixed amplitude radiation pattern diagram and current amplitude distribution along the radiator.

Initial Concepts

In what is to follow, for simplicity's sake, we shall consider only a linear radiator whose radiation pattern diagram can be written in the following form [1]:

$$D(\Theta) = \int_{-a}^{a} F(t) \exp i t \kappa \sin\Theta \, dt, \qquad (1)$$

where $\kappa = \frac{2\pi}{\lambda}$; λ is the wavelength at which the radiator functions.

We shall introduce a substitution for the variables: $\pi \sin\Theta = u$, $t = \frac{\lambda x}{2}$. Then the function $D(\Theta)$ is transformed into a certain function $R(u)$, and function $F(t)$ into function $f_0(x)$. After a series of noncomplex transformations, equation (1) may be reduced to the following equation:

$$R(u) \exp i\varphi(u) = \int_{-\sigma}^{\sigma} f(x) \exp i\psi(x) \exp iux \, dx, \qquad (2)$$

where the function of $f(x) = \frac{\lambda}{2} f_0(x)$; $2\sigma = \frac{4a}{\lambda}$ is the electric length of the radiator; $\varphi(u)$ is the phase radiation pattern diagram; $\psi(x)$ is the current phase distribution in the radiator.

We shall assume that function $R(u)$ belongs to the class W_σ (this does not disturb the generality of the comments here, inasmuch as all radiation pattern

diagrams that can be realized belong to this class). Then, in accordance with the Wiener-Paley theorem [3], the following equation holds:

$$2\pi\int_{-\infty}^{\infty}|R(u)|^2\,du=\int_{-\sigma}^{\sigma}|\varphi(x)|^2\,dx<\infty. \qquad (3)$$

It should be noted that for functions of the class W_2, the following inequality is derived from equation (3):

$$\int_{-\infty}^{\infty}|R(u)|\,du<\infty;\quad \int_{-\sigma}^{\sigma}|f(x)|\,dx<\infty. \qquad (4)$$

As is well known, under the conditions indicated above, the function of the amplitude-phase distribution of current along a radiator is determined from the following formula:

$$f(x)\exp i\varphi(x)=\int_{-\infty}^{\infty}R(u)\exp i\varphi(u)\exp -iux\,du. \qquad (5)$$

while outside the segment $[-\sigma,\sigma]$ $f(x)\equiv 0$.

Equations (2) and (5) are baseline equations in considerations of questions in the theory of mixed problems in the synthesis and design of radiating systems. Consequently, the four types of mixed problems indicated in the introduction reduce mathematically to the following:

(1) known functions $\varphi(u)$ and $f(x)$; it is necessary to find the function $\psi(x)$;
(2) the functions $R(u)$ and $\psi(x)$ are known, and it is necessary to find the function $f(x)$;
(3) the functions $\varphi(u)$ and $\psi(x)$ are known, and it is necessary to find the function $f(x)$;
(4) the functions $R(u)$ and $f(x)$ are known, and it is necessary to find the function $\psi(x)$.

We shall demonstrate that the solution to each of these problems may be represented as a solution either of a system of integral equations, or as a solution of a linear integral equation. With this end in mind, we shall transform expression (2) into the following equation:

$$R(u)=\int_{-\sigma}^{\sigma}f(x)\exp i[\psi(x)-\varphi(u)-ux]\,dx. \qquad (6)$$

which, after separating the real and imaginary portions, makes it possible to reduce the consideration of all types of the mixed problems to a consideration of the following system of integral equations with two unknown functions:

$$\left.\begin{aligned}\int_{-\infty}^{\infty} f(x)\cos[\varphi(x)-\psi(u)-ux]\,dx &= R(u)\\ \int_{-\infty}^{\infty} f(x)\sin[\varphi(x)-\psi(u)-ux]\,dx &= 0\end{aligned}\right| \qquad (7)$$

As a result of similar calculations, formula (5) can also be represented as a system of equations:

$$\left.\begin{aligned}\int_{-\infty}^{\infty} R(u)\cos[\psi(u)-\varphi(x)-ux]\,du &= f(x)\\ \int_{-\infty}^{\infty} R(u)\sin[\psi(u)-\varphi(x)-ux]\,du &= 0\end{aligned}\right| \qquad (8)$$

The reduction of mixed problems to systems of integral equations is also convenient from the point of view that these systems may be solved with the aid of approximate methods in numerical analysis, which will not be examined here. One of these kinds of approximative methods is cited in work [11]. It is a simple matter to see that equation (2), after simple transformations, can be written in the form of the following system of equations:

$$\left.\begin{aligned}R(u)\cos\psi(u) &= \int_{-\infty}^{\infty} f(x)\cos[\varphi(x)-ux]\,dx\\ R(u)\sin\psi(u) &= \int_{-\infty}^{\infty} f(x)\sin[\varphi(x)-ux]\,dx\end{aligned}\right| \qquad (9)$$

and equation (5) is equivalent to the following kind of system of equations:

$$\left.\begin{aligned}f(x)\cos\varphi(x) &= \int_{-\infty}^{\infty} R(u)\cos[\psi(u)-ux]\,du\\ f(x)\sin\varphi(x) &= \int_{-\infty}^{\infty} R(u)\sin[\psi(u)-ux]\,du\end{aligned}\right| \qquad (10)$$

We shall examine in more detail the reduction of problem 1 into a nonlinear, integral equation, with the reduction method for the other problems to integral equations being similar. Multiplying equations (9) by sin $\phi(u)$ and cos $\phi(u)$ respectively, and assuming that sin $\phi(u)\neq 0$ and that cos $\phi(u)\neq 0$, after transformation we get:

$$\int_{-\infty}^{\infty} f(x)\sin[\psi(u)-\varphi(x)-ux]\,dx = 0. \qquad (11)$$

In the case when $\sin \varphi(u) \equiv 0 [\varphi(u) = \pi k$, where $k=0, 1, 2]$, or $\cos \varphi(u) \equiv 0 [\varphi(u) = \frac{\pi}{2} + \pi k$, where $k=0, \pm 1]$, it is also a simple matter to be convinced that from equation (11) one of the nonlinear equations of system (9) drops out, and when they are solved, it is possible to find the current phase distribution along the antenna. Equation (11) is a nonlinear, integral equation with respect to the unknown function $\varphi(x)$. By means of similar considerations, it is possible to demonstrate that problem 2 reduces to the following nonlinear integral equation with respect to $\varphi(u)$:

$$\int_{-\infty}^{\infty} R(u) \sin [\varphi(u) - \psi(x) - ux] du = 0. \qquad (12)$$

It is clear that if as a result of the solution to equation (12) a function $\varphi(u)$ is found, then from equation (5) the function $f(x)$ will be determined easily, and as a result, problem 2 will be solved. Problem 3, as it is clearly seen, can also be reduced to a solution of equation (11), which with respect to the desired function $f(x)$, is nonlinear. And, finally, problem 4 reduces to a nonlinear, integral equation after simple transformations, which is different from the foregoing ones, that is:

$$R^2(u) = \left| \int_{-\infty}^{\infty} f(x) \cos [\psi(x) - ux] dx \right|^2 + \left| \int_{-\infty}^{\infty} f(x) \sin [\psi(x) - ux] dx \right|^2. \qquad (13)$$

Equations (11), (12), and (13) may be written in the operational form:

$$P(X) = 0, \qquad (14)$$

where P is the integral operator corresponding to the equations, and X is the function sought.

The Solution to the Operational Equation P(X)=0

Let G be a measurable set of finite or infinite cardinality. It is possible to demonstrate [4] that the aggregate of all continuous real functions $\alpha(x)$ on G forms a Banach space E_1, if the norm $\alpha(x)$ is set by the equation:

$$\|\alpha(x)\| = \sup_{x \in G} |\alpha(x)|.$$

It is possible to show in the same way that the aggregate of all continuous real functions $\beta(u) = P\{\alpha(x)\}$ on G forms a Banach space E_2, if we assign the norm $\beta(u)$ by the equation:

It is possible to prove by using the theory of operators [5] that the operator P(X) determined above acts out of the space E_1 into the space E_2. Then equation (14) is solved by means of a single step method of constructing a series that converges to its solution:

$$X_{n+1} = X_n - A_n(X_n)$$

where A_n is a certain operator acting out of space E_1 into space E_2.

The justification for this suggestion is grounded on a series of theorems [4, 5, 10], which make it possible to indicate several conditions that are sufficient for the existence of an exact solution to mixed problems of synthesis and design. It follows from the formulations of the majority of theorems indicated that the important features for their applicability in the case under consideration here is proving the differentiability (according to Fréchet) of the operator P(X) and the fulfillment of the Lipschitz condition for the derivative P'(X) [6, 7, 8]:

$$\|P'(X_1) - P'(Y_1)\| \leq L\|X - Y\|,$$

where L is some constant not depending on X and Y.

The fulfillment of the other requirements of the theorem is assured by a suitable selection of an auxiliary operator $A_n(X_n)$ and an initial approximation X_0. In calculations, it is often the case that it is convenient to take the operator BP(X) for the $A_n(X_n)$ operator: $A_n(X)=BP(X)$, where B is a linear operator acting out of the space E_2 into E_1. /5

If, in particular, $B=[P'(X_0)]^{-1}$, then the series (15) gives a modified Newton method; if, however, $E_2=E_1$ and $B=\alpha I$, where I is a unique operator, then a method of sequential approximations is forthcoming [4].

The Correctness of Mixed Problems in Synthesis and Design

In considering mixed problems in the synthesis of radiating systems for the determination of desired current amplitude and current phase characteristics in

a radiator, it is not equations (2) and (5) that were used, but the integral equations of the form P(X)=0 arising out of them. For this reason, it is necessary to make clear whether or not the solutions found for this equation satisfy the initial integral equations (2) and (5). For concreteness, we shall consider problem 2 and prove that the function $\bar{\varphi}(u)$ derived from equation (12), together with the assigned functions R(u) and $\psi(x)$ satisfy the initial integral equations.

We shall suggest that the phase radiation pattern diagram $\bar{\varphi}(u)$ determines, after it is substituted into equation (13), a second current distribution $f_1(x)$ and a second current phase distribution $\psi_1(x)$ in the radiator. Then, after some simple transformations, it is possible to reduce equation (5) to the following form:

$$\int_{-\infty}^{\infty} R(u)\sin\left[\bar{\varphi}(u)-\psi_1(x)-ux\right]du=0. \qquad (16)$$

As $\bar{\varphi}(x)$ is a solution to equation (12), the following relationship also holds:

$$\int_{-\infty}^{\infty} R(u)\sin\left[\bar{\varphi}(u)-\psi(x)-ux\right]du=0. \qquad (17)$$

After adding and subtracting termwise equations (16) and (17), and after elementary transformations, we arrive at:

$$\int_{-\infty}^{\infty} R(u)\sin\left[\bar{\varphi}(u)-\frac{\psi(x)+\psi_1(x)}{2}-ux\right]\cos\frac{\psi(x)-\psi_1(x)}{2}du=0,$$

$$\int_{-\infty}^{\infty} R(u)\cos\left[\bar{\varphi}(u)-\frac{\psi(x)+\psi_1(x)}{2}-ux\right]\sin\frac{\psi(x)-\psi_1(x)}{2}du=0.$$

Taking into consideration that $\cos\frac{\psi(x)-\psi_1(x)}{2}\neq 0$, and that $\sin\frac{\psi(x)-\psi_1(x)}{2}\neq 0$, /5
we can write:

$$\int_{-\infty}^{\infty} R(u)\sin\left[\bar{\varphi}(u)-\frac{\psi(x)+\psi_1(x)}{2}-ux\right]du=0,$$

$$\int_{-\infty}^{\infty} R(u)\cos\left[\bar{\varphi}(u)-\frac{\psi(x)+\psi_1(x)}{2}-ux\right]du=0.$$

Multiplying both members of equation (18) by i and adding both equations termwise, we receive after a series of computations:

$$\exp\left[-i\frac{\psi(x)+\psi_1(x)}{2}\right]\int_{-\infty}^{\infty} R(u)\exp\left[i\bar{\varphi}(u)-iux\right]du=0.$$

The left-hand member of equation (20) may be considered to be a radiation pattern diagram of a radiator with an amplitude distribution of R(u) and a phase distribution of $\psi(u)$. From physical considerations, it is clear that it may be identical to zero only in the case when $R(u)\equiv 0$, which has no physical sense. In this way, the solution $\bar{\psi}(u)$ of equation (12) is the solution for problem 2 in the synthesis of a radiator. We should note that if $\sin\frac{\psi(x)-\psi_1(x)}{2}\equiv 0$, then $\psi(x)=\psi_1(x)\pm 2\pi k (k=0\pm 1)$. But this means that physically, by means of the solution $\bar{\psi}(u)$, one and the same current phase distribution is realized in the radiator. If $\cos\frac{\psi(x)-\psi_1(x)}{2}\equiv 0$, then $\psi(x)=\psi_1(x)\pm\pi$. In this case, as one may easily be convinced, problem 2 may be resolved by means of a simple substitution of the value of $\psi(x)$ into equation (2), if equation (12) has a solution $\bar{\psi}(u)\pm\pi$, and if, obviously, it has this solution. Thus, the determination of the function $\bar{\psi}(u)$ completely resolves the mixed problem 2 in the synthesis of a radiator. In the same way, it may be demonstrated that solutions to equations (11), (12), and (13) are also solutions to the corresponding mixed synthesis problems.

It is interesting to note that the theorem presented in [10], when all requirements indicated are met, yields the possibility of finding the necessary current amplitude and current phase distribution along a radiator that realize the assigned radiation pattern diagram, but they do not guarantee the uniqueness of the distributions found in this way. As is well known, nonlinear integral equations, speaking in general, do not have unique solutions; this has also been observed in the kinds of synthesis problems under consideration here. In fact, if attempts are made to synthesize or design an antenna with a phase radiation diagram equal to zero, that is:

$$\varphi(u)\equiv 0,$$

under the condition that the current amplitude distribution along the antenna is a positive function with respect to the zero point of the selected coordinate system, then a synthesis of the desired radiation system can be carried out if the current phase distribution along the radiator can be realized physically in the form of any odd function. In this case:

$$\int_{-l}^{l} f(x)\sin[-\psi(x)-ux]\,dx=-\int_{-l}^{l} f(x)\sin[\psi(x)-ux]\,dx=0,$$

when $\sin|\psi(-x)+u(-x)|=-\sin|\psi(x)+ux|$. A similar situation may be observed, for example, in the synthesis of an antenna with a positive amplitude radiation pattern

diagram $R(u)$ and a current phase distribution in the radiator $\varphi(x)\equiv 0$. We shall produce a synthesis if one of the infinite set of the following current amplitude distributions can be practically realized in the antenna:

$$f(x) = \int_{-\infty}^{\infty} R(u)\exp\left[i(\varphi(u) - ux)\right] du,$$

where $\varphi(u)$ is any arbitrary odd function with respect to the coordinate system zero point.

Calculations of concrete current distributions corresponding to this case can be found in the work cited [1]. Finally, by means of a direct substitution in equation (13), it is possible to convince oneself that if $\bar{\varphi}(x)$ resolves the mixed synthesis problem number 4, then any current phase distribution along the radiator of a form:

$$\varphi(x) = \bar{\varphi}(x) + \varphi_0,$$

where φ_0 is an arbitrary constant, will also resolve this problem.

From what has been explained above, it follows that mixed synthesis problems of radiation systems, in the absence of the normal kinds of synthesis problems considered, have (in the case when they are realizable), generally speaking, no unique solutions. The questions in the theory of mixed synthesis problems under determined conditions examined in the present work may be generalized also for a two-dimensional radiating system, and also for systems of discrete radiators (with the help of the Stieltjes integral).

In conclusion, we should note that the integral equation (12), corresponding to problem 3, is linear, and for that reason, after transforming it into an equation with a symmetrical core:

$$\int_{-l}^{l} f(x) K(z, x)\, dx = 0.$$

where:

$$K(z, x) = \int_{-\infty}^{\infty} \sin\left[\varphi(u) - \varphi(x) - ux\right] \sin\left[\varphi(u) - \varphi(z) - uz\right] du,$$

it is possible to apply the following recurrent series for determining a desired function of current amplitude distribution (if a solution exists) [9]:

where $\lambda > 0$, $\Omega \subset R^n$, and λ_1 is the smallest characteristic number of the nucleus $K(x,s)$.

1. Belkin, E. C. Postroenive izluchayushchey sistemy po zadannov diagramme napravlennosti [The Construction of a Radiating System with an Assigned Radiation Pattern]. Gosenergoizdat [State Scientific and Technical Power-Engineering Publishing House], 1962.

2. _____. "Fazovaya digramma napravlennosti i zadacha sinteza antenn" [Phase Radiation Pattern Diagrams and the Problem of Antenna Synthesis and Design], Radio Technology and Electronics, No. 1, Vol. 8, 1963.

3. Levin, B. Ya. Raspredeleniye korney tselykh funktsiy [The Distribution of Roots of Integral Functions]. Gostekhizdat [State Publishing House of Technical and Theoretical Literature], 1956.

4. Kantorovich, L. V., Akilov, G. P. Funktsional'nyy analyz v normirovannykh prostranstvakh [Functional Analysis in Normed Spaces]. Fizmatgiz [State Publishing House of Literature on Physics and Mathematics], 1959.

5. Krasnocel'skiy, M. A. Topologicheskiye metody v teorii nelineynykh integral'nykh uravneniy [Topological Methods in the Theory of Nonlinear Integral Equations]. Gostekhizdat, 1956.

6. Vaynberg, M. M. Variatsionnye metody issledovaniy nelineynykh operatorov [Variational Methods in the Study of Nonlinear Operators]. Gostekhizdat, 1956.

7. _____. "Nekotorye voprosy differentsial'nogo ischisleniya v lineynykh prostranstvakh" [Some Problems in Differential Calculus in Linear Spaces], Advances in the Mathematical Sciences, No. 4, Vol. 7, 1952.

8. Marinescu, G. "Asupra diferentialei si derivatei in spatile normate" [translation from Romanian unknown], Bull. stunt Academy R. R. Romane, Sect mat si fiz 6, No. 2, Vol. 6, 1954, pp. 213-219.

9. Fridman, V. M. "Metod posledovatel'nykh priblizheniy dlya integral'nogo uravneniya Fredgol'ma 1 roda" [A Method of Series Approximations for an Integral Fredholm Equation of the First Kind], Advances in the Mathematical Sciences, No. 1, Vol. 11, 1956, p. 67.

10. Polyak, B. T. "Gradientnye metody resheniya uravneniya i neravenstv" [Gradient Methods in Solving Equations and Inequalities], The Journal of Computational Mathematics and Mathematical Physics, No. 6, Vol. 4, 1964.

ON A METHOD OF STUDYING BINARY SOURCES OF RADIOFREQUENCY RADIATION WITH THE AID OF AN INTERFEROMETER /5

A. A. Pistol'kors

A methodology for studying binary sources of extraterrestrial radiofrequency emissions is analyzed; the methodology is based on the theory of the complex coefficient of Zernike coherence and on the application of an interferometer with a phase shifter. Methods for determining the angular distance between the sources are examined, as well as the ratio of their intensities and their relative positions.

Introduction

Two methods are used for studying the structure of complex extraterrestrial radiofrequency sources. One of them is based on the apparent retardation in the source as it passes across the meridian [1]. In the second method, suggested by Jennison [2], a triple-antenna interferometer is used. Both methods are quite complex.

In the present article, a particular case of the complex structure is studied, that is, binary sources. A comparatively simple method may be suggested for measuring their parameters. It is based on an analysis of the complex coefficient of fluctuation coherence in the interferometer antennas corresponding to the sources [3] and on the experimental determination of the magnitudes characterizing this coefficient. This latter is connected with a luminance distribution in the source by means of a Fourier transformation.

Assuming the sources to be point sources, we will look for an angular separation between them, the ratio between the source intensities, and their positions with respect to each other.

The Coefficient of Coherence for the Case of Binary Sources

Let at the points P_1 and P_2 on the Earth's surface (we shall take it to be flat) antennas 1 and 2 of an interferometer be set up with a base d (Fig. 1). At point Q in the feeder line, a receiver is hooked in. The intensity of fluctuations arising at input is ([4], p. 507):

$$I(Q) = I_1(Q) + I_2(Q) + 2\sqrt{I_1(Q)I_2(Q)}\,|\gamma_{12}|\cos(\beta_{12} - \delta). \qquad (1)$$

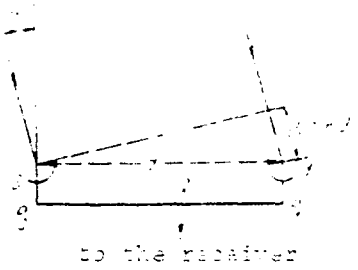

Fig. 1. Diagram of a double-antenna interferometer.

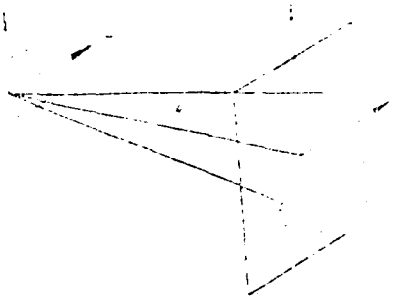

Fig. 2. On calculating the intensity of fluctuations at the interferometer output.

Here, $I_1(Q)$ and $I_2(Q)$ are the intensities of the fluctuations picked up individually by the first and second interferometer antennas; $\gamma_{12} = |\gamma_{12}|e^{-i\beta_{12}}$ is the complex coefficient of the fluctuation coherence at points P_1 and P_2; δ is the phase shift corresponding to the difference in the passage of the waves along the feeder from the antennas to the place where the receiver is connected. /3

Expression (1) is good for small shifts across time τ in the signals picked up by both antennas and combined at point Q, when:

$$\tau \ll \frac{1}{\Delta f},$$

where Δf is the bandwidth of the frequencies picked up.

We shall examine first of all a source near the zenith. Let this source be disposed on a plane σ with a coordinate system $\xi o \eta$, and let there be a parallel surface A, in which the interferometer is disposed (Fig. 2). The distance between the surfaces is designated by R, and we construct on surface A a coordinate system XoY, whose axis is parallel to the axes of $\xi o \eta$, with the zero point lying normal to oO. Then, according to the Van-Zittert and Zernike theorem ([4], p. 510):

$$\gamma_{12} = e^{i\varphi}\frac{\int\int_{\sigma} I(\xi,\eta)e^{-i\varkappa(\rho_2 - \rho_1)}\,d\xi\,d\eta}{\int\int_{\sigma} I(\xi,\eta)\,d\xi\,d\eta}. \qquad (2)$$

Where $\varkappa = \frac{2\pi}{\bar{\lambda}}$, where $\bar{\lambda}$ is the mean wavelength of the noise radiation picked up; φ is the phase difference in fluctuations arriving at points P_1 and P_2 from the zero point in the coordinate system $\xi o \eta$, equal to $\frac{2\pi}{\lambda}(oP_1 - oP_2)$; $I(\xi,\eta)$ is the

function of luminous distribution on the source surface:

$$x = \frac{x_1 - x_2}{\lambda}, \quad y = \frac{y_1 - y_2}{\lambda}$$

where x_1, y_1, and x_2, y_2 are the coordinates of the points P_1 and P_2.

In what is to follow, we shall call the magnitude μ'_{12} the nucleus of the coefficient of coherence. The nucleus μ'_{12} does not depend on the positioning of the interferometer antennas; it only depends on the projection of the base of the interferometer antennas onto the x-axis (with a magnitude of p) and y-axis (with a magnitude of q). We shall dispose the point P_1 and P_2 along the x-axis. Then $x_1-x_2=d$ (if $x_1>x_2$) and $p\frac{d\xi}{R}=d\nu$, where φ is the angle formed by the direction from point O onto the abscissa of the point $\xi\eta$ with the normal to the surfaces Σ and A; at the same time, q=0. Let the coordinates of the point sources be respectively $\xi_1\eta_1$ and $\xi_2\eta_2$, and their intensities be respectively a and b.

We shall choose the zero point of the coordinate system $\xi O\eta$ in such a way that $\nu_1=\frac{\xi_1}{R}=-\nu$, and $\nu_2=\nu$ (Fig. 3). Then, the projection of the angular distance between the sources onto the surface ξO will be 2ν, and the nucleus is:

$$\mu'_{12} = \frac{ae^{i\kappa d\nu} + be^{-i\kappa d\nu}}{a+b} = \frac{(a+b)\cos\kappa d\nu + i(a-b)\sin\kappa d\nu}{a+b} =$$

$$= \cos\kappa d\nu - i\frac{a-b}{a+b}\sin\kappa d\nu. \qquad (4)$$

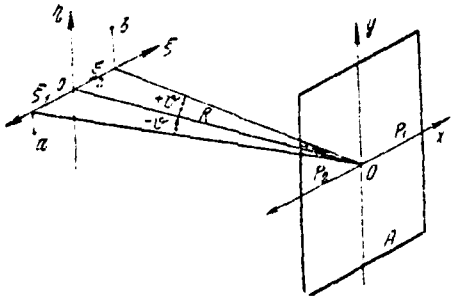

Fig. 3. On calculating the nucleus of the coefficient of coherence.

The nucleus of the coefficient of coherence μ'_{12}, as it is a function of the electric length κd, describes a picture of field voltage distribution in the interference bands on the surface A, with the interference bands corresponding to the pair of sources under consideration here, not in terms of their intensities,

but in terms of the points a and b.

We take into consideration the periodic 24-hour movement of the source, fixing its position on surface Σ and shifting the base of the interferometer along the x-axis, a parallel line from east to west. However, because the nucleus γ_{12} does not depend on the positioning of the base, it is possible to study the interferometer, one antenna of which is always located at the zero point of the coordinate system XOY, and the second antenna of which shifts. Subtracting the electric length $\omega\tau$ along the OX-axis from the zero point of the coordinate system, we derive maximums for the interference bands at $\cos \omega\tau = \pm 1$ and minimums at $\sin \omega\tau = \pm 1$. The field voltage phase on surface A depends on the magnitude $\omega\tau$, as well as on the sign of the difference between a-b.

If it would be possible to explain the picture of interference bands mentioned above by means of measurements, it would be possible to determine by means of this the parameters for the sources a and b.

Up to the present time, a radiofrequency source has been studied close to the zenith. Conclusions drawn for it are easily extended to the case of any position for the source. They will remain justified if we take the projection of the angular separation between the constituent binary sources onto the orientation of the interferometer base at an angle of 2π.

The Current on the Output of an Interferometer with a Phase Shifter

We take $I_1(Q)=M(a+b)$ and $I_2(Q)=N(a+b)$. Then, expression (1) may be written in the form:

$$I(Q) = M + N(a+b) + 2\sqrt{MN}(a+b)\gamma_{12}\cos(\beta_{12} - \beta_1 - \dots)$$

We note also that:

$$\gamma_{12}\cos(\beta_{12} - \beta_1) = \mathrm{Re}\,\gamma_{12}e^{-i(\beta_{12}-\beta_1)} = \mathrm{Re}\,\gamma_{12}e^{-i\gamma} = \dots$$

where $\gamma=\phi+\delta$.

The measurement method suggested here is based on a shift in the lobes of the interferometer diagram. The methods for this kind of shift using phase shifters

were suggested by Payne-Scott and Little [5] as well as by Hanbury.Brown, Palmer, and Thompson [6]. They use interferometers at the present state of the art [7].

With a translation of the source together with the sky profile, the phase shift φ in the signals arriving from point o on the surface to antennas 1 and 2 decreases. For this reason, $\varphi = -\omega_D t$, where:

$$\omega_D = \omega_E \frac{l}{\lambda} \cos\delta \cos\alpha \quad [illegible]$$

Here, ω_E is the angular velocity corresponding to the Earth's rotation; δ is the source declination; α is the angle between the base and the east-west line.

Using a phase shifter, it is possible to derive the frequency of the output current:

$$\Omega = \omega_D \pm \omega_\Phi [illegible]$$

where ω_Φ is the phase shifter frequency.

Then:

$$\varphi_{12} e^{[illegible]} = \frac{[illegible]}{a+b}, \quad [illegible]$$

and expression (5) takes the following form: /6

$$I(\Omega) = (M + N)(a + b) + 2\sqrt{MN}[(a - b)\cos\kappa dv \cos\Omega t +$$
$$+ (a - b)\sin\kappa dv \sin\Omega t]. \quad (10)$$

The current amplitude I_Ω of the frequency Ω is proportional to:

$$\sqrt{(a-b)^2\cos^2\kappa dv + (a-b)^2\sin^2\kappa dv} = \sqrt{a^2+b^2-2ab\cos 2\kappa dv}, \quad (11)$$

and its phase ψ is determined by means of the equation:

$$\operatorname{tg}\psi = \frac{a-b}{a+b}\operatorname{tg}\kappa dv. \quad (12)$$

Determining the Angular Separation Between the Sources

In order to determine the angular separation $2v$, it is necessary to know the period of the interference bands on the Earth mentioned above. In order to find this period, it is sufficient, by varying the base d, to determine the distance between the pole maximum and the nearest minimum. We shall substitute variations

in the distance between the antennas with variations in the reception frequency.

In the frequency range under consideration here, we find at first the frequency ω_1, giving a maximum value to the picked-up power. For this, it is necessary that:

$$2\kappa_1 d\vartheta = 2p\pi, \qquad (12)$$

where p is a whole number.

Then, we search for a frequency ω_2, larger or smaller than ω_1, at which the power received from the binary source has a minimum value. It is clear that:

$$2\kappa_2 d\vartheta = (2p \pm 1)\pi, \qquad (14)$$

from which:

$$2\vartheta = \frac{1}{m_2 - m_1} \qquad (15)$$

where $m_i = \frac{d}{\lambda_i}$.

The distance d between the antennas must be taken beforehand to be sufficiently large, in order that at a fixed maximum frequency dispersion between ω_1 and ω_2, the measurement of the determined minimum angular separation between the sources will be assured. Thus, for a minimum angular separation of $2\vartheta = 1' = 0.291 \cdot 10^{-3}$ rad, at p=5, $m_1 = \frac{5}{2 \cdot 0.291} = \frac{5,000}{2 \cdot 0.291} = 8,600$. It is clear that $m_2 = 8,600 \pm 860$, that is, $m_2 = 9,460$, or $m_2 = 7,740$.

Taking $m_2 > m_1$, we get for a mean frequency ω_0: $m_0 = 9,030$. Consequently, $\frac{\omega_2 - \omega_1}{\omega_0} \approx 0.095$.

The distance between the interferometer antennas is determined by a fixed minimum angular separation $2\vartheta_{min}$ for the measurement and a frequency dispersion of f_1 and f_2. From expressions (13) and (14), it follows that:

$$\frac{f_1}{2f_2 - f_1} = p,$$

where p is a whole number.

On the other hand, from expression (13), it follows that:

$$m_1 = \frac{d}{\lambda_1} = \frac{c}{2\vartheta_{min} f_1} = \frac{1}{2\vartheta_{min}} \cdot \frac{f_2}{2f_2 - f_1}.$$

For measuring the angular separation 2ν between the components of the binary system, it is necessary to know, although even only in an approximate way, the curve of amplification in the system "interferometer antenna-receiver" within the frequency range f_1-f_2, in order to be able to find correctly the frequencies of the maximum and minimum of the picked-up energy. This curve, naturally, should not have sections with great steepness.

Determining the Ratio of the Source Intensities

In order to find the relationship of the intensities a and b of the sources, it is sufficient to find the ratio of the field voltage minimum of the interference bands on Earth (the field voltage proportional to $|a-b|$) to the field voltage maximum (proportional to a+b). For this, it is necessary to know the ratio of the amplification of the system "antenna-receiver" at the frequencies mentioned above ω_1 and ω_2, and with a large dispersion of these frequencies, to know also the relationship of the source radiation intensity to the frequency at the pertinent frequencies.

We shall denote a correction factor, which takes into account the joint effects of the factors mentioned above, by means of $\frac{q_1}{q_2}$. Comparing the current amplitudes I_1 and I_2 at the frequencies ω_1 and ω_2, and noting that $I_1 \sim (a+b)q_1$ and $I_2 \sim |a-b|q_2$, we find:

$$\frac{\text{intensity of the weak source}}{\text{intensity of the strong source}} = \frac{1-\frac{f_1}{f_2}\frac{\nu}{D}}{1-\frac{f_2}{f_1}\frac{\nu}{D}}.$$

In order to explain which of the sources a and b is the weaker, it is necessary to determine the sign of the imaginary portion of the nucleus of the coherence coefficient u'_{12}; this requires special measurements.

Below we shall cite yet one more method for measuring the ratio of source intensities.

Determining the Mutual Positionings of Sources with Different Intensities

As has already been indicated, for this it is necessary to determine the sign of the difference a-b; this can be carried out by means of elucidating the relationship between the phase of the current I_2 and the observation conditions.

Measurements may be carried out in several ways; they all require the presence of two channels connected in parallel to the antennas of an interferometer (Fig. 4), and phase shifts between the currents I_1 and I_2, which must be compared as well.

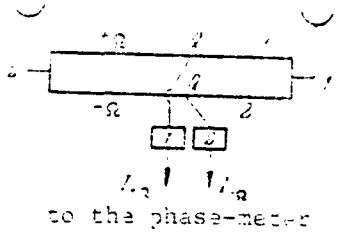

Fig. 4. Diagram of an interferometer with two channels for determining the mutual positionings of sources with different intensities.

Thus, channel 1 can be used for receiving at frequency ω_1, corresponding to the maximum of the interference bands, and channel 2 for receiving at frequencies $\omega_2>\omega_1$, corresponding to the minimum of the bands. Then:

$$\left.\begin{aligned} i_{21} &= a_1(a-b)\cos\Omega t \\ i_{22} &= a_2(a-b)\sin\Omega t \end{aligned}\right\} \quad (19)$$

The phase shifts between the points i_{21} and i_{22} must be $\pm\frac{\pi}{2}$. The purpose for the measurements is to establish the sign of this shift and to determine the sign of a-b. The phase of the lobes in the interferometer diagram can vary with a frequency Ω on the order of 25-50 Hz. At these frequencies, the phase shifts of two currents may be measured sufficiently accurately. In this case, the following method may be suggested. Let the phase shifter in channel 1 maintain a frequency Ω, and in channel 2 the phase shifter maintain a frequency of Ω, corresponding to the displacement of the lobes of the diagram to the opposite side. For measurements, it is most convenient of all to take the frequency at which $\cos \kappa d\upsilon = \pm\sin \kappa d\upsilon$. We shall consider further the case corresponding to a positive sign, as this takes place for the mean frequency ω_0 in the numerical example cited. For this case:

$$\left.\begin{aligned} i_{21} &= C[(a-b)\cos\Omega t - (a-b)\sin\Omega t] \\ i_{22} &= C[(a-b)\cos\Omega t - (a-b)\sin\Omega t] \end{aligned}\right\} \quad (20)$$

where C is the coefficient of proportionality.

We shall find the phase ψ of the current i_{22} according to the ratio to i_{21}; then:

$$\operatorname{tg}\frac{\psi}{2} = -\frac{a-b}{a+b}, \quad (21)$$

which yields the possibility of determining not only the sign of the difference a-b, but also the ratio $\frac{b}{a}$, which in the given instance can be greater than unity (at $\vartheta>0$).

Supplementary Remarks

It has been presumed up to the present time that a shift across the time τ of two signals combined at point Q is small and satisfies the inequality (2). This condition can be disrupted with a translation in the source together with the sky profile with respect to the base of the interferometer. We shall consider a base oriented along the line "east-west," when this kind of translation makes itself most strongly felt.

For a source in the region of culmination:

$$\tau = \frac{d}{c} \sin \vartheta,$$

where ϑ is the angle formed by the line to the source with the normal to the base (Fig. 1).

In the case under consideration, the following factor is added to the last term in expression (1):

$$\frac{\sin \frac{\Delta\omega \tau}{2}}{\frac{\Delta\omega \tau}{2}} = \frac{\sin \pi \Delta f \frac{d}{c} \sin \vartheta}{\pi \Delta f \frac{d}{c} \sin \vartheta},$$

a factor characterizing the envelope of the interferometer diagram. If the observation zone is restricted by values for the angles ϑ, at which the envelope does not fall below half the maximum value, then, taking $\sin \vartheta \approx \vartheta$, we get values for the corresponding sector of the angles ϑ:

$$\Delta\Theta = \frac{1,2c}{d\Delta f},$$

that is, it will depend only on the band of the frequencies picked up and the length of the base.

Using expression (17), it is not difficult to find that:

$$\Delta\Theta = 2,4 \frac{f_2 - f_1}{\Delta f} 2\vartheta_{\min}.$$

Formula (23) determines the observation sector $\Delta\theta$ across the number of minimum angular separations θ_{min} contained within it and for which the interferometer is calculated. Thus, if $\theta_{min}=1'$ and $\frac{f_2-f_1}{f_1}=0.1$, then at $\frac{\Delta f}{f_1}=10^{-2}$, $\Delta\theta=24'$, and at $\frac{\Delta f}{f_1}=10^{-3}$, $\Delta\theta=4°$.

If the time for finding a source within the limits of the sector $\Delta\theta$ is insufficient for carrying out observations, then the ratio between the feeder lengths leading to point Q should be either periodically or continually corrected.

In conclusion, we should note that the methods suggested here for measuring are only slightly sensitive to arbitrary variations in the phase shifts in the interferometer antennas, because they are oriented on the mean frequency of the intersection of the source by the lobes of the radiation pattern diagram of an interferometer built together with a phase shifter.

BIBLIOGRAPHY

1. Maltby, P., Moffet, A. T. Astrophysical Journal, No. 67, Vol. 7, Suppl. Series 1962.

2. Jennison, R. C. Monthly Notices of the Royal Astronom. Soc., No. 3. Vol. 118, 1958, pp. 276-284.

3. Zernike, F. Physica, Vol. 5, 1938, p. 785.

4. Born, M., Wolf, E. Principles of Optics. Pergamon Press, 1964.

5. Payne-Scott, R., Little, A. G. Austral. J. Sci. Res., A4, No. 489, 1951.

6. Hanbury Brown, R., Palmer, H. P., Thompson, A. F. Phil. Magazine, Series 7, No. 379, Vol. 46, August 1955, pp. 857-866.

7. Anderson, B., et al. Nature, No. 4969, Vol. 205, 1965, pp. 375-376.

SOLUTIONS TO A PROBLEM IN THE ANALYSIS OF A NONHOMOGENEOUS LINE (STRATUM) BY MEANS OF A METHOD EMPLOYING PARTIAL WAVES

D. I. Mirovitskiy, I. F. Budagyan

In the present work, a new method for solving an analysis problem (a primal problem in the propagation of waves in nonhomogeneous carrier lines or media) based on the conception of partial waves is examined; this makes it possible to determine by means of a sufficiently uniform method the space and reflected partial waves, and as a consequence, the complete field and internal coefficient of reflection for any arbitrary, nonhomogeneous line or medium. The recurrent relationships derived assure great accuracy in solving problems connected with wave propagation in a weakly nonhomogeneous system; these problems are usually considered in short-wave approximations (the Wentzel-Cramers-Brillouin method). These relationships are, however, good also with a shift to calculations for a system with a sharply expressed dependence of the parameters on the coordinates, where normally long-wave approximations are usually used (the Born and Kirchhoff methods).

Introduction

A precise solution to the problem of wave propagation in a nonhomogeneous system (a line, carrier, or medium) has been found up to the present only for several principles of variation in the wave number. In connection with this, different approximation methods [1, 2, 3] have gained great significance by taking account of the demands of high frequency signal technology and radio physics. In solving this problem a start is usually made from the equation $\psi''+\varkappa^2\psi=0$ [4, 5, 6], which connects only the full field ψ with the parameters of the medium. This is explained by the fact that the subdivision of ψ into two parts, to which, beginning from these or other particular considerations [7], may be ascribed the sense of space and reflected waves in a nonhomogeneous medium, is ambiguous [8, 9]. The conception of partial waves [10, 11] makes it possible to formulate requirements that must be satisfied by a partial space wave A and a partial reflected wave B in a medium.

It is well known that the field outside a homogeneous layer extending from 0 to a is expressed as $\psi=e^{i\varkappa_0 x}+re^{-i\varkappa_0 x}$, $(x\leq 0)$, $\psi=txe^{i\varkappa_a(x-a)}$, $(x\geq a)$, where r and t are its reflection factor and transmission coefficient, $\varkappa_0$ and $\varkappa_a$ are the wave numbers for the left and right homogeneous half-spaces. The partial space wave a should be transformed into an incident wave as it enters the layer ($a=e^{i\varkappa_0 x}$,

$x<0$), and upon output, into a transmitted wave ($\alpha=te^{i\kappa_a(x-a)}$, $x\geq a$), and then as a reflected wave it should satisfy the conditions:

$$\beta=re^{-i\kappa_0 x},\quad x=0;\qquad \beta=0,\quad x=a.$$

The ratio of the partial waves $\beta\alpha^{-1}$ should be taken (beginning with the physical sense of the functions of α and β) in the sense of the interior reflection factor R. This factor satisfies the corresponding Riccati equation:

$$R'(x)-2i\kappa(x)R(x)+\varkappa(x)[R^2(x)-1]=0, \qquad (1)$$

derived in the normal manner [12]. For a layer (carrier line) with pronounced boundaries on its interior, the reflection factor upon input R(0) should be connected with an output reflection factor $r(\kappa_0)$ by the relationship:

$$r=[R(0)-\Gamma][1-\Gamma R(0)]^{-1},\quad \Gamma=[z_0-z(0)][z_0-z(0)]^{-1}. \qquad (2)$$

Here, z(0) and z_0 are the characteristic impedances for the entry plane ($x=+0$) and the left-hand homogeneous half-space. At the layer output, this factor should be transformed into the Frenel reflection factor for the interface between two homogeneous media [z(a) and z_a]. For a stratum with even input and output [$z(0)=z_0$, $z(a)=z_a$], the internal reflection factor should be transformed at input into a layer reflection factor $R(0)=r(\kappa_0)$, and at output, it should be equal to zero.

Space and reflected partial waves in a nonhomogeneous line (layer, stratum) satisfy a system of two first order equations [9, 10]:

$$\left.\begin{aligned}\alpha'-\alpha(\varkappa-i\kappa)&=\beta\varkappa\\ \beta'-\beta(\varkappa-i\kappa)&=\alpha\varkappa\end{aligned}\right\}, \qquad (3)$$

which connect the wave number κ and the normed gradient $\varkappa$ of the characteristic impedance z of the nonhomogeneous line with space α and reflected β waves of the field w:

$$\kappa=\kappa_0\sqrt{\varepsilon\rho},\quad \varkappa=-\frac{z'}{2z}=-\frac{1}{2}(\ln z)'=$$
$$=-\frac{1}{4}[(\ln\rho)'-(\ln\varepsilon)'],\quad z=\sqrt{\frac{\rho}{\varepsilon}}. \qquad (4)$$

The equations (3) derived by means of an approximation of a determined, smoothly nonhomogeneous stepped line [13], for each j-th jump of which, with a thickness of d_j, the field may be represented uniquely in the form $w_j=\alpha_j+\beta_j$, where $\alpha_j=A_je^{i\kappa_j x}$, and $\beta_j=B_je^{-i\kappa_j x}$. Here, the amplitude coefficients A_j and B_j, as well as the wave number κ_j and the characteristic impedance z_j are constants.

The subsequent reciprocal substitution of the stepped line by means of the smoothly nonhomogeneous line (using a passage to the limit of $d_j \to 0$) leads to a Volterra integral equation, whose differentiation with respect to the coordinate taking into account the internal conditions of equations (13) and (14) in the cited work [14] yields equation (3) in the present article. In the work cited [9], the equations under (3) were derived earlier by means of another method.

In deriving the system (3), there was no assumption as to the slowness of variation in the features $\varkappa(x)$ and $\sigma(x)$ in the medium along the coordinate x, and as a consequence, there are also no foundations in the solution for this system to introduce the small variable δ, writing thus, for example ([9], p. 182), the solution for the wave propagation problem in a nonhomogeneous medium thusly:

$$\chi_1^m = \chi_1^{(0)} - \delta\chi_1^{(1)} + \delta^2\chi_1^{(2)} - \ldots \quad \chi_2^m = \chi_2^{(0)} - \delta\chi_2^{(1)} + \delta^2\chi_2^{(2)} - \ldots,$$

where χ_1^m and χ_2^m are functions corresponding approximately to the space and reflected waves α and β, but not derived with the help of system (3), but from the equation for the full field u.

From the Picard theorem for a normal system of first order equations, it follows [15] that system (3) has a natural solution, which may be found by means of series approximations. The series of the functions derived for this converges smoothly in the fixed interval, and as a consequence, the boundary functions are continuous. It is essential that the solution to system (3), generated by means of the method cited, does not depend on the choice of a zero approximation, and for that reason, for both weakly nonhomogeneous media, as well as for strongly nonhomogeneous media, it is possible to apply the same calculational scheme. For this, the solutions normally found by various methods ([16], pp. 63-103) (short wave and long wave approximations) will be derived by means of a completely uniform method. A certain increase in the volume of calculations, caused by the use of a zero approximation which is nonoptimal for one or another particular problem, is compensated for here by taking into account the rapid working times of computers in applications of one or another computation program for the various problems in the theory of wave propagation.

Cases when the functions $f_1(x) = \varkappa_{-1}\varkappa_{-1}(x)$ and $f_2(x) = \varkappa_{-1}\beta(x_+(x)$ are not continuous in the assigned interval ($x=0$ or $x=\infty$), require further study ([15], p. 254).

They are considered in work [17], in which a method for solving the problem of wave propagation is developed, and which is based on the investigation of amplitude-phase relationships in the solution of the first order equation:

$$u' - p\alpha' - q\alpha = 0, \quad \text{где } q = \ldots, \quad p = \ldots$$

for a partial space wave α.

The Fundamental Recurrent Relationships

In the selection of a zero approximation $\alpha_0(x)$ and $\beta_0(x)$ in any variant of the problem, it is convenient to begin with a solution for a quite weakly nonhomogeneous carrier line ($\varkappa$ is very small), computing for this the number of approximations corresponding to the degree of nonhomogeneity in the line or layer under consideration, that is, the more approximations there are, the greater will be the nonhomogeneity of the line. The base equations for finding $\alpha_0(x)$ and $\beta_0(x)$ are first order approximative differential equations, but they are not interconnected:

$$\alpha_0'(x) + \alpha_0(x)[\varkappa(x) - i\kappa(x)] = 0, \quad \beta_0'(x) - \beta_0(x)[\varkappa(x) - i\kappa(x)] = 0. \quad (5)$$

derived from system (3) by equating the right-hand portions of the equations to zero. /6

The solution for equations (5) for a semi-infinite layer, whose entry plane is disposed at x=0, leads to the following expressions:

$$\left.\begin{aligned} \alpha_0(x) &= \alpha_0(0)\exp\left[-\int_0^x(\varkappa - i\kappa)\,dx\right] = \alpha_0(0)K(x)\exp\left[i\int_0^x \kappa\,dx\right] \\ \beta_0(x) &= \beta_0(0)K(x)\exp\left[-i\int_0^x \kappa\,dx\right] \end{aligned}\right| \quad (6)$$

where:

$$K(x) = \sqrt{\kappa(0)\kappa^{-1}(x)}.$$

The sum of these waves, found at the zero approximation, has the form:

$$\psi_0(x) = \alpha_0(x) - \beta_0(x) = K(x)\left[\alpha_0(0)\,e^{i\int_0^x \kappa(x_1)\,dx_1} - \beta_0(0)\,e^{-i\int_0^x \kappa(x_1)\,dx_1}\right]. \quad (7)$$

We should note that this result overlaps with the expression for the field in a nonhomogeneous medium, found ([9], p. 174) by the VKB [expansion unknown] method on the basis of the equation for the complete field ψ with the absence of

corresponding expressions in the work cited [18]. It is possible to demonstrate [19] that with x=0, the following relationship holds for subsequent approximations:

$$\left.\begin{aligned} z_0(0) = z_1(0) = z_2(0) = \ldots = z_n(0) = z(0) \\ \beta_0(0) = \beta_1(0) = \beta_2(0) = \ldots = \beta_n(0) = \beta(0) \end{aligned}\right\}. \qquad (8)$$

For this reason, the solution of two independent equations for the n-th approximation:

$$z_n' - z_n(x - i\kappa) = \beta_{n-1} x \quad \text{и} \quad \beta_n' - \beta_n(x - i\kappa) = z_{n-1} x \qquad (9)$$

may be conveniently represented at n=1 thusly:

$$\left.\begin{aligned} z_1(x) = K(x) e^{-i\int_0^x \kappa(x_1)\,dx_1} \left[z(0) + \beta(0) \int_0^x \kappa(x_1) e^{i\int_0^{x_1} \kappa(x_2)\,dx_2}\,dx_1 \right] \\ \beta_1(x) = K(x) e^{-i\int_0^x \kappa(x_1)\,dx_1} \left[\beta(0) - z(0) \int_0^x \kappa(x_1) e^{i\int_0^{x_1} \kappa(x_2)\,dx_2}\,dx_1 \right] \end{aligned}\right\}. \qquad (10)$$

We shall introduce for brevity sake the following notational symbols:

$$J_+(x) = \int_0^x \kappa(x_1) e^{i\int_0^{x_1} \kappa(x_2)\,dx_2}\,dx_1,$$

$$J_-(x) J_+(x_1) = \int_0^x \kappa(x_1) e^{-i\int_0^{x_1} \kappa(x_2)\,dx_2}\,dx_1 \int_0^{x_1} \kappa(x_2) e^{i\int_0^{x_2} \kappa(x_3)\,dx_3}\,dx_2,$$

$$\Phi_-(x) = K(x) e^{-i\int_0^x \kappa(x_1)\,dx_1}, \quad G(x) = e^{-i\int_0^x \kappa(x_1)\,dx_1}.$$

Then, the recurrent relationships at n=2 take the form:

$$\left.\begin{aligned} z_2(x) = \Phi_-(x)\, z(0)\,[1 - J_-(x) J_+(x_1)] - \beta(0) J_-(x) \\ \beta_2(x) = \Phi_-(x)\, \beta(0)\,[1 - J_-(x) J_-(x_1)] - z(0) J_-(x) \end{aligned}\right\}. \qquad (11)$$

For the third approximation (n=3), we get respectively:

$$\alpha_3(x)=\Phi_-(x)\ \alpha(0)[1-J_-(x)J_-(x_1)-\beta(0)J_-(x)-J_-(x)J_-(x_1)J_-(x_2)J_-(x_3)+\ldots$$
$$\beta_3(x)=\Phi_-(x)\ \beta(0)[1-J_-(x)J_-(x_1)+\alpha(0)[J_-(x)-J_-(x)J_-(x_1)J_-(x_2)+\ldots$$

It is not difficult to find by induction expressions for the subsequent approximation as well:

$$\alpha_4(x)=\Phi_-(x)\ \alpha(0)[1-J_-(x)J_-(x_1)-J_-(x)J_-(x_1)J_-(x_2)J_-(x_3)-$$
$$-\beta(0)[J_-(x)-J_-(x)J_-(x_1)J_-(x_2)],$$
$$\beta_4(x)=\Phi_-(x)\ \beta(0)[1-J_-(x)J_-(x_1)-J_-(x)J_-(x_1)J_-(x_2)J_-(x_3)-$$
$$-\alpha(0)[J_-(x)-J_-(x)J_-(x_1)J_-(x_2)].$$

In this way, we shall note the recurrent formulas for positive and odd approximations:

$$\alpha_{2n}(x)=\Phi_-(x)\ \alpha(0)[1-J_-(x)J_-(x_1)-\ldots-$$
$$-J_-(x)J_-(x_1)\ldots J_-(x_{2n-2})J_-(x_{2n-1})]-\beta(0)[J_-(x)-$$
$$-J_-(x)J_-(x_1)J_-(x_2)-\ldots-J_-(x)J_-(x_1)\ldots J_-(x_{2n-2})],$$
$$\beta_{2n}(x)=\Phi_-(x)\ \beta(0)[1-J_-(x)J_-(x_1)-\ldots-J_-(x)J_-(x_1)$$
$$\ldots J_-(x_{2n-2})J_-(x_{2n-1})]-\alpha(0)[J_-(x)-J_-(x)J_-(x_1)J_-(x_2)-$$
$$-\ldots-J_-(x)J_-(x_1)\ldots J_-(x_{2n-2})],$$
$$\alpha_{2n+1}(x)=\Phi_-(x)[\alpha(0)[1-J_-(x)J_-(x_1)-\ldots-J_-(x)J_-(x_1)\ldots$$
$$\ldots J_-(x_{2n-2})J_+(x_{2n-1})]-\beta(0)[J_-(x)-J_-(x)J_+(x_1)J_-(x_2)-\ldots$$
$$\ldots-J_-(x)J_-(x_1)\ldots J_-(x_{2n})]],$$
$$\beta_{2n+1}(x)=\Phi_-(x)\ \beta(0)[1-J_-(x)J_-(x_1)-\ldots-J_-(x)J_-(x_1)\ldots$$
$$\ldots J_+(x_{2n-2})J_-(x_{2n-1})]-\alpha(0)[J_-(x)-J_-(x)J_-(x_1)J_-(x_2)-$$
$$-\ldots-J_-(x)J_-(x_1)\ldots J_-(x_{2n})]].$$

The internal reflection factor $R=\beta\alpha^{-1}$, and consequently the input reflection factor $r(\kappa_0)$ of a nonhomogeneous line (layer) connected with it by expression (2), is determined in the following manner.

In using recurrent formulas that describe partial waves, it is necessary above all to determine the kinds of approximations for the partial waves that express the desired internal reflection factor R_n (at the n-th approximation) in the relation. With this end in mind, we use the Riccati equation (1) and the linear system (3). We rewrite equation (1) in the form:

$$R'-\varkappa-(2i\kappa+\varkappa R)R=0$$

and we shall use the first equation in system (3), which, taking into account

that according to the determination $R=\beta\alpha^{-1}$, may be represented in the following form:

$$\alpha'\alpha^{-1} - \varkappa = i\kappa - \varkappa R.$$

Then:

$$R' + R(\varkappa - i\kappa + \alpha'\alpha^{-1}) = \varkappa. \qquad (13a)$$

We shall start from the determined space wave α_n found at the n-th approximation, writing equation (13a) with respect to R_n in the following manner:

$$R_n' + R_n(\varkappa - i\kappa + \alpha_n'\alpha_n^{-1}) = \varkappa. \qquad (13b)$$

Assuming that in this equation $R_n=\beta_j\alpha_n^{-1}$, we shall find the number of the j-th successive approximation assuring the feasibility of the first equation in the base-line linear system (3), which earlier was represented in the form of equation (9). Differentiating the expression for R_n, we get:

$$R_n' = \beta_j'\alpha_n^{-1} - \beta_j\alpha_n^{-2}.$$

We shall introduce this expression into equation (13a). For this, $\beta_j'+\beta_j(\varkappa+i\kappa)=\alpha_n\varkappa$. Comparing the equation just derived with the second equation in system (9), we immediately establish that j=n+1.

In this way, the n-th approximation for the internal reflection factor is $R_n=\beta_{n+1}\alpha_n^{-1}$, that is, this is the relation of the reflected wave in the successive approximation to the space wave taken in the foregoing approximation; this situation has a definite physical sense. At the same time, function R_n satisfies the equation derived from equation (13b) by means of substituting into it the expression $\alpha_n'\alpha_n^{-1}$, which is determined from the first equation in system (9):

$$R_n' + 2i\kappa R_n + \varkappa\left(\frac{\beta_{n-1}}{\alpha_n}\frac{\beta_{n-1}}{\alpha_n} - 1\right) = 0, \qquad (14)$$

which with $\beta_{n-1}\to\beta_{n+1}$ is transformed into equation (1).

A direct consideration of the process of wave propagation makes it possible to establish the fact that the optimal sequentiality of relations of partial waves is the series including even numbered approximations for the space wave, that is, α_{2n}, n=0,1,2... In fact, the space wave at the zero approximation generates a reflected wave (in the first approximation). This process at any arbitrary point within the nonhomogeneous medium is characterized by an internal reflection factor $R_1=\beta_1\alpha_0^{-1}$. In its turn, the wave β_1, being reflected in its

movement as a return wave, creates another space wave α_2, which then generates a reflected wave β_3. In this way, in fact, the internal reflection factor at the second approximation is $R_{II}=\beta_3\alpha_2^{-1}$. The process described in this way is fully characterized by system (9).

Taking into account what has been analyzed above, as well as the tradition sponsored by applications of the VKB method, in which the zero approximation (an approximation of geometric optics) gives two waves which do not interact between each other [$R_0(x)=0$], we shall use the following notation in what is to follow for successive approximations of the internal reflection factor:

$$R_1=\beta_1\alpha_1^{-1},\quad R_2=\beta_2\alpha_2^{-1},\quad R_3=\beta_3\alpha_3^{-1},\quad R_4=\beta_4\alpha_4^{-1},\quad R_5\quad\beta_5\alpha_5^{-1}. \tag{15}$$

Using the recurrent formulas (10) and (12), we write:

$$R_0(x)=0,\quad R_1(x)=G(x)[R(0)-J_+(x)],$$
$$R_2(x)=G(x)\{R(0)[1-J_+(x)J_-(x_1)]+[J_-(x)-J_-(x)J_-(x_1)J_-(x_2)]$$
$$[1-J_-(x)J_-(x_1)-R(0)J_-(x)]^{-1}. \tag{16a}$$

These formulas bring the reflection factor R(x) at any instantaneous point x within a nonhomogeneous line into conformance with the exact value of the internal reflection factor R(0) on the entry plane for the same line. They are used in problems with an assigned input reflection factor (and synthesis problems), if the relations in (8) are justified, establishing that $R(0)=R_j(0)$, where j=0,1,2...

If we assume an assigned R(a), that is, the internal reflection factor at the output of the line, then it is necessary, in the recurrent expressions $J_{\pm}(x)$; $J_{\pm}(x)J_{\mp}(x_1)$:... for the partial waves entering into the formulas for the internal reflection factor, to vary the integration limits (instead of 0-x, use x-a). For this, formulas (16a) must be written in the following form:

$$R_0(x)=0,\quad R_1(x)=Q(x)[R(a)-I_-(x)],$$
$$R_2(x)=Q(x)\{R(a)[1-I_-(x)I_+(x_1)]-[I_-(x)-I_-(x)I_-(x_1)I_-(x_2)]$$
$$\times[[1-I_+(x)I_-(x_1)]-R(a)I_+(x)]^{-1}, \tag{16b}$$

keeping in mind that expressions (8) are transformed in the following manner: /7

$$\alpha_0(a)=\alpha_1(a)=\alpha_2(a)=\ldots=\alpha_n(a)=\alpha(a),$$
$$\beta_0(a)=\beta_1(a)=\beta_2(a)=\ldots=\beta_n(a)=\beta(a).$$

Here, the following symbolic notations are used:

$$J_-(x) = \int_x^a \varkappa(x_1)\, e^{-2\int_{x_1}^a \varkappa(x_2)\,dx_2}\,dx_1, \qquad Q(x) = e^{-2\int_x^a \varkappa(x_1)\,dx_1},$$

$$J_-(x)J_-(x_1) = \int_x^a \varkappa(x_1)\, e^{-2\int_{x_1}^a \varkappa(x_2)\,dx_2}\,dx_1 \int_{x_1}^a \varkappa(x_2) e^{-2\int_{x_2}^a \varkappa(x_3)\,dx_3}\,dx_2.$$

In solving problems connected with determining a reflection factor according to a given principle of variation in the characteristic wave impedance $\rho=\rho(x)$ along the coordinate x, two cases are usually encountered:

1. A nonhomogeneous line (layer, stratum), extending from x=0 to x=a, matched with an input homogeneous line, that is, one that has no reflections, making it necessary to find R(x) according to a fixed or assigned $\rho(x)$. For this case, it is necessary, once having defined the desired reflection factor and terms of $R_n(x)$, to use the following recurrent relations coming out of formulas (16a) with R(0)=0, and which remain good for the entry plane of the nonhomogeneous line as well (that is, at x=a):

$$R_1(x) = G(x)J_-(x), \tag{17}$$

$$R_2(x) = G(x)[J_+(x) - J_-(x)J_-(x_1)J_-(x_2)][1 - J_-(x)J_-(x_1)]^{-1}, \tag{18}$$

$$R_3(x) = G(x)[J_-(x) - J_-(x)J_-(x_1)J_-(x_2) - J_-(x)J_-(x_1)J_-(x_2)J_-(x_3)J_-(x_4)] \cdot [1 - J_-(x)J_-(x_1) - J_-(x)J_+(x_1)J_-(x_2)J_-(x_3)]^{-1}. \tag{19}$$

2. A nonhomogeneous line matched with a homogeneous, input line, that is, at the line output there are no jumps in the characteristic impedances [$\rho(a)=\rho_a$, where ρ_a characterizes the output line], making it necessary to find the $R_n(0)$ connected with the input reflection factor r of formula (2) according to the assigned $\rho=\rho(x)$. Taking x=0 from expression (16b), we get for this case [R(a)=0]:

$$R_1(0) = -Q(0)I_-(0), \tag{20}$$

$$R_2(0) = -Q(0)[I_-(0) - I_-(0)I_-(x)I_-(x_1)][1 - I_+(0)I_-(x)]^{-1}, \tag{21}$$

$$R_3(0) = -Q(0)[I_-(0) + I_-(0)I_+(x)I_-(x_1) - I_-(0)I_-(x)I_-(x_1) \times I_+(x_2)I_-(x_3)][1 - I_+(0)I_-(x) - I_-(0)I_-(x)I_-(x_1)I_-(x_2)]^{-1}. \tag{22}$$

In a similar manner, it is not difficult to derive from expressions (16a) and (16b) the recurrent relations for other variants of the problem of wave propagation

as well, in which neither R(0) nor R(a) is equal to zero. We shall consider an example which clarifies the possibilities represented by using the formulas suggested above for the solution of problems in the analysis and synthesis of a nonhomogeneous line (layer, stratum). The generally accepted method [20, 21] for the approximative solution to these kinds of problems reduces to the integration of equation $R'_{\pi}(x)+2ik(x)R\times(x)-\times(x)=0$, derived from the linearization of equation (1). This method leads to the following result:

$$R_{\pi}(x)=e^{-i2\int_0^x \varkappa(x_1)\,dx_1}\left[R(0)-\int_0^x \varkappa(x_1)e^{i2\int_0^{x_1}\varkappa(x_2)\,dx_2}\,dx_1\right]. \qquad (23)$$

It is not difficult to convince oneself that $R_{\pi}(x)$ is here in fact the first expression from the series of relations for partial waves given by formulas (15), as $R_{\pi}(x)=\beta_1(x)\alpha_0^{-1}(x)$, where $\beta_1(x)$ is determined by the second equation in system (10), and $\alpha_0(x)$ is determined by the first equation in system (6). At the same time, the equation $R(0)=\beta(0)\alpha^{-1}(0)$ must also be taken account of. In this way, the first approximation for the reflected wave $\beta_1(x)$ is the product of the partial space wave at the zero approximation $\alpha_0(x)$ by the internal reflection factor $R_{\pi}(x)$, found from the linearized Riccati equation.

By means of manual computation, which necessitates restricting to a small number of approximations (n), when the following conditions of the Picard theorem are <u>a fortiori</u> not fulfilled:

$$\alpha_{n-1}-\alpha_{n-2},\ \beta_{n-1}-\beta_{n-2},$$

it is advisable and expedient, without using the symmetrical form of the expressions for the partial waves, to go to the optimal series for them. In accordance with formula (14), the following waves should be chosen for this:

$$\alpha_0, \alpha_2, \alpha_4, \ldots \text{ и } \beta_1, \beta_3, \beta_5, \ldots, \qquad (24)$$

which are determined by the expressions (6), (11), ... and (10), (12), ..., and the full field is determined as:

$$\psi_0=\alpha_0,\ \psi_1=\alpha_0+\beta_1,\ \psi_2=\alpha_2-\beta_3,\ \psi_3=\alpha_4-\beta_5,\ \ldots, \qquad (25)$$

which for ψ_0 and ψ_1, is in accordance with the position of [1].

All that has been analyzed above holds for a change from a finite, nonhomogeneous line to an infinite, nonhomogeneous line (medium). This change brings

with it the necessity only for a corresponding substitution of the limits on all the integral expressions in the derived recurrent formulas.

The Determination of the Internal and Input Reflection Factors /7

We shall consider a geometrically nonhomogeneous, coaxial line with a homogeneous filler, for which $\partial\kappa(x)/\partial x=0$, and the characteristic impedance is $\rho(x)=[\mu(x)/\varepsilon(x)]^{1/2}$. The driving capacitance and inductance satisfy the following relations: $\varepsilon(x)=\kappa\kappa_0^{-1}\xi(x)$, $\mu(x)=\kappa\kappa_0^{-1}\xi^{-1}(x)$, and for this reason, introducing the normed function for the characteristic impedance $P(x)=\rho^{1/2}(x)\rho^{-1/2}(0)$ to the line input, it is possible in accordance with formulas (6), (10), and (11), to write the following:

$$z_0(x)=P(x)e^{i\kappa x}z(0),\quad \beta_0(x)=P(x)e^{-i\kappa x}\beta(0),$$

$$z_1(x)=P(x)e^{i\kappa x}\left[z(0)-\beta(0)\int_0^x\varkappa(x_1)e^{-i2\kappa x_1}\,dx_1\right],$$

$$\beta_1(x)=P(x)e^{-i\kappa x}\left[\beta(0)+z(0)\int_0^x\varkappa(x_1)e^{i2\kappa x_1}\,dx_1\right],$$

$$z_2(x)=P(x)e^{i\kappa x}\left\{z(0)\left[1-\int_0^x\varkappa(x_1)e^{-i2\kappa x_1}\,dx_1\int_0^{x_1}\varkappa(x_2)e^{i2\kappa x_2}\,dx_2\right]-\right.$$
$$\left.-\beta(0)\int_0^x\varkappa(x_1)e^{-i2\kappa x_1}\,dx_1\right\},$$

$$\beta_2(x)=P(x)e^{-i\kappa x}\left\{\beta(0)\left[1-\int_0^x\varkappa(x_1)e^{i2\kappa x_1}\,dx_1\int_0^{x_1}\varkappa(x_2)e^{-i2\kappa x_2}\,dx_2\right]-\right.$$
$$\left.+z(0)\int_0^x\varkappa(x_1)e^{i2\kappa x_1}\,dx_1\right\},$$

where the normed characteristic impedance gradient $\varkappa$ is expressed by formula (4).

We shall limit ourselves to a case where a section of nonhomogeneous line is matched on its output side, that is, $\rho(a)=\rho_a$. For this, $R(a)=0$ and it is necessary to determine, according to the given dependency relationship $\rho=\rho(x)$, $0\leq x\leq a$, the input reflection factor r connected with the internal reflection factor for input $R(\kappa_0+0)$, by means of relation (2). Formulas (20), (21), and (22) are good also for this case, with the exception that the symbolic notation used in them now has the following form:

$$I(0)=\int_0^a\varkappa(x)e^{-i2\kappa(a-x)}\,dx,\quad Q(0)=e^{i2\kappa a},$$

$$I_1(0)I_2(x)=\int_0^a \varkappa(x)\,e^{-i2\varkappa(a-x)}\,dx\int_x^a \varkappa(x_1)\,e^{-i2\varkappa(x_1-x)}\,dx_1. \qquad (26)$$

/7

For the sake of ease in comparing the method presented here with the exact solution for this problem, as well as with the normally used approximation solution [9], we shall choose the following principle of variation in the characteristic impedance of the nonhomogeneous line:

$$\rho(x)=\rho(0)e^{-2\rho x}. \qquad (27)$$

For the selected principle $\varkappa=\rho$, and as a consequence, it is possible to rewrite formula (1) in the form:

$$R'(x)-2i\kappa R(x)+\rho[R^2(x)-1]=0. \qquad (28)$$

We find the exact solution for this equation by substituting into it the expression $u(x)=\exp[\rho\int_0^x R(y)dy]$. At the same time, it is transformed into a linear equation with constant coefficients:

$$u''(x)-2i\kappa u'(x)-\rho^2u(x)=0.$$

Insofar as the solution to this equation has, as is well known, the following form:

$$u(x)=C_1\exp\left[-ix\left(\kappa-\sqrt{\kappa^2-\rho^2}\right)\right]-C_2\exp\left[-ix\left(\kappa-\sqrt{\kappa^2-\rho^2}\right)\right],$$

the exact solution to equation (28) may be represented in the form:

$$R(x)=-\frac{i\kappa}{\rho}-\frac{i}{\rho}\sqrt{\kappa^2-\rho^2}\,G,\quad G=(F-D)(F-D)^{-1},$$
$$F=\exp\left(i2\kappa\sqrt{\kappa^2-\rho^2}\right),\ D=\frac{C_1}{C_2}. \qquad (29)$$

The constant of integration D is determined from the boundary condition R(a)=0:

$$D=\left[(\kappa^2-\rho^2)^{\frac{1}{2}}-\kappa\right]\left[(\kappa^2-\rho^2)^{\frac{1}{2}}-\kappa\right]^{-1}\exp 2ia(\kappa^2-\rho^2)^{\frac{1}{2}}.$$

For a semi-infinite, nonhomogeneous line, D=0. Introducing the value found for D into expression (29), we can determine the desired exact expression:

$$R(0)=-\frac{i\kappa}{\rho}-\frac{i}{\rho}\sqrt{\kappa^2-\rho^2}(1-D)(1-D)^{-1}=$$
$$=ip\left[e^{i2a\sqrt{\kappa^2-\rho^2}}-1\right]\left[\kappa+\sqrt{\kappa^2-\rho^2}+\left[\sqrt{\kappa^2-\rho^2}-\kappa\right]\times e^{i2a\sqrt{\kappa^2-\rho^2}}\right]^{-1}. \qquad (30)$$

The module of this reflection factor R(0) is expressed as:

$$|R_1(0)| = A \sin \left[\sqrt{B^2 - A^2} \left(B^2 - A^2 \cos^2 \right) \sqrt{B^2 - A^2} \right]^{-\frac{1}{2}}, \quad A = ap, \; B = a\kappa, \ldots$$

The relations determined by the recurrent formulas (20)-(22), taking into account (26), have the following form in this case: /7

$$R_1(0) = -e^{i2\kappa a} \int_0^a p\, e^{-i2\kappa(a-x)}\, dx = iqe_-, \quad q = \frac{p}{2\kappa}, \quad e_- = e^{i2\kappa a} - 1,$$

$$R_2(0) = -e^{i2\kappa a} \left[p \int_0^a e^{-i2\kappa(a-x)}\, dx - p^2 \int_0^a e^{-i2\kappa(a-x)}\, dx \cdot \right.$$

$$\cdot \int_x^a e^{i2\kappa(a-x_1)}\, dx_1 \int_{x_1}^a e^{-i2\kappa(a-x_2)}\, dx_2 \Big] \Big[1 - p^2 \int_0^a e^{i2\kappa(a-x)}\, dx \cdot$$

$$\left. \cdot \int_0^a e^{-i2\kappa(a-x_1)}\, dx_1 \right]^{-1} = iq[e_- - q^2(2e_- - 2i\kappa a e_-)][1 - q^2(2i\kappa a - e_-)]^{-1}$$

$$R_3(0) = iq\, e_- - 2q^2(e_- - i\kappa a e_-) - 2q^3[(3 - \kappa^2 a^2)e_- - 3i\kappa a e_-] \cdot$$
$$\cdot 1 - q^2(2i\kappa a - e_-) - q^3[-2\kappa^2 a^2 - 2i\kappa a(e_- - 1) - 3e_-]^{-1}.$$

For $|R_n(0)|$, we get respectively:

$$|R_1(0)| = AB^{-1} S, \tag{32}$$

$$|R_2(0)| = AB^{-1} \left[1 - LM^{-1} \right]^2 \Big]^{-\frac{1}{2}}, \tag{33}$$

$$|R_3(0)| = AB^{-1} \left\{ 1 - \left[\frac{L - A^4 (8B^3)^{-1} N}{M + A^4 (8B^4)^{-1} (B^2 S - 3N)} \right]^2 \right\}^{-\frac{1}{2}}. \tag{34}$$

Here:

$$A = ap, \quad B = a\kappa, \quad S = \sin B, \quad C = \cos B,$$
$$N = S - BC, \quad L = C - A^2 S (2B)^{-1}, \quad M = A^2 C (2B)^{-1} -$$
$$- S \left[1 - A^2 (2B^2)^{-1} \right].$$

The effectiveness of the recurrent formulas may be assessed by means of comparing the calculation results according to the recurrent and the exact formulas. For this comparison, it is convenient to use two methodologies somewhat differing from each other and conditioned by the special features of the recurrent formulas derived. In the first instance, the parameter pa, the product of the coefficient p characterizing, in accordance with formula (27), the velocity in the variation of the characteristic impedance ρ of the nonhomogeneous line along the coordinate x must be fixed, as well as the length a of the section of nonhomogeneous line. In the second instance, the parameter $p\kappa^{-1}$ must be fixed;

it enters both into the exact formula (31), as well as into formulas (32)-(34), which contain the factor $AB^{-1}=p\kappa^{-1}$, characterizing the degree of nonhomogeneity of the line.

The first instance corresponds to the conditions under which variations in the length a of the nonhomogeneous section of the line lead automatically to a corresponding change in the coefficient p. Thus, a successive increase in length, that is, a transition from a_1 to a_2, a_3, etc., where $a_1<a_2<a_3<\ldots$, occasions the necessity for considering nonhomogeneous sections of lines with the coefficients p_1, p_2, p_3, ..., where $p_1>p_2>p_3>\ldots$, with $p_1a_1=p_2a_2=\ldots=\text{const}$. Similar conditions are encountered frequently in practice, when the section of nonhomogeneous line is disposed between two homogeneous portions with fixed characteristic impedances ρ_0 and ρ_a. In Fig. 1a, two sections with lengths a_1 and a_2 are pictured together with corresponding curves characterizing the velocity of the variation in the characteristic impedance in the nonhomogeneous portion.

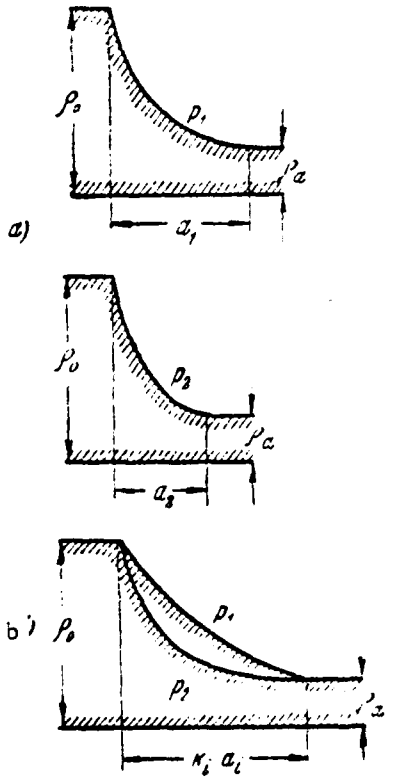

Fig. 1. Variation of characteristic impedance in a nonhomogeneous portion of line for the cases when: (a) $p_1a_1=p_2a_2=\text{const}$. (b) $p_1\kappa_1^{-1}=p_2\kappa_2^{-1}=\text{const}$.

The frequency relationship $|R(0)|=f(\kappa a)$ is given in Fig. 2 by the solid line with $pa=0.5$. Here, the broken line plots the results of calculations

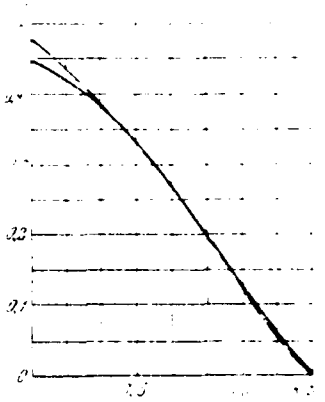

Fig. 2. Comparison of results of calculations according to the exact and recurrent formulas for the relationship between the internal reflection factor at input and the electrical length of a nonhomogeneous line for the case pa=const.

according to the recurrent formula (32), that is, at the first approximation. It is easy to see that only where $\varkappa a>1$, the first approximation begins to give high values for the module of the internal reflection factor.

The second instance, when the parameter $p\varkappa^{-1}$ is fixed, corresponds to conditions under which a variation in the wavelength (frequency) occasions a corresponding variation in the coefficient p. This last is necessary in order to retain as constant the jump in the characteristic impedances (ρ_0 and ρ_a) in the semi-infinite, homogeneous lines. At the same time, the electrical length (but not the geometrical length) of the nonhomogeneous section remains invariant across any arbitrary wave or frequency range. In this way, the relation $p\varkappa^{-1}$ characterizes the degree of nonhomogeneity of the line, that is, the magnitude of the jump in characteristic impedances at a distance equal to the wavelength. A diagram showing the physical sense of the variation in the parameter $p\varkappa^{-1}$ is shown in Fig. 1b. Here, $p_1\varkappa_1^{-1}=p_2\varkappa_2^{-1}=c_1$, $\varkappa_1 a_1=\varkappa_2 a_2=c_2$, with c_1 and c_2 being constants.

We shall compare the computation results arrived at by the recurrent formula, not only with the exact results, but also with the computations carried out with the help of other variants of the method of successive approximations. Several modifications to this method are well known. The most exact is taken to be the second variant of the two described in the cited work [9] (pp. 194-203). This variant reduces in fact to the solution of the Riccati equation by means of successive approximations. As a result, it is possible to derive the following expressions (see the Supplement):

$$R_1^*(x) = -e^{-i2\varkappa x}\int_x^a \varkappa(x_1)\,e^{i2\varkappa x_1}\,dx_1, \tag{35}$$

$$R_2^*(x) = -e^{-i2\varkappa x}\int_x^a \varkappa(x_1)\left[1 - R_1^2(x_1)\right]e^{i2\varkappa x_1}\,dx_1, \tag{36}$$

$$R_1^*(0) = -\int_0^a \varkappa(x)\,e^{i2\varkappa x}\,dx, \tag{37}$$

$$R_2^*(0) = -\int_0^a \varkappa(x)\left[1 - R_1^2(x)\right]e^{i2\varkappa x}\,dx. \tag{38}$$

Taking into account that $\varkappa(x)=p$, in accordance with formulas (35) and (38), we may write:

$$R_1^*(x) = -e^{-i2\varkappa x}\int_x^a p\,e^{i2\varkappa x_1}\,dx_1 = \frac{ip}{2\varkappa}\left[e^{2i\varkappa(a-x)} - 1\right], \tag{39}$$

$$R_2^*(0) = \frac{p}{\varkappa}e^{-i2\varkappa a}\left[\frac{p^2 a}{2\varkappa} - \frac{1}{2}\sin 2\varkappa a\left(1 + \frac{p^2}{2\varkappa^2}\right) + i\sin^2\varkappa a\right]. \tag{40}$$

The second approximation according to the method described in work [9] will consequently have the following form:

$$|R_2^*(0)| = \frac{A}{B}\left\{\left[\frac{A^2}{2B} - \frac{1}{2}\left(1 + \frac{A^2}{2B^2}\right)\sin 2B\right]^2 + \sin^4 B\right\}^{\frac{1}{2}}. \tag{41}$$

The calculation results arrived at by the exact formula (31) and the recurrent formulas (32), (33), and (34), as well as according to formula (41) are shown in Figs. 3 and 4 for the two cases: (a) a smoothly nonhomogeneous stratum ($p\varkappa^{-1}$= =0.5), and (b) a stratum with an abrupt change in features across its thickness ($p\varkappa^{-1}$=0.8). The data used in constructing these curves are cited in the table. /7

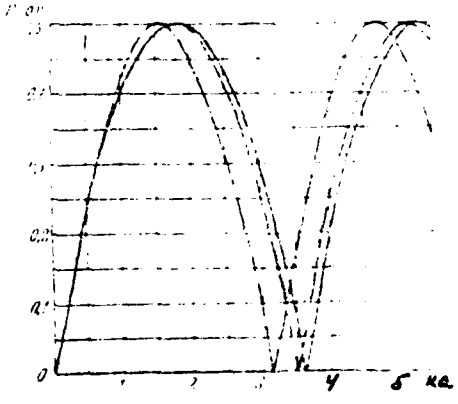

Fig. 3. Comparison of calculation results for $|R(0)|$ according to the exact formula, recurrent formulas, and according to the method given in work [9] for the case $p\varkappa^{-1}$=0.5.

AD-A115 394 FOREIGN TECHNOLOGY DIV WRIGHT-PATTERSON AFB OH F/G 9/5
ANTENNAS.(U)
MAY 82
UNCLASSIFIED FTD-ID(RS)T-1170-81 NL

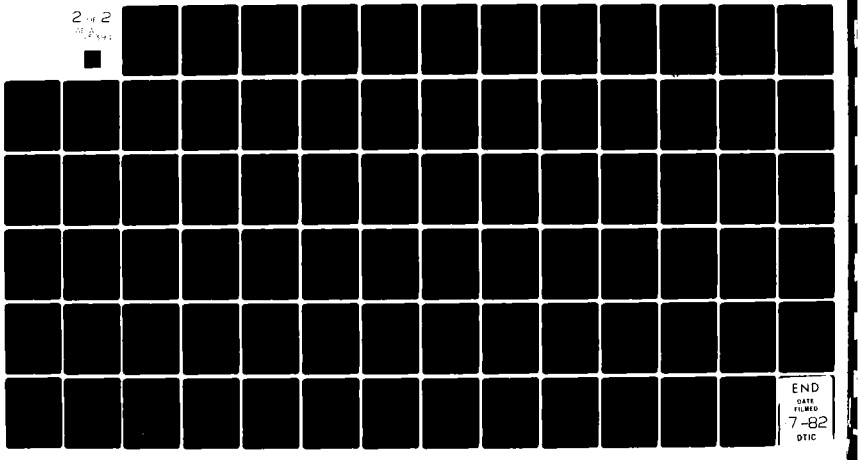

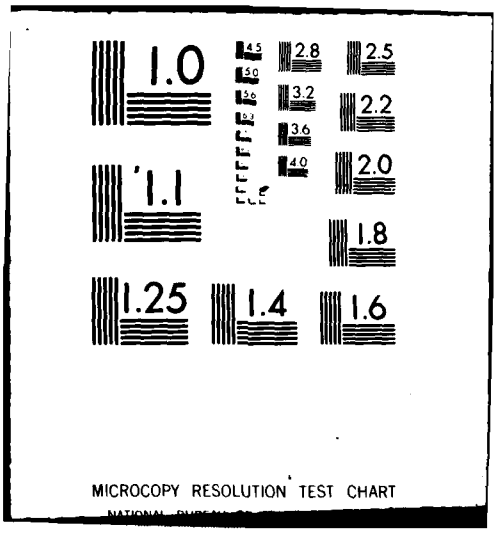
1.0
1.1
1.25
1.4
1.6
1.8
2.0
2.2
2.5
2.8
3.2
3.6
4.0
4.5
5.0
5.6
MICROCOPY RESOLUTION TEST CHART

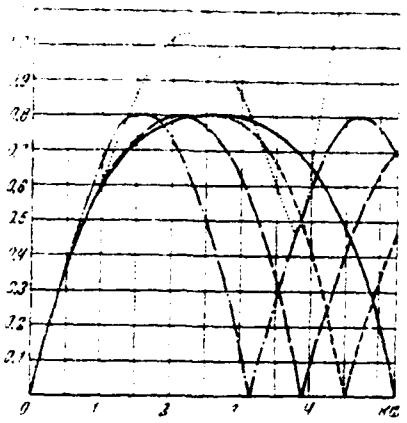

Fig. 4. Comparison of calculation results for $|R(0)|$ according to the exact formula, recurrent formulas, and the method given in work [9] for the case $p\kappa^{-1}=0.8$.

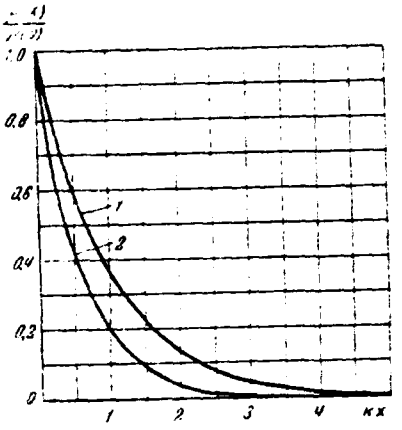

Fig. 5. Relationship of normed characteristic impedance for nonhomogeneous line and the "electric coordinate" κx for the cases.
1) $p\kappa^{-1}=0.5$, 2) $p\kappa^{-1}=0.8$

Table

κx	0	1	2	3	4
$P(x)=\exp(-2x\cdot0.5)$	1	0.368	0.135	0.0498	0.0183
$P(x)=\exp(-2x\cdot0.8)$	1	0.202	0.0408	0.0082	0.0017

The exact solution is shown in the figures as the solid line, the first approximation by the line made up of dots and bar sections, the second approximation by means of the barred line, and the third approximation by means of the line with smaller bars. The point curve shows data for comparison of the calculation results according to formula (41). From an analysis of the curves, it emerges that at $p\kappa^{-1}=0.5$, the point curve differs only slightly from the curve with large bar sections describing the second approximation for $R_2(0)$ and plotted according to formula (33). The substantial distortion is noted only in the area of the first minimum (near the point $\kappa a=3.6$). However, with a transition to the less smooth line ($p\kappa^{-1}=0.8$), the correspondence noted above is completely disrupted. Although the abscissas of the first minimums of the point and the large bar curves almost coincide, the magnitudes for these minimums are substantially different, /8

while it is not only the nature of the point curve [plotted according to formula (41)] that differs significantly from the exact curve, but at $\kappa a \approx 2.5$ and $\kappa a > 4.2$, the module of the reflection factor $|R_2(0)|$ becomes greater than unity. This contradicts the law of the conservation of energy. At the same time, the maximums and the minimums of the curves plotted according to formulas (32)-(34) for various approximations, overlap according to their magnitudes with corresponding extrema of the point curve. The shape of the approximation curves, beginning with the first approximation, is close in form to the point curve and differs /8
from it practically only in terms of the period of oscillation $T(\kappa a)$. With a transition from the first approximation to the second, and further to the third approximation, the period of oscillation of the curves goes in a monotone fashion to the period of oscillation of the point curve [$T_1(\kappa a)=3.2\kappa a$; $T_2(\kappa a)=3.9\kappa a$; $T_3(\kappa a)=4.5\kappa a$], and then as $T_{\text{точн}}(\kappa a)=5.2\kappa a$.

Fig. 5 shows the corresponding graphs (see the table) characterizing the relationship between the normed characteristic impedance $\frac{\rho(x)}{\rho(0)}$ of a nonhomogeneous line and the argument κx for the two cases under consideration (weakly and strongly nonhomogeneous lines).

Conclusions

The effectiveness of the recurrent formulas derived here is explained by the following facts.

The base equations (3) for the method suggested here constitute a linear system of the first degree, and they determine the partial waves α and β, the full field $\psi=\alpha+\beta$, the internal reflection factor $R=\beta\alpha^{-1}$, and with the help of (2), the input reflection factor r.. It follows from the linearity of the system, as was noted earlier, that its solution, found by means of the Picard method, naturally converges uniformly to the boundary functions ($\alpha_n \to \alpha$, $\beta_n \to \beta$), not dependent on the zero approximation chosen (α_0, β_0) and the initial conditions [$\alpha(0)$, $\beta(0)$, or $\alpha(a)$, $\beta(a)$]. The solution for R_n of the exact equation (14) tends toward the internal reflection factor R, if the function β_n has a limit, and insofar as the latter is always fulfilled at $\kappa \neq 0$ or $x \neq \infty$, then the method for determining (from the recurrent formulas suggested) R_n also possesses the advantages noted.

The method used in work [9] converges to a direct solution for the equation $R'_n+2i\varkappa R_n=\varkappa(1-R^2_{n-1})$ by means of the Picard method, which is required in carrying out the ancillary investigations (see [15], pp. 233-258, 263-276, [22], pp. 23-27).

Recurrent formulas are characterized by rapid convergence, which is maintained with the transition to strongly nonhomogeneous lines (media) with large $\varkappa$, as well as with a module of the reflection factor $|R_n|$ close to unity; this is confirmed by the examples that were worked through, and then confirmed also in the fact that the method in [9] assures a sufficiently rapid convergence only if $\varkappa$ is small, and $|R_n|^2\ll 1$. This latter holds only for a weakly nonhomogeneous medium (see [9], p. 200) and for a small jump in parameters or variables at the output of a nonhomogeneous stratum.

As has been demonstrated, the internal reflection factor R is a limit, toward which the series $R_n=\beta_{n+1}\alpha_{n-1}$ tends. At the same time, in finding R_n by means of the Picard method for solving equation (1), it is assumed that R is a boundary function for the second series.

It should be noted that with any arbitrary $\varkappa$, for the purposes of unifying /8
the program, it is convenient to start from the zero approximation derived assuming $\varkappa$ to be small. This makes it possible to substitute calculation relations differing significantly from each other (VKB, Born, Kirchhoff, et al.) in short wave and long wave approximations by a system of unique recurrent formulas. This feasibility, noted above, is explained by the advantages brought about by the transition from considerations of an equation for the full field $\psi''+\varkappa^2\psi=0$ to a consideration of equations for a partial space wave α and a partial reflected wave β.

In conclusion, we note that with the help of recurrent formulas, it is possible to calculate not only nonhomogeneous lines and media both with electromagnetic losses, as well as without losses, but also nonhomogeneous systems that do not allow for wave propagation [17].

SUPPLEMENT

Solution of the Riccatti Equation by Means of the Method of Successive Approximations

We transfer the quadratic member of the Riccatti equation (1) into the right-hand member:

$$R'(x) + 2i\varkappa(x)R(x) = \varkappa(x)[1 - R^2(x)]$$

and rewrite the equation, in accordance with formula (17.30) in work [9], in the form:

$$\frac{d}{dx}R(x)\,e^{i2\int_{x_0}^{x}\varkappa(x_1)\,dx_1} = \varkappa(x)[1 - R^2(x)]\,e^{i2\int_{x_0}^{x}\varkappa(x_1)\,dx_1}. \qquad (1^*)$$

We integrate expression (1*) within the limits x to ∞ and use the boundary condition $\lim_{x\to\infty} R(x)=0$. Restricting ourselves to weakly nonhomogeneous lines, we use the method of successive approximations (see [9], p. 197 and 200), taking the internal reflection factor to be small (that is, $|R|^2 \ll 1$). The zero approximation $R_0(x)=0$ is then for successive approximations ([9], formula (17.38)]:

$$R_n(x) = -e^{-i2\int_{x_0}^{x}\varkappa(x_1)\,dx_1}\int_{x}^{\infty}\varkappa(x_1)\left[1 - R_{n-1}^2(x_1)\right]e^{i2\int_{x_0}^{x_1}\varkappa(x_2)\,dx_2}\,dx_1. \qquad (2^*)$$

For convenience in comparing the calculation results by means of this method with the calculations according to the recurrent formulas in the article for the case under consideration of a nonhomogeneous line matched at its output (x=a), it is necessary to integrate expression (1*) not over x to ∞, but over x to a, and to use the boundary condition R(a)=0:

$$R_n(x) = -e^{-i2\int_{x_0}^{x}\varkappa(x_1)\,dx_1}\int_{x}^{a}\varkappa(x_1)\left[1 - R_{n-1}^2(x_1)\right]e^{i2\int_{x_0}^{x_1}\varkappa(x_2)\,dx_2}\,dx_1. \qquad (3^*)$$

In accordance with [9] (p. 204), we take $x_0=0$, that is, we presume that an arbitrary observation point is located on the entry plane. Then, instead of expression (3*), we have: /8

$$R_n(x) = -e^{-i2\int_{0}^{x}\varkappa(x_1)\,dx_1}\int_{x}^{a}\varkappa(x_1)\left[1 - R_{n-1}^2(x_1)\right]e^{i2\int_{0}^{x_1}\varkappa(x_2)\,dx_2}\,dx_1. \qquad (4^*)$$

In work [9] (p. 200), the internal reflection factor was taken at the input to the nonhomogeneous line (x=0), that is, $R_n(0)$, which, in the absence of a jump in characteristic impedances at x=0 when $\rho(0)=\rho_0$, will in accordance with (2) be equal to the input reflection factor r. At the same time, from expression (4*), we have:

$$R_n(0) = -\int_0^a \varkappa(x_1)\left[1 - R_{n-1}^2(x_1)\right] e^{i2\int_0^{x_1}\varkappa(x_2)\,dx_2}\,dx_1. \qquad (5^*)$$

In the present work, it was a line with homogeneous filler [$\varkappa'(x)=0$] that was under consideration. For this reason, from formula (4*) and (5*), we get:

$$R_n(x) = -e^{-i2\varkappa x}\int_x^a \varkappa(x_1)\left[1 - R_{n-1}^2(x_1)\right] e^{i2\varkappa x_1}\,dx_1, \qquad (6^*)$$

$$R_n(0) = -\int_0^a \varkappa(x_1)\left[1 - R_{n-1}^2(x_1)\right] e^{i2\varkappa x_1}\,dx_1. \qquad (7^*)$$

The computational formulas (48), (49), (50), and (51) are derived directly from (6*) and (7*). At the same time, in accordance with the explanation after formula (13b), it was accepted, as was done in work [9], that the internal reflection factor at the zero approximation[1] is equal to zero, that is, that $R_0(x)=0$.

[1]The approximation in geometrical optics that takes into consideration two waves not interacting between themselves.

BIBLIOGRAPHY

1. Ginzburg, V. L. Rasprostraneniye elektromagnitnykh voln v plazme [The Propagation of Electromagnetic Waves in a Plasma]. Fizmatgiz [State Publishing House of Literature on Physics and Mathematics], 1960.

2. Wait, J. Electromagnetic Waves in Stratified Media, Vol. 3. Pergamon Press, 1962.

3. Bremmer, H. Electromagnetic Theory and Antennas. Pergamon Press, 1963, p. 2.

4. Chen Jung Ming. J. Res. NBS, Vol. D-68, No. 6, 1964, p. 743.

5. Holmes, D. A. Proc. IEEE, Vol. 52, No. 2, 1964, p. 201.

6. Collin, R. E., Oliner, A. J. Res NBS, Vol. D-68, No. 4, p. 469.

7. Gans, R. Ann. der Physik [Annals of Physics], Vol. 47, 1915, p. 709.

8. Schelkunoff, S. A. Commun. Pure Appl. Math, Vol. 4, 1951, p. 117.

9. Brekhovskikh, L. M. Volny v sloistykh sredakh [Waves in Stratified Media]. Publishing House of the Academy of Sciences of the USSR, 1957.

10. Mirovitskiy, D. I. "Vzaimodeystviye poley v mikroskopicheskoy elektrodinamike" [Interaction Between Fields in Microscopic Electrodynamics], The Theses of Articles Presented at the 13th Conference of VZEI [All-Union Correspondence Power-Engineering Institute], 1963, p. 86.

11. Mirovitskiy, D. I. "Rasprostraneniye zvuka v neodnorodnoy srede i vnutrenniye usloviya" [Sound Propagation in a Nonhomogeneous Medium and the Internal Conditions], Acoustics Journal, Vol. 10, No. 1, 1964, p. 668. /8

12. Walter, K. IRE Trans., Vol. AP-8, No. 6, 1960, p. 608.

13. Mirovitskiy, D. I. "K zadache sinteza neodnorodnogo sloya i rasseivayushchey oblasti" [On the Problem of Synthesizing a Nonhomogeneous Layer and a Dispersing Area], Works of the VZEI, Issue 26, 1964, p. 48.

14. Mirovitskiy, D. I. "O dvukh variantakh zadachi sinteza opticheski neodnorodnogo sloya" [On Two Variants of the Synthesis Problem for an Optically Nonhomogeneous Layer], Optics and Spectroscopy, Vol. 18, No. 4, 1965, p. 668.

15. Matveev, N. M. "Metody integrirovaniya obyknovennykh differentsial'nykh uravneniy" [Methods for Integrating Normal Differential Equations], Higher Education, 1963.

16. Mors, F., Fëshbakh, G. Methods in Theoretical Physics, Vol. 2, Publishing House for Foreign Literature, 1960.

17. Budagyan, I. F., Mirovitskiy, D. I. "Primeneniye k zadache rasprostraneniya voln asimptoticheskikh metodov teorii nelineynykh kolebaniy" [The Application of Asymptotic Methods in the Theory of Nonlinear Oscillations for the Problem of Wave Propagation], Journal of PMTF [Applied Mechanics and Technical Physics], 1, 1966, p. 82.

18. Lyubarskiy, G. Ya., Povzner, A. Ya. Journal of Technical Physics, Vol. 29, No. 2, 1959, p. 170.

19. Mirovitskiy, D. I., Budyagyan, I. F. "Modifitsirovannyy metod korotkovolnovogo i dlinnovolnovogo preblizheniy" [A Modified Method for Short Wave and Long Wave Approximations], Theses of the Articles of the 15th Conference of the VZEI, 1965, p. 61.

20. Fel'dshteyn, A. L. "Sintez neodnorodnykh liniy po zadannym chastotnym kharakteristikam" [The Synthesis of Nonhomogeneous Lines According to Fixed Frequency Characteristics], Radio Technology, Vol. 6, No. 7, 1952.

21. Bolinder, E. Proc. IRE, Vol. 38, No. 11, 1950, p. 1354; Klopfenstein, R. W. Proc. IRE, Vol. 44, No. 1, 1956, p. 31.

22. Trikomi, F. Differentsial'nye uravneniya [Differential Equations]. Publishing House of Foreign Literature, 1962.

ON ONE METHOD FOR SOLVING EXTERIOR PROBLEMS IN ELECTRODYNAMICS /8

M. B. Zakson

A method for solving first and second boundary problems in electrodynamics, based on the application of single component Hertz vectors (Bromvich functions), is presented. The solution to the primal problems is demonstrated on the example of calculating several characteristics of planar antennas, and conversely, on the example of synthesizing linear antennas.

Introduction

As is well known [1, 2, 3, 4], in curvilinear systems with coordinates ξ, η, ζ, the Lamé coefficients which satisfy the Bromvich conditions are:

$$\frac{\partial}{\partial \zeta}\left(\frac{h_\xi}{h_\eta}\right)=0;\ h_\zeta=1,$$

the electromagnetic pole outside the regions occupied by the sources may be taken in the form of a superposition of electrical (TM) and magnetic (TE) waves [Translator's note: It is possible that the author transposed the symbols "TM" and "TE"]. These waves are completely determined by appropriate single component Hertz vectors, scalar Bromvich functions.

As has been demonstrated, only two kinds of coordinate systems satisfy the conditions mentioned here: generalized cylindrical coordinate systems and generalized spherical coordinate systems. The Lamé coefficients of these kinds of systems can be taken in the form: $h_\xi=M(\zeta)h_1(\xi,\eta)$; $h_\eta=M(\zeta)h_2(\xi,\eta)$. Despite this restriction, the Bromvich functions have found application in solving a series of important problems in electrodynamics.

In the present work, a method for determining, according to assigned sources, the electromagnetic field in the form of a superposition of TM and TE waves is presented, and in addition, several possibilities for solving exterior problems in electrodynamics for this case are demonstrated.

Formulating the Problem. Baseline Formulas

We shall search for an electromagnetic field of fixed sources in the exterior region V_e, limited within by the surface, $\zeta=\frac{L}{2}$, and by one or more surfaces s,

determined by equations of the form $f(\xi,\eta)=0$. At the same time, we assume /8
that in the case $\zeta>\frac{L}{2}$, one of the following two conditions is realized:

$$E_\tau|_s = 0, \qquad \text{(I)}$$

or:

$$H_\tau|_s = 0. \qquad \text{(II)}$$

Sources for an electromagnetic field are found in the region restricted by the surfaces s_1 and $\zeta=\frac{L}{2}$. They consist of the steady volume currents $\underline{j}$, as well as of sources disposed along the surface s_1: in the case of condition (I), tangential components of the vector $\underline{E}_0$, and in the case of condition (II), tangential components of the vector $\underline{H}_0$.

In this way, condition (I) corresponds to the first boundary problem in electrodynamics, and condition (II) to the second.

In the region V_e, the Bromvich functions may be taken in the following form (the time dependency is expressed as $e^{\omega t}$):

$$\left.\begin{aligned} U(\xi,\eta,\zeta) &= \sum_{n=0}^{\infty} A_n \psi_{en}(\xi,\eta) q_{en}^{(2)}(\zeta) \\ V(\xi,\eta,\zeta) &= \sum_{n=0}^{\infty} B_n \psi_{hn}(\xi,\eta) q_{hn}^{(2)}(\zeta) \end{aligned}\right\}, \qquad (1)$$

where A_n and B_n are complex amplitudes of the respective electric and magnetic waves, and the functions ψ_n and q_n satisfy the well-known equations in the work cited [2].

The boundary conditions for the functions $\psi_n(\xi,\eta)$ in the case of conditions (I) are:

$$\psi_e^{(I)}|_s = 0; \quad \left.\frac{d\psi_h^{(I)}}{\partial n}\right|_s = 0, \qquad (2)$$

and in the case of conditions (II):

$$\psi_h^{(II)}|_s = 0; \quad \left.\frac{d\psi_e^{(II)}}{\partial n}\right|_s = 0. \qquad (3)$$

For determining the amplitudes A_n and B_n, we shall apply a method similar to the one described in work [5], which is a modification of the method of Ya. N. Fel'd [6].

The sought for amplitudes are expressed as: /8

$$\left.\begin{aligned} A_n^{(I)} &= -\frac{\int_{v_i} \mathbf{j}\,\mathbf{e}_{vn}^{(I)}\,dv - \int_{s_i} [\mathbf{E}_0,\ \mathbf{h}_{en}]\,ds}{i\omega\varepsilon\varkappa_{en}^2\,\gamma_{en}^{(I)}\,W\left[q_{en}^{(1)},\ q_{en}^{(2)}\right]} \\ B_n^{(I)} &= -\frac{\int_{v_i} \mathbf{j}\,\mathbf{e}_{hn}^{(I)}\,dv - \int_{s_i} [\mathbf{E}_0,\ \mathbf{h}_{hn}]\,ds}{i\omega\mu\varkappa_{hn}^2\,\gamma_{hn}^{(I)}\,W\left[q_{hn}^{(1)},\ q_{hn}^{(2)}\right]} \\ A_n^{(II)} &= -\frac{\int_{v_i} \mathbf{j}\,\mathbf{e}_{en}^{(II)}\,dv + \int_{s_i} \mathbf{j}_s\,\mathbf{e}_{en}^{(II)}\,ds}{i\omega\varepsilon\varkappa_{en}^2\,\gamma_{en}^{(II)}\,W\left[q_{en}^{(1)},\ q_{en}^{(2)}\right]} \\ B_n^{(II)} &= -\frac{\int_{v_i} \mathbf{j}\,\mathbf{e}_{hn}^{(II)}\,dv + \int_{s_i} \mathbf{j}_s\,\mathbf{e}_{hn}^{(II)}\,ds}{i\omega\mu\varkappa_{hn}^2\,\gamma_{hn}^{(II)}\,W\left[q_{hn}^{(1)},\ q_{hn}^{(2)}\right]} \end{aligned}\right| \qquad (4)$$

where $\underline{j}_s$ is the surface current density,

$$\delta_n = \int |\psi_n(\xi,\tau)|^2\,ds,$$

$\underline{e}$, $\underline{h}$ -- are voltage vectors of the auxiliary field in the regions ν_e and ν_i excited at infinity and satisfying the boundary conditions (I) or (II) on the surfaces s and s_i and the Wronskian:

$$W\left[q_n^{(1)},\ q_n^{(2)}\right] = q_n^{(1)}(\zeta)\frac{dq_n^{(2)}(\zeta)}{d\zeta} - q_n^{(2)}(\zeta)\frac{dq_n^{(1)}(\zeta)}{d\zeta}.$$

In the case $M(\zeta)\equiv 1$ (generalized cylindrical coordinate system), the expressions for $A_n^{(I)}$ and $B_n^{(I)}$ are converted into the calculational formulas for the excitation of normal waveguides with ideally conducting walls [5], and the expressions for $A_n^{(II)}$ and $B_n^{(II)}$ are converted into the formulas for the excitation of waveguides with walls possessing infinite permeance.

At $M(\zeta)\equiv\zeta$ (generalized spherical coordinate system), the expressions derived can be applied in the theory of antennas. These relationships may be directly employed for solving primal and inverse problems in electrodynamics.

Applications of the Relationships Derived in the Theory of Antennas

The results derived may be applied both in the general theory of antennas, as well as in calculating characteristics of several types of radiating devices.

The representation of an electromagnetic field of an antenna in the form of the superposition of TE and TM waves creates in a series of cases additional possibilities for investigations, calculations, and the physical treatment of phenomena in the theory of antennas. /8

We shall examine the field of a planar antenna disposed within the limits of a sphere with a radius $\frac{L}{2}$, whose center is the zero point of the spherical coordinate system r, Θ, ϕ. It is apparent that the electromagnetic field of diffraction antennas in the form of apertures of any arbitrary shape in an infinite, ideally conducting plane with a fixed field $\underline{E}_0$ satisfies condition (I), and that condition (II) is met by a field of infinitely thin, planar continuous and discrete radiators with a fixed current density $\underline{j}_s$. The section of the plane occupied by the antenna aperture is the surface s_j in this given case.

In a spherical coordinate system, the Bromvich functions have the form:

$$\left.\begin{aligned} U(r,\ \Theta,\ \varphi) &= \sum_{l=1}^{\infty}\sum_{m=0}^{l} A_{lm}\left|\begin{matrix}\sin m\varphi\\ \cos m\varphi\end{matrix}\right. \sqrt{kr}\, H^{(2)}_{l-\frac{1}{2}}(kr)\, P_l^{(m)}(\cos\Theta)\\ V(r,\ \Theta,\ \varphi) &= \sum_{l=1}^{\infty}\sum_{m=0}^{l} B_{lm}\left|\begin{matrix}\cos m\varphi\\ \sin m\varphi\end{matrix}\right. \sqrt{kr}\, H^{(2)}_{l+\frac{1}{2}}(kr)\, P_l^{(m)}(\cos\Theta) \end{aligned}\right| \quad (5)$$

Denoting $a_{lm} = \sqrt{\frac{2}{\pi}} e^{-i\frac{l-1}{2}\pi} A_{lm}$, $b_{lm} = \sqrt{\frac{2}{\pi}} e^{-i\frac{l-1}{2}\pi} B_{lm}$,

we derive the following expressions for the Bromvich functions in a further zone:

$$\left.\begin{aligned} U(r,\ \Theta,\ \varphi) &= e^{-ikr}\sum_{l=1}^{\infty}\sum_{m=0}^{l} a_{lm}\, P_l^{(m)}(\cos\Theta)\left|\begin{matrix}\sin m\varphi\\ \cos m\varphi\end{matrix}\right.\\ V(r,\ \Theta,\ \varphi) &= e^{-ikr}\sum_{l=1}^{\infty}\sum_{m=0}^{l} b_{lm}\, P_l^{(m)}(\cos\Theta)\left|\begin{matrix}\cos m\varphi\\ \sin m\varphi\end{matrix}\right. \end{aligned}\right| \quad (6)$$

The amplitudes A_{1m} and B_{1m} may be calculated according to (4), after which the Bromvich functions may be found, and then consequently, both in the further

zone [see expression (6)], as well as in the near zone [according to formula (5)].

The expressions derived in this way make it possible also to calculate the full radiating power:

$$P_{\Sigma} = 2k^2 \sum_{l=1}^{\infty} \frac{l(l+1)}{l+\frac{1}{2}} \left\{ \sqrt{\frac{\varepsilon}{\mu}} |A_{l_0}|^2 - \sqrt{\frac{\mu}{\varepsilon}} |B_{l_0}|^2 - \right.$$
$$\left. - 2 \sum_{m=1}^{l} \frac{(l-m)!}{(l-m)!} \left(\sqrt{\frac{\varepsilon}{\mu}} |A_{l_m}|^2 + \sqrt{\frac{\mu}{\varepsilon}} |B_{l_m}|^2 \right) \right\}. \qquad (7)$$

At the same time, it is necessary to take into account that $A_{1_0}^{(I)}=0$ and $B_{1_0}^{(II)}=0$.

We shall examine in further detail linear antennas. We shall analyze the case of an infinitely thin wire antenna of length L, disposed along the z-axis, /8 with current I(z). Its center is disposed as the center of a spherical coordinate system. In this case, m=0 and $B^{(II)}=0$.

The magnetic field for these kinds of antennas in the far zone may be represented in the form:

$$H_{\varphi} = i\omega\varepsilon \sqrt{\frac{2}{\pi}} \frac{e^{-ikr}}{r} \sum_{l=1}^{\infty} A_l P_l^{(1)}(\cos\theta) e^{-i\frac{l\pi}{2}}.$$

The amplitudes of the electric wave types:

$$A_l = \frac{\int_{-\frac{L}{2}}^{+\frac{L}{2}} I(z) e_{l_z}(z)\, dz}{16k^2 \sqrt{\frac{\varepsilon}{\mu}} \frac{l(l-1)}{2l-1}} \quad (l = 1, 2, 3 \ldots),$$

where:

$$l_{l_z}(z)|_{z>0} = \frac{2l(l-1)}{z^2} \sqrt{kz}\, J_{l-\frac{1}{2}}(kz),$$

$$l_{l_z}(z)|_{z<0} = (-1)^{l-1} \frac{2l(l-1)}{z^2} \sqrt{k|z|}\, J_{l+\frac{1}{2}}(k|z|)$$

the value of the z-th component of the electric field vector of the wave TM_{10} along the z-axis.

In this way:

$$A_l = 15\pi(2l+1)\int_{-\frac{L}{2}}^{\frac{L}{2}} \left(\frac{z}{\frac{L}{2}}\right)^{l+1} I(z)\frac{J_{l+\frac{1}{2}}(kz)}{(kz)^{\frac{1}{2}}}dz. \qquad (10)$$

In the case of an even current distribution [symmetrical antenna with current I(z)=I(-z)], only odd waves l=2q+1 remain, and the expression for the amplitudes takes the form:

$$A_{2q+1} = 60\pi\left(2q+\frac{3}{2}\right)\int_0^{\frac{L}{2}} I(z)\frac{J_{2q+\frac{3}{2}}(kz)}{(kz)^{\frac{3}{2}}}dz. \qquad (11)$$

If the antenna consists of N discrete radiators (dipole) of length dL with currents I_n, disposed at the points z_n, then the amplitudes are:

$$A_l = 15\pi(2l+1)\sum_{n=1}^{N}\left(\frac{z_n}{|z_n|}\right)^{l+1} p_n\frac{J_{l+\frac{1}{2}}(kz_n)}{(kz_n)^{\frac{1}{2}}}, \qquad (12)$$

where $p_n = I_n dL$.

With a symmetrical array and even N: /9

$$A_{2q+1} = 60\pi\left(2q+\frac{3}{2}\right)\sum_{n=1}^{\frac{N}{2}} p_n\frac{J_{2q+\frac{3}{2}}(kz_n)}{(kz_n)^{\frac{3}{2}}}. \qquad (12)$$

We shall examine briefly the problem of the number of wave types that must be taken into account in the calculation. As was shown above, a radiator p disposed at point z excites an l-th wave type with the amplitude:

$$A_l = 15\pi(2l+1)\frac{J_{l+\frac{1}{2}}(kz)}{(kz)^{\frac{1}{2}}}p.$$

If $kz=\alpha(l+\frac{1}{2})$ $(0<\alpha<)$, then in accordance with [7], we get:

$$A_l \approx \frac{15\sqrt{2\pi}}{kz}\frac{(\alpha e^{\beta})^{(l+\frac{1}{2})}}{\sqrt{2\pi(l+\frac{1}{2})}}p, \qquad (13)$$

where $\beta=\sqrt{1-\alpha^2}$.

It is obvious that at l>kz, with an increase in the index l, the wave

amplitude abruptly decreases. In this way, in addition to the wave types with indices less than kz, there are practically sufficient restrictions in terms of only a few wave types having indices greater than kz.

Consequently, if we take into consideration a linear antenna of length L whose center is disposed at point z=0, then, as a rule, it is possible to restrict oneself to wave types with amplitudes whose indices are smaller than $\frac{kL}{2}$+(2 to 4). An exception involves cases with superdirective antennas ("small-dimension antennas"), where it is necessary to consider waves of higher types with larger indices. The high directionality in these kinds of antennas is caused by the excitation of these kinds of waves. In order to derive the necessary amplitudes of the higher wave types, the value of the current I (or p) in these kinds of antennas, as follows from formula (13), must be sharply increased in comparison with antennas of normal dimensions. However, the necessity of observing the required relationship between amplitudes of all existing wave types (including also low wave types) leads to a feature characteristic for these kinds of antennas of variable-phase current distribution along the antenna and supplementary increases in the current amplitudes.

The Synthesis and Design of Linear Antennas

As was mentioned above, the relationships derived may be applied in solutions for inverse problems in electrodynamics, that is, a determination of a principle of source distribution according to assigned fields in space. We shall examine /9
the essence of the solution method for these kinds of problems using the example of the synthesis of discrete, linear antennas. For the sake of simplicity of explanation, we shall limit ourselves to cases of symmetrical radiation pattern diagrams, for which the Bromvich functions contain only odd wave types.

Introducing the variable x=cosθ, we represent the fixed radiation pattern diagram in the form of an angular multiplier of the Bromvich function $U(x) \in L^2$ [-1, 1]. At the same time, as is well known, the function U(x) may be interpreted in the sense of a convergence on the average along the section [-1, 1] to a series according to Legendre polynomials. In this way:

$$U(x) = \sum_{n=1}^{\infty} a_{2n-1} P_{2n-1}(x). \qquad (11)$$

We shall introduce the coefficients $A_{2q+1} = a_{2q+1} \sqrt{\frac{\pi}{2}} (-1)^q$

The Bromvich function for the given field in the far zone takes a form corresponding to expression (6) for the case m=0:

$$U(x, r) = e^{-ikr} \sqrt{\frac{2}{\pi}} \sum_{q=0}^{\infty} (-1)^q A_{2q+1} P_{2q+1}(x) \qquad (11)$$

We represent the linear antenna being synthesized in the form of a series of N dipoles disposed at the points $\pm z_n$. The amplitudes A_{2q+1} in this case are determined by expression (12), and the problem reduces to finding the values of p_n. Above all, we should note the possibilities for an approximation solution to the problem. Taking the given function U(x) in the form of a finite series:

$$U_Q(x) = \sum_{q=0}^{Q-1} a_{2q+1} P_{2q+1}(x)$$

and assigning a number of dipoles N=2Q in the antenna being sought, such that:

$$A_{2q+1} = 60\pi \left(2q + \frac{3}{2}\right) \sum_{n=1}^{\frac{N}{2}} p_n \frac{J_{2q+\frac{3}{2}}(kz_n)}{(kz_n)^{\frac{3}{2}}}$$

we reduce the synthesis problem to solving a system composed of $Q=\frac{N}{2}$ equations with the same number of unknown p_n.

From what has been analyzed above, it follows that in determining the number N, it is necessary to take into account, in particular, the dimensions of the antenna, in order that the waves excited by the antenna being synthesized with amplitudes $A_{2q+1}\Big|_{q \geq \frac{N}{2}}$ can be ignored. It is especially necessary to take care in doing this and in checking for the synthesis of superdirective antennas.

It should be noted that this method of solution can also be convenient for /9 synthesizing nonequivalent arrays.

For the synthesis problem, it is also possible to apply a method of solving a system of linear equations.

We take the given function U(x) in the form of a finite harmonic series:

$$U(x) = \sum_{n=1}^{\frac{N}{2}} C_n \sin nax, \qquad (17)$$

where $a=\frac{2\pi}{T}$, T being the expansion period:

$$C_n = \frac{2}{T}\int_{-\frac{T}{2}}^{\frac{T}{2}} U(x)\sin naxdx.$$

Equalizing the right members of expressions (14) and (17) to each other, multiplying them by $P_{2q+1}(x)$, and integrating with respect to x across the intervals -1 to +1, we get, taking into account [8]:

$$A_{2q+1} = -\left(2q-\frac{3}{2}\right) = \sum_{n=1}^{\frac{N}{2}} C_n \frac{j_{2q+\frac{3}{2}}(an)}{\sqrt{an}}. \qquad (18)$$

Comparing the derived expression with formula (12), we note that if $kz_n=an$, then:

$$p_n = -\frac{ja\,C_n}{60}. \qquad (19)$$

The antenna being synthesized in this case is an equivalent array of dipoles disposed at the points $z_n=\pm\frac{an}{k}$.

The antenna length $L=\frac{aN}{k}$.

BIBLIOGRAPHY

1. Bromvich, T. Phyl. Mag., 38, 223, 1919, p. 143.

2. Kisun'ko, G. B. Elektrodinamika polykh sistem [The Electrodynamics of Field Systems]. VKAS [expansion unknown] publishers, Leningrad, 1949.

3. Borgnis. Ann. D. Physik [Annals of German Physics], 35, 1939, p. 276.

4. Louie de Broglie. Elektromagnitnye volny v volnovodakh i rezonatorakh [Electromagnetic Waves in Waveguides and Resonators]. Publishing House of Foreign Literature, 1948.

5. Zakson, M. B. Articles from the Academy of Sciences, No. 4, Vol. 66, 1949.

6. Fel'd, Ya. N. Osnovnye teorii shchelevykh antenn [Basic Theories in Slot Antennas]. Soviet Radio Publishing House, 1948.

7. Vatson, G. N. Teoriya besselevykh funktsiy [The Theory of Bessel Functions], No. 1. Publishing House of Foreign Literature, 1949.

OPTIMAL DIFFERENTIAL ELECTRIC FIELD DISTRIBUTIONS IN AN ANTENNA APERTURE /9

R. A. Konoplëv, L. N. Zakhar'ev

Formulas are derived for optimal field distributions in an aperture assuring the maximum magnitude and slope for the major lobes in a differential radiation pattern for a broad class of antennas.

Introduction

This article is dedicated to finding optimal field distributions in an antenna aperture creating a radiation pattern of the differential type. The amplitude-phase electric field distribution is optimized in accordance with the demands to generate maximum values for the slope in an equisignal direction and amplitudes for the main maxima in an antenna's differential radiation pattern.

Optimal electric field distributions make it possible to find the maximum possible achievable parameters for antenna equipment. Comparing them with parameters derived from actual equipment, it is possible to give an objective estimation of the quality of development. Together with this, an optimal distribution may serve as a limit, towards which there is a convergence in selecting an actual distribution. In several cases, for example, in constructing multielement antenna arrays, the optimal distributions can be directly applied.

A large number of articles, written both in the USSR and abroad, is dedicated to the problem of optimizing electric field distribution in an antenna aperture. Thus, in the works [1, 2, 3, 4], field distributions in linear and round apertures are found which realize a minimum level of side lobes and a maximum kpd [efficiency factor]. Several generalizations and advances have been generated in the works cited [1, 2, and 5, 6]. In works [7, 8], optimal coefficients of excitation for a finite number of wave types in a reflector radiator have been determined, which make it possible to derive extrema features for overall differential radiation patterns for a reflector antenna. In the works cited [1, 9], coefficients of excitation for an equidistant antenna array are optimized. /9

Some results in the present work are well known, in particular, the optimality

of a linear electric field distribution in an antenna aperture for a maximum slope in the differential radiation pattern, and these results will be presented here only for the sake of filling out the analysis.

Maximum Slope of a Differential Radiation Pattern for a Linear Aperture

The electric field distribution in an antenna aperture creating a differential radiation pattern is written in the form of a trigonometric series:

$$A(x) = \sum_{n=1}^{\infty} B_n \sin n\pi x, \qquad (1)$$

where x is the relative coordinate in the antenna aperture, B_n are unknown constant coefficients.

The radiation pattern R(u) corresponding to distribution (1) may be calculated using the integral relationship:

$$R(u) = \int_{-1}^{1} A(x) e^{iux} dx, \qquad (2)$$

where $u=\kappa a \sin\theta$, $\kappa=\frac{2\pi}{\lambda}$ is the wave number, a is half the antenna aperture, and θ is an angle taken from the normal to the antenna aperture.

Substituting expression (1) into formula (2), and integrating it, we get:

$$R(u) = \frac{2\pi}{i} \sin u \sum_{1}^{\infty} (-1)^n \frac{nB_n}{u^2-(n\pi)^2}. \qquad (3)$$

Differentiating this expression with respect to u and taking u=0, we find a formula for the slope of the differential radiation diagram S in the equisignal direction:

$$S = \frac{2i}{\pi} \sum_{1}^{\infty} (-1)^n \frac{B_n}{n}. \qquad (4)$$

The coefficients B_n must satisfy the normalization condition $\int_{-1}^{1} A^2(x)\,dx = P_\Sigma$. Here, p_Σ is the full power radiated (received) by the antenna. In what is to follow, we shall take $P_\Sigma=1$. At the same time, the normalization condition may be written in the form:

$$\int_{-1}^{1} A^2(x)\,dx = 1.$$

Taking formula (1) into account, this condition is expressed as:

$$\sum_{1}^{\infty} B_n^2 = 1. \qquad (6)$$

The Lagrange method is used for finding the conditional extremum. We shall introduce the new function:

$$\Phi(B_n, \mu) = F(B_n) - \mu g, \qquad (7)$$

where $g=\Sigma B_n^2-1$ is the normalization condition, μ is an undetermined multiplier.

The condition of the function extremum $\Phi(B_n,\mu)$ yields a system of equations with unknown B_n and μ:

$$\left.\frac{\partial \Phi}{\partial B_n} = 0,\ g = 0\right|. \qquad (8)$$

Using the second equation from the system so generated, we determine:

$$B_n = -\frac{2}{\pi}(-1)^n \frac{1}{2n}. \qquad (9)$$

The undetermined multiplier μ is found from the normalization condition:

$$\mu = \sqrt{-\frac{1}{\pi^2}\sum_{1}^{\infty}\frac{1}{n^2} - \frac{1}{12}}. \qquad (10)$$

In this way, the electric field distribution in a linear aperture that assures a maximum slope S in the equisignal direction is:

$$A(x) = -\frac{\sqrt{6}}{\pi}\sum_{1}^{\infty}(-1)^n \frac{\sin n\pi x}{n}. \qquad (11)$$

This expression may be easily transformed into the form:

$$A(x) = \sqrt{\frac{3}{2}}\, x. \qquad (12)$$

The linear distribution (12) is transformed in accordance with expression (2) into the radiation pattern:

$$R(u) = \sqrt{6}\,\frac{\sin u - u\cos u}{u^2}, \qquad (13)$$

which is pictured in Fig. 1. The characteristics of this radiation pattern are:

$$S(0) = 0{,}82; \quad f_{\text{макс}} = 1{,}07; \quad u_{\text{макс}} = 2{,}081.$$

The value of S(0) is given in dimensionless units. The slope is given in absolute units:

$$Sa = 0{,}82\ ka. \qquad (14)$$

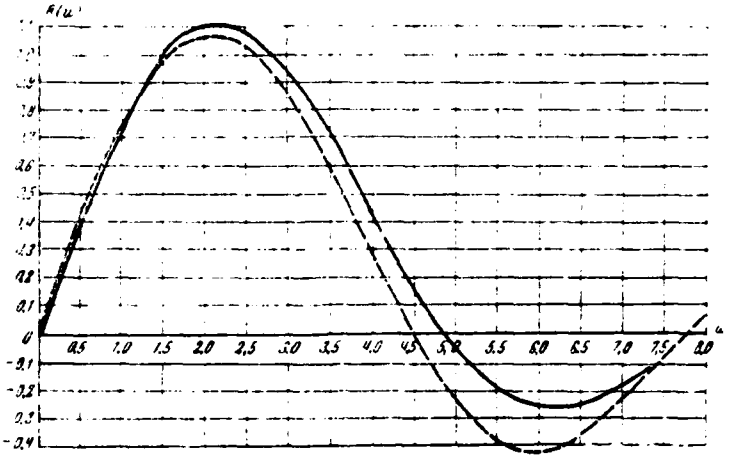

Fig. 1. Optimal radiation patterns for a linear aperture:
– – – – – with maximum slope at u=0;
———·· · with a maximum level of the first lobe.

/9

The Highest Value of the First Lobe of a Differential Radiation Pattern for a Linear Aperture

We shall determine the electric field distribution in an antenna aperture by means of the conditions for deriving the greatest value of the first maximum of a differential radiation diagram. We shall find an auxiliary function using expressions (3) and (6) in accordance with the demands of the problem:

$$\Phi(u, B_n, \mu) = f(uB_n) - \mu\left(\sum_1^\infty B_n^2 - 1\right) = 0. \qquad (15)$$

The conditions of the extremum of function Φ will give a system of equations:

$$\left.\begin{aligned} &\frac{\partial \Phi}{\partial B_n} = 0,\ \frac{\partial \Phi}{\partial u} = 0,\ g = \sum_1^\infty B_n^2 - 1 = 0 \\ &n = 1, 2 \ldots \end{aligned}\right\}. \qquad (16)$$

Solving this system, we find: /9

$$B_n = \frac{i\pi}{\mu}(-1)^n \frac{n \sin U_m}{U_m^2 - (n\pi)^2}. \qquad (17)$$

For finding the value $u=U_m$, the corresponding maximum of the radiation pattern, it is necessary to solve a quite complex transcendental equation $\frac{\partial \Phi}{\partial u}=0$, in which the coefficients have the optimal values (17). However, this problem may

be resolved by means of a simpler method. In fact, the coefficients found according to formula (17), with an accuracy to within the value of the constant multiplier, are in agreement with the coefficients of an expansion of the function into a Fourier series: $A(x) = N \sin Vx,\ V = U_{макс}.$ (18)

From condition (5), it follows that:

$$N = \frac{1}{\sqrt{1 - \frac{\sin 2V}{2V}}}. \quad (19)$$

The radiation pattern corresponding to the distribution according to (18) has the form:

$$R(u) = \frac{1}{\sqrt{1 - \frac{\sin 2V}{2V}}}\left[\frac{\sin(u-V)}{u-V} - \frac{\sin(u+V)}{u+V}\right]. \quad (20)$$

It is now necessary to determine the optimal value of V and the value u to which corresponds the maximum of the radiation pattern. From considerations of symmetry, it follows that expression (20) reaches a maximum at V=u. In this way, it is sufficient to determine the maximum of the function in the following manner:

$$R(uV)|_{u=V} = \sqrt{1 - \frac{\sin 2V}{2V}}. \quad (21)$$

Taking the derivative of expression (21) equal to zero, we arrive at the transcendental equation:

$$\operatorname{tg} 2V = 2V, \quad (22)$$

the solution to which is V=2.247. This solution could have been generated directly from the system of equations:

$$R'_u(u, V) = 0,\ R'_V(u, V) = 0. \quad (23)$$

It is easy to convince oneself that this is the case if the value u=V=2.247 be substituted into equation (23). The optimal radiation pattern is shown in Fig. 1. Its basic parameters are: S(0)=0.78, R_M=1.103, U_M=2.247.

Maximum Slope of a Differential Radiation Pattern with a Round Aperture /9

We shall examine a planar round aperture, in which an arbitrary field is assigned:

$$A(r, \varphi) = \sum_{0}^{\infty} \sum_{1}^{\infty} (A_{ml} \cos m\varphi + B_{ml} \sin m\varphi) J_m(\alpha_{ml} r), \qquad (24)$$

where A_{ml}, B_{ml} are unknown coefficients, J_m is the Bessel function, α_{ml} is the 1-th root of the equation $J_m(x)=0$.

The radiation pattern (Fig. 2) may be written in the form:

$$D(\Theta, \psi) = \int_{-\pi}^{\pi} \int_{0}^{1} A(r\varphi) e^{iur\cos(\varphi-\psi)} r dr d\varphi. \qquad (25)$$

where $u=\kappa a \sin\Theta$; $a=1$.

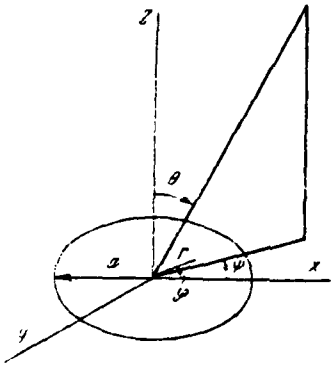

Fig. 2. Round aperture.

We shall examine the radiation pattern in a fixed plane, for example in the plane $\psi=\frac{\pi}{2}$:

$$R(u) = \int_{-\pi}^{\pi} \int_{0}^{1} A(r\varphi) e^{iur\sin\varphi} r dr d\varphi. \qquad (26)$$

In this plane, only those members of the amplitude distribution (24) which contain the multiplier $\sin m_{\phi}$ have an influence on the formation of the differential radiation pattern, and for this reason we get:

$$A_{ml} = 0. \qquad (27)$$

Taking expression (27) into account, the radiation pattern may be expressed thusly:

$$R(u) = \frac{\pi}{i} \sum_{l=1}^{\infty} \sum_{m=0}^{\infty} B_{ml} [(-1)^m - 1] \frac{\alpha_{ml} J_{m-1}(\alpha_{ml}) J_m(u)}{u^2 - \alpha_{ml}^2}. \qquad (28)$$

It is clear from this that only odd numbered harmonics contribute to the differential radiation pattern. We shall calculate the slope of the radiation pattern [formula (5)] in the equisignal direction. Taking into account that:

$$J_m^{-1}(0) = \begin{cases} 0 \text{ when } m \neq 1 \\ \frac{1}{2} \text{ when } m = 1 \end{cases}, \qquad (29)$$

we get:

/9

$$S = f(0) = -\pi i \sum_{0}^{\infty} B_{1l} \frac{J_0(z_{1l})}{z_{1l}}. \qquad (30)$$

The normalization condition, similar to condition (5), is written in the form in this case:

$$\int_{-\pi}^{\pi}\int_{0}^{1} A^2(r, \varphi)\, r dr d\varphi = -\sum_{0}^{\infty} \frac{\pi}{2} B_{1l}^2 J_2(z_{1l}) J_0(z_{1l}) = 1. \qquad (31)$$

In order to determine the coefficients assuring a maximum slope S, we construct the auxiliary function:

$$\Phi(B_{1l}, \mu) = F(B_{1l}) + \mu g, \qquad (32)$$

where $g = \frac{\pi}{2} \sum_{0}^{\infty} B_{1l}^2 J_2(z_{1l}) J_0(z_{1l}) - 1 = 0.$

In accordance with the Lagrange method, we have the system of equations:

$$\left.\frac{\partial \Phi}{\partial B_{1l}} = 0,\ g = 0\right|, \qquad (33)$$

whose solution is found:

$$B_{1l} = -\frac{i}{\mu} \frac{1}{z_{1l} J_2(z_{1l})}. \qquad (34)$$

In this way:

$$A(r\varphi) = -\frac{i}{\mu} \sin\varphi \sum_{0}^{\infty} \frac{J_1(z_{1l} r)}{z_{1l} J_2(z_{1l})}. \qquad (35)$$

From a comparison of this expression with the well-known expansion:

$$r = 2 \sum_{0}^{\infty} \frac{J_1(z_{1l} r)}{z_{1l} J(z_{1l})}, \qquad (36)$$

it follows that with the normalization:

$$A(r\varphi) = \frac{2}{\sqrt{\pi}} r \sin\varphi = \frac{2}{\sqrt{\pi}} y, \qquad (37)$$

with an accuracy to within the value of the constant multiplier, this expression is in agreement with the optimal amplitude distribution of an antenna having a linear aperture. The radiation pattern corresponding to distribution (37):

$$R(u) = 4\sqrt{\pi} \frac{J_2(u)}{u}, \qquad (38)$$

is pictured in Fig. 3. The basic parameters of this graph are: S(0)=0.88; /1

f_M=1.26; U_m=2.3.

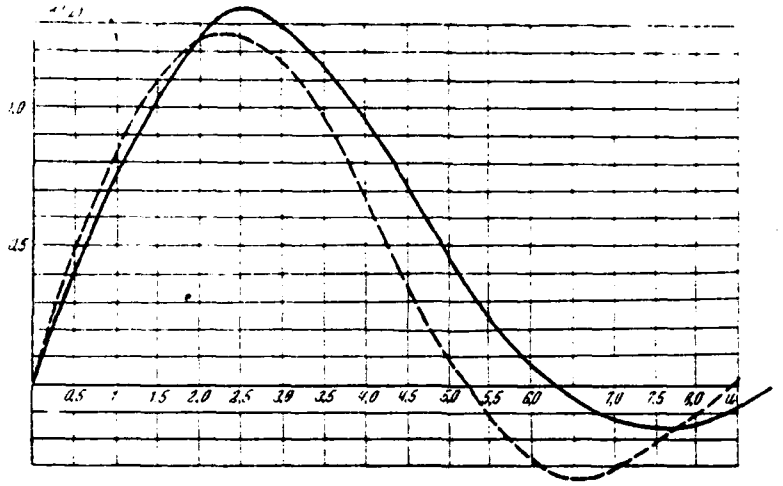

Fig. 3. Optimal radiation patterns for a round aperture:
– – – – – with maximum slope at u=0;
———— with a maximum level of first lobe.

Maximizing the Amplitude of the Major Lobes of a Differential Radiation Pattern

We shall turn once again to a radiation pattern [formula (28)] formed by an arbitrary electric field distribution [formula (24)] in a round antenna aperture, and we shall select amplitudes B_{ml} of the field disposition in the aperture in such a way that when fulfilling the normalization condition:

$$g = \sum_{m=0}^{\infty} \sum_{l=0}^{\infty} \pi B_{ml}^2 \int_0^1 J_m^2(z_{ml} r)\, r dr - 1 = 0 \qquad (39)$$

a round aperture will create a differential radiation pattern with a maximum amplitude of the major lobes. As earlier, we shall use the Lagrange method and introduce the auxiliary function:

$$\Phi(B_{ml}, u, \mu) = f(u, B_{ml}) + \mu g.$$

Setting the derivative of the auxiliary function in terms of B_{ml}, u, and μ equal to zero, we generate a system of equations for finding B_{ml}, U_M and μ (U_M is the value corresponding to the direction of the principal maximum of the radiation pattern):

$$\left.\frac{\partial \Phi}{\partial B_{ml}} = 0,\ \frac{\partial \Phi}{\partial u} = 0,\ g = 0\right\}.$$

From this system of equations, it follows that:

$$B_{ml} = \frac{1}{V} \frac{[(-1)^m - 1]\, x_{ml} J_m(V)}{(V^2 - x_{ml}^2) J_{m\pm1}(x_{ml})}. \qquad (40)$$

In expression (40), the value $V=U_M$ is the solution to the transcendental equation derived by substituting the found values of B_{ml} into the equation $\frac{\partial \Phi}{\partial u}$. The solution to this equation represents substantial difficulties; however, the value V may be found by means of an indirect method.

It turns out that if the function:

$$A(r, \varphi) = \sin(Vr \sin\varphi) \qquad (41)$$

is expanded into a series similar to series (24), the coefficients of the expansion derived with an accuracy to within the value of the constant multiplier are in agreement with expression (40). From this, it follows that the electric field distribution (41) is optimal, that is, it assures a maximum value for the first lobe in the differential radiation pattern. The radiation pattern corresponding to the optimal field distribution has the form:

$$R(u) = \frac{1}{\sqrt{1 - \frac{J_1(2V)}{V}}} \left[\frac{J_1(u-V)}{u-V} - \frac{J_1(u+V)}{V+u}\right]. \qquad (42)$$

The value $V=U_{макс}$ is determined in the same way as in the foregoing case.

We take u=V and find the value V at which R(V) reaches a maximum value. For this, we solve the equation:

$$\frac{\partial R(V)}{\partial V} = \frac{\partial}{\partial V}\left[\sqrt{\frac{\pi}{2}} \sqrt{1 - \frac{J_1(2V)}{V}}\right] = 0. \qquad (43)$$

This equation reduces to the transcendental equation:

$$J_1(2V) = -J_3(2V), \qquad (44)$$

from which it follows that V=2.568. Thus, the value for the first maximum of the radiation pattern is $R_M(u)=1.33$, and the slope of the radiation pattern in the equisignal direction is S(0)=0.82.

The graph of the optimal radiation pattern is presented in Fig. 3.

The Case of an Arbitrary Aperture

Comparing the results derived earlier, it is not difficult to note that the character of an optimal field distribution does not change with the transition

from a linear aperture to a round aperture. A similar result may be derived for a square aperture. From this, it follows that the optimal field distribution under /1
consideration here does not in general depend on the shape of the aperture. Another special feature of the derived optimal distributions is their dependency on the coordinate of the plane (x=0) in which the differential radiation pattern is formed. This is explained by the fact that the optimal field distribution must assure a maximum orientation in the plane y=0, which is achieved with a uniform field distribution along the x-coordinate in the antenna aperture (Fig. 2).

We shall attempt to generalize the presumption made with respect to the optimal field distribution for an arbitrary aperture using the example of deriving the maximum slope. We shall consider that a field distribution depends only on the y-coordinate.

We shall examine an arbitrary aperture (not necessarily a singly connected aperture) whose extent along the y-coordinate takes up a portion along the OY-axis from -1 to +1 (Fig. 4). For calculating the radiation pattern in the plane x=0,

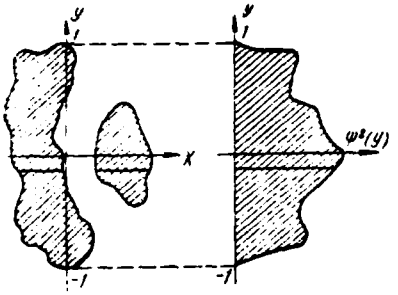

Fig. 4. Arbitrary planar aperture.

it is convenient to introduce an equivalent aperture with respect to the y-coordinate (Fig. 4). The shape of the aperture will be described essentially by means of the positive function $\psi^2(y)$. Then, the radiation pattern in the plane under consideration may be represented in the following form:

$$R(u) = \iint_S A(x, y)\, e^{iuy}\, dxdy = \int_{-1}^{+1} \psi^2(y)\, A(y)\, e^{iuy}\, dy. \qquad (45)$$

Insofar as it is differential radiation patterns that are being considered here, we shall assume first of all that:

$$R(0) = \int_{-1}^{+1} \psi^2(y)\, A(y)\, dy = 0. \qquad (46)$$

From condition (46), it follows that the zero point of the coordinate system in the equivalent aperture should be chosen in such a way that it overlaps with the "center of gravity" of the adduced distribution. The expression for the slope S at u=0 may be easily generated from expression (45):

$$S(0) = \int_{-l}^{l} \psi^2(y)\, y A(y)\, dy. \qquad (47)$$

We shall introduce the normalization condition: /1

$$g = \int_{-l}^{l} \psi^2(y)\, A^2(y)\, dy - 1 = 0. \qquad (48)$$

In order to abbreviate the notation, we shall denote:

$$\psi(y)\, A(y) = B(y),\ \psi(y)\, y = \varphi(y). \qquad (49)$$

We shall represent the unknown functions B(y) and ϕ(y) in the form of Fourier series:

$$\left.\begin{aligned} S(0) &= \sum_{0}^{\infty} A_n \cos n\pi y + B_n \sin n\pi y \\ \varphi(y) &= \sum_{0}^{\infty} \Phi_n \cos n\pi y - \psi_n \sin n\pi y \end{aligned}\right\}. \qquad (50)$$

Taking into account formula (50), expressions (47) and (48) may be transformed into the following forms:

$$\left.\begin{aligned} S(0) &= \sum_{0}^{\infty} A_n \Phi_n \varepsilon_n + B_n \psi_n \\ g &= \sum_{0}^{\infty} \varepsilon_n A_n^2 + B_n^2 - 1 = 0 \end{aligned}\right\}. \qquad (51)$$

In accordance with the Lagrange method, we form the auxiliary function:

$$\Phi = F + \mu g. \qquad (52)$$

The system of equations:

$$\left.\frac{\partial \Phi}{\partial A_n} = 0,\ \frac{\partial \Phi}{\partial B_n} = 0,\ g = 0\right|, \qquad (53)$$

makes it possible to determine the unknown constant coefficients A_n, B_n:

$$A_n = \frac{1}{2\mu} \Phi_n,\ B_n = \frac{1}{2\mu} \psi_n. \qquad (54)$$

From the expressions in (54), it follows that in the case of an optimal electric field distribution in the aperture B(y) and ϕ(y) with an accuracy within the value of the constant multiplier, they should be in agreement, that is:

$$B(y) = \frac{1}{2A}\varphi(y), \tag{55}$$

or, taking into account formula (49):

$$A(y) = \frac{1}{2A}\,y. \tag{56}$$

The constant multiplier may be easily determined from condition (48): /1

$$\frac{1}{2A} = \frac{1}{\sqrt{\int_{-1}^{1} \psi^2(y)\, y^2 dy}}. \tag{57}$$

In this way, the optimal distribution assuring a maximum of the slope S in the equisignal direction does not in fact depend on the shape of the aperture, and is always equal to:

$$A(y) = \frac{y}{\sqrt{\int_{-1}^{1} \psi^2(y)\, y^2 dy}}. \tag{58}$$

The slope S corresponding to this distribution is:

$$S(0) = \sqrt{\int_{-1}^{1} \psi^2(y)\, y^2 dy}. \tag{59}$$

Conclusions

1. For a broad class of antennas, expressions have been derived for optimal field distributions at an aperture which assure a maximum slope for a radiation pattern of the differential type and a maximum value for the major lobes of the radiation pattern.

2. The phase characteristics of the field in the aperture for assuring maximum values of S(0) and $R_m(u)$ must be constant.

3. The optimal distributions derived depend only on one coordinate in the antenna aperture, the coordinate corresponding to the plane of the formation of the differential radiation pattern, and it does not depend on the shape of the aperture.

BIBLIOGRAPHY

1. Dol'f. Proceedings of the JRE, Vol. 34, No. 6, 1946, p. 335.

2. Taylor. IRE Transactions, Vol. AP-3, No. 1, 1955, p. 16.

3. Taylor. JRE Transactions, Vol. AP-8, No. 1, 1960, p. 17.

4. Fel'd, Ya. N. (ed.). Antenny santimetrovykh voln [Antennas for the Centimetric Waves]. Soviet Radio Publishing House, 1950.

5. Pokrovskiy, V. I. Radio Technology and Electronics, Vol. II, No. 5, 1957, p. 559.

6. Sokolov, I. F., Vakman, D. E. Radio Technology and Electronics, Vol. III, No. 1, 1958, p. 46.

7. Khannan. JRE Transactions, Vol. AP-9, No. 5, 1961, pp. 444 and 445.

8. Crompton. Proceedings of the JRE, Vol. 42, No. 2, 1954, p. 371.

9. Krupitskiy, E. I., Sapozhnikova, T. N. Radio Technology and Electronics, Vol. 10, No. 11, 1965, 1967.

CALCULATING THE CHARACTERISTICS OF A JUNCTION OF TWO WAVEGUIDES BY MEANS OF A RESONATING COUPLING APERTURE /1

G. A. Yevstropov, A. M. Yevseyev

A problem in coupling two waveguides by means of a resonating coupling aperture is solved. The equivalent circuit for the junction is determined. The calculation methodology for the parameters of the equivalent circuit is cited. Particular cases of junctions of rectangular waveguides and a rectangular waveguide with a round waveguide are examined. The theoretical conclusions are compared with experimental results.

Introduction

The coupling of waveguides by means of resonating coupling apertures is widely used in the creation of antennas and other devices for superhigh frequencies. In order to carry out computations for this kind of equipment, it is necessary to know the equivalent circuits for the various waveguide junctions by means of an aperture, as well as the coupling of the parameters of the equivalent circuit together with the geometrical dimensions and the wavelength.

Despite the fact that a coupling of two waveguides by means of an arbitrary coupling aperture may be computed for the most part, still it is possible to generate a simple equivalent circuit and computational formulas only for a narrow resonating (half-wave) aperture.

Works [1, 2, 3] are dedicated to the question under consideration here. The methods for solution used in them, however, did not make it possible to derive formulas convenient for engineering calculations, nor equivalent circuits. In this article, a determination method for the characteristics of a junction of two waveguides by means of a resonating coupling aperture is used; this method was developed in work [4] for a rectangular waveguide and aperture radiating into a half-space. The results from work [4] are generalized for a waveguide of any arbitrary cross section and for a resonating aperture radiating into another waveguide.

The Formulation of the Problem and the Method for Solving It

The possible methods of joining waveguides by means of a coupling aperture are presented in Table 1 (using the example of rectangular and round waveguides). For the sake of simplicity, we shall assume that in the waveguides only a principal type of wave may be propagated. The field source in the problem under consideration here is a wave being propagated in a waveguide 1 or 2 and incident to the coupling aperture from the left. /1

Under the influence of the incident wave (with an effective amplitude of A_0 and power P_0), a voltage with a complex amplitude U is induced in the aperture. Once the coupling aperture has been excited, it begins to radiate energy both into waveguide 1, as well as into waveguide 2. The amplitudes of the waves induced in the waveguides and being propagated to the left of A and to the right of B away from the aperture are expressed thusly:

$$\left.\begin{aligned} A_{1,2} &= U(p_{1,2} + iq_{1,2}) \\ B_{1,2} &= -U(p_{1,2} - iq_{1,2}) \end{aligned}\right\}^{1)} \qquad (1)$$

These formulas were derived in work [4] for a rectangular cross section waveguide, but it is an easy affair to demonstrate that they are justified also for a waveguide of any arbitrary cross sectional area. The parameters $p_{1,2}$ and $q_{1,2}$ depend on the geometrical dimensions of the waveguide and the disposition of the aperture on it. We shall consider that the problem of excitation of each waveguide by means of the coupling aperture with a voltage U at the center has been resolved, that is, the parameters $p_{1,2}$ and $q_{1,2}$ have been found.

The power of the wave being propagated in the waveguide:

$$P_{1,2} = |A_{1,2}|^2 S_{1,2}, \qquad (2a)$$

where $S_{1,2}$ is a coefficient depending on the shape and dimensions of the cross sectional area of the waveguide and the wave type.

In this way, the power re-emitted into one of the waveguides with power delivered to the other is:

$$P_{изл.\,1,2} = 2S_{1,2}U_0^2(p_{1,2}^2 + q_{1,2}^2) = \frac{U_0^2}{R_{\Sigma 1,2}}, \qquad (2b)$$

[1]Here and further, the indices 1 and 2 relate to the first and second waveguides respectively.

Table 1

№ пп.	Diagram of junction	Equivalent circuit	Conductance	Notes
1	2	3	4	5
1	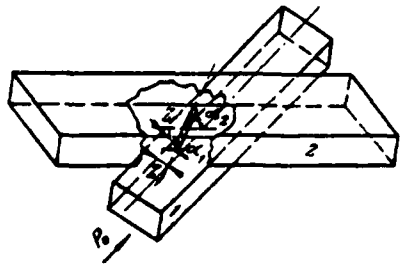	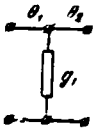	$g_1 = 2\frac{a_1 b_1 \beta_1}{a_2 b_2 \beta_2}\frac{p_1^2 + q_1^2}{p_2^2 + q_2^2}$	$p_{1,2}$ and $q_{1,2}$ are calculated according to formula (11)
2	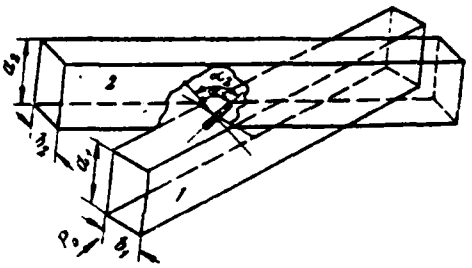		$g_1 = 2\frac{\beta_1 a_1^3 b_1}{\beta_2 a_2^3 b_2}\frac{1-\beta_2^2\sin^2\alpha_2}{1-\beta_1^2\sin^2\alpha_1} \times \frac{\cos\left(\frac{\pi}{2}\beta_1\sin\alpha_1\right)}{\cos\left(\frac{\pi}{2}\beta_2\sin\alpha_2\right)}$	
3	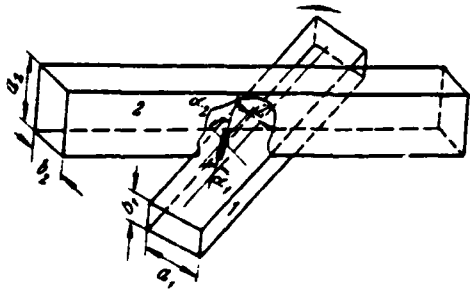	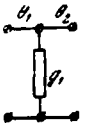	$g_1 = 2\frac{\beta_1 a_1 b_1}{\beta_2 a_2 b_2}\frac{p_1^2 + q_1^2}{q_2^2}$	p_1 and q_1 according to formula (11) q_2 according to formula (15)
4		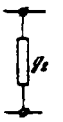	$g_2 = 2\frac{\beta_2 a_2 b_2}{\beta_1 a_1 b_1}\frac{q_2^2}{p_1^2 + q_1^2}$	q_2 according to formula (15) p_1 and q_1 according to formula (11)
5	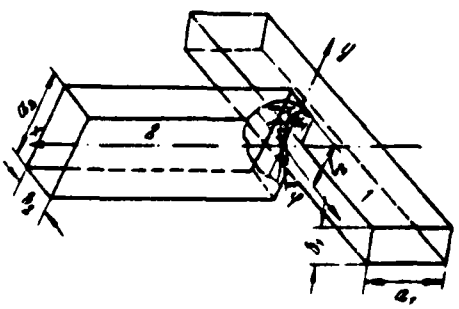		$g_1 = 1\frac{\beta_1 a_1 b_1}{\beta_2 a_2 b_2}\frac{q_1^2}{p_2^2}$	q_1 according to formula (15) p_2 according to formula (20)
6			$g_2 = \frac{\beta_2 a_2 b_2}{2\beta_1 a_1 b_1}\frac{p_2^2}{q_1^2}$	p_2 according to formula (20) q_1 according to formula (15)

1	2	3	4	5
7	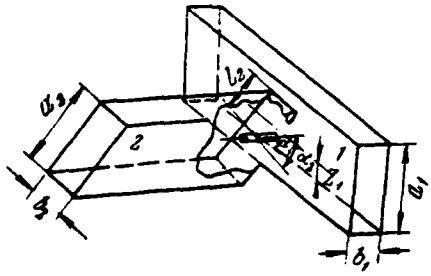	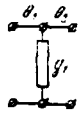	$g_1 = 4\frac{\beta_1 a_1 b_1}{\beta_2 a_2 b_2}\frac{p_1^2+q_1^2}{p_2^2}$	p_1 and q_1 according to formula (11) p_2 according to formula (20) /1
8		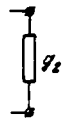	$g_2 = \frac{\beta_2 a_2 b_2}{2\beta_1 a_1 b_1}\frac{p_2^2}{p_1^2+q_1^2}$	p_1 and q_1 according to formula (11) p_2 according to formula (20)
9	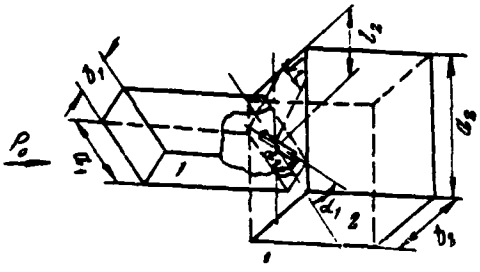		$g_1 = \frac{\beta_1 a_1 b_2 \cos^2\alpha_1 \sin^2\frac{\pi}{a_1} l_1}{\beta_2 a_2 b_1 \cos^2\alpha_2 \sin^2\frac{\pi}{a_2} l_2} \times \frac{\cos^2\left(\frac{\pi}{4}\frac{\lambda}{a_1}\cos\alpha_1\right)}{\cos^2\left(\frac{\pi}{4}\frac{\lambda}{a_2}\cos\alpha_2\right)} \times \left\{\frac{\left(\frac{2a_2}{\lambda}\right)^2-\cos^2\alpha_2}{\left(\frac{2a_1}{\lambda}\right)^2-\cos^2\alpha_1}\right\}^2$	
10	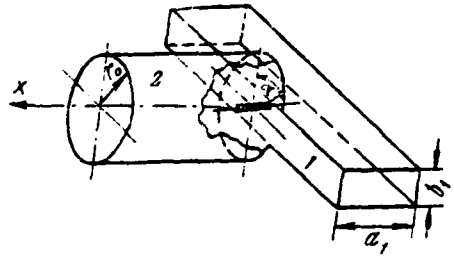	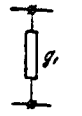	$g_1 = \frac{2\beta_1 a_1 b_1 S q_1^2}{Z_0 Q^2\left[\left(\frac{\lambda}{\lambda_{кр}}\right)^2-1\right]}$	q_1 according to formula (15) S according to formula (22) Q acc. to form. (23)
11		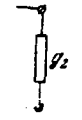	$g_2 = \frac{Z_0 Q^2\left[\left(\frac{\lambda}{\lambda_{кр}}\right)^2-1\right]}{2\beta_1 a_1 b_1 S q_1^2}$	q_1 according to formula (15) S according to formula (22) Q according to formula (23)
12	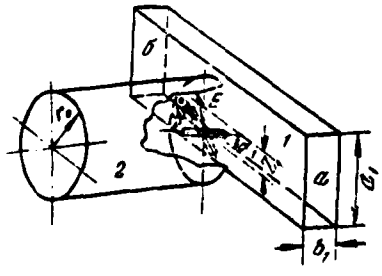	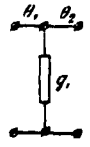	$g_1 = \frac{2\beta_1 a_1 b_1 S\left(p_1^2+q_1^2\right)}{Z_0 Q^2\left[\left(\frac{\lambda}{\lambda_{кр}}\right)^2-1\right]}$	p_1 and q_1 according to formula (11) S according to formula (22) Q according to formula (23) /1
13		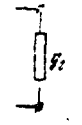	$g_2 = \frac{Z_0 Q^2\left[\left(\frac{\lambda}{\lambda_{кр}}\right)^2-1\right]}{2\beta_1 a_1 b_1 S\left(p_1^2+q_1^2\right)}$	p_1 and q_1 according to formula (11) S according to formula (22) Q according to formula (23)

where:

$$R_{1,2} = \frac{1}{2S_{1,2}(p_{1,2}^2 + q_{1,2}^2)},$$

$U_0 = |U|$ is the effective value of the pulse height at the center of the aperture.

In this case, if the coupling aperture is cut on the face end of the waveguide, or if there is a plunger located in the shoulders of one of the waveguides, the pulse heights of the waves in formulas (1) must be taken to be equal to zero; this must be taken into account by excluding the two from formula (2b).

It is not only the power re-emitted into the waveguide that is of great interest, but also the phase of the re-emitted fields. For waves re-emitted respectively to the left and to the right of waveguide 1 and waveguide 2 (with an index of two) or conversely (with an index of one), we get: /1

$$\psi_{1,2n} = \arg U + \operatorname{arc\,tg}\frac{q_{1,2}}{p_{1,2}}, \quad \psi_{1,2n} = \pi - \arg U - \operatorname{arc\,tg}\frac{q_{1,2}}{p_{1,2}}. \quad (3)$$

The phase of the voltage U may be determined by using the reciprocity principle, from which it follows that the phase shift between the voltage in the aperture and the wave in the waveguide remains constant, both for the excitation of the waveguide by means of the aperture, as well as with the excitation of the aperture due to the wave being propagated in the waveguide:

$$U = U_0 \frac{p_{1,2} + iq_{1,2}}{\sqrt{p_{1,2}^2 - q_{1,2}^2}},$$

$$\psi_{2n} = \operatorname{arc\,tg}\frac{q_1}{p_1} + \operatorname{arc\,tg}\frac{q_2}{p_2}, \quad (4)$$

$$\psi_{2n} = \pi + \operatorname{arc\,tg}\frac{q_1}{p_1} - \operatorname{arc\,tg}\frac{q_2}{p_2} \quad (5)$$

under the condition that the wave is incident on the aperture from the left in waveguide 1.

Formulas (1), (2), and (4) are in agreement in form with similar baseline formulas in the work cited [4]. For this reason, all the results of this work, including problems in the matching of an aperture with a waveguide, hold for the case when the aperture is cut in a side wall of an exciting infinite waveguide.

In this way:

$$\left.\begin{aligned} P_{изл.\,1,\,2} &= \frac{g_{1,\,2}}{\left(\frac{g_{1,\,2}}{2}+1\right)^2} \\ g_{1,\,2} &= 4S_{1,\,2}\left(p^2_{1,\,2}-q^2_{1,\,2}\right)R_{22,\,1} \end{aligned}\right\}. \qquad (6)$$

The power of the wave incident upon the aperture is taken to be equal to unity. The equivalent connection circuit is shown in Fig. 1. The electrical lengths are:

$$\Theta_1 = -\Theta_2 = \frac{\pi}{2} - \operatorname{arc\,tg}\frac{q_{1,\,2}}{p_{1,\,2}}. \qquad (7)$$

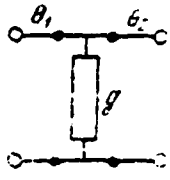

Fig. 1. Equivalent connection circuit of waveguies (waveguide being excited with aperture in a side wall) joined by a resonating coupling aperture.

For the analysis of the functioning and computations for the devices using the coupling types considered here, it is perfectly possible to use the methods analyzed in [5, 6].

If the aperture is cut in the face end of the exciting waveguide 2, the results of work [4] are not applicable. In this case, the voltage U may be found from the equation for the energy balance having the form:

$$P_{пад} = P_{изл} + P_{отр}, \qquad (8)$$

where $P_{пад}=S_{1,2}A_0^2$; $P_{изл}$ is determined by formula (2) and:

$$P_{отр} = S_{1,\,2}\left(U_0\sqrt{p^2_{1,\,2}+q^2_{1,\,2}}-A_0\right)^2. \qquad (9)$$

Here, it has been taken that the reflection factor off the face end without an aperture is equal to 1.

From expressions (2) and (8), we get:

$$\left.\begin{aligned} P_{изл.\,1,\,2} &= \frac{4g_{1,\,2}}{(g_{1,\,2}+1)^2} \\ g_{1,\,2} &= S_{1,\,2}\left(p^2_{1,\,2}+q^2_{1,\,2}\right)R_{22,\,1} \end{aligned}\right\}. \qquad (10)$$

The formula for $P_{изл\ 1,2}$ is in agreement with the expression for the power

dispersed in the load for a double-wire line with conductance $g_{1,2}$. The power reflected from the aperture [formula (9)] is also in agreement with the power reflected from the load $g_{1,2}$ in a double-wire line, that is:

$$P_{отр}=\left(\frac{1-g_{1,2}}{1+g_{1,2}}\right)^2.$$

In this way, the equivalent circuit of a waveguide with resonating coupling aperture in the face end is a double-wire line with load $g_{1,2}$ (Fig. 2).

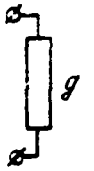

Fig. 2. The equivalent connection circuit of waveguides (waveguide being excited with aperture in face end) connected by a resonating coupling aperture.

The methodology derived here is used for calculating the most widely used types of coupling two rectangular waveguides, as well as for connecting a rectangular waveguide with a round waveguide. For this, it is necessary to determine the coefficients $p_{1,2}$, $q_{1,2}$ and the radiation resistance $R_{\Sigma 1,2}$.

Derivation of Formulas for the Coefficients of Excitation and Radiation Resistance of an Aperture Cut on Rectangular and Round Waveguides

We shall examine the case when an aperture is cut on the side walls of a rectangular waveguide. We shall use the formulas derived already in solving the problem of the excitation of a waveguide by means of an aperture and the formulas cited in the accompanying works.

When exciting a waveguide by means of an aperture cut into the long wall of a waveguide and inclined on the bias (Fig. 3a), from work [4], we have:

$$p_{1,2}=\frac{1}{\kappa\beta_{1,2}a_{1,2}b_{1,2}}\cos\left(\frac{\pi}{a_{1,2}}z_{1,2}\right)\left\{\sin\varkappa_{1,2}\left[\frac{\cos\gamma_{1,2}\frac{\lambda}{4}}{1-\left(\frac{\eta_{1,2}}{\kappa}\right)^2}+\right.\right.$$

$$\left.+\frac{\cos\xi_{1,2}\frac{\lambda}{4}}{1-\left(\frac{\xi_{1,2}}{\kappa}\right)^2}\right]+\frac{\pi\cos\varkappa_{1,2}}{\kappa a_{1,2}\beta_{1,2}}\left[\frac{\cos\xi_{1,2}\frac{\lambda}{4}}{1-\left(\frac{\xi_{1,2}}{\kappa}\right)^2}-\frac{\cos\eta_{1,2}\frac{\lambda}{4}}{1-\left(\frac{\eta_{1,2}}{\kappa}\right)^2}\right]\left.\right\}; \quad (11)$$

$$q_{1,2}=\frac{\sin\left(\frac{\pi}{a_{1,2}}z_{1,2}\right)}{\kappa\beta_{1,2}a_{1,2}b_{1,2}}\left\{\sin\varkappa_{1,2}\left[\frac{\cos\xi_{1,2}\frac{\lambda}{4}}{1-\left(\frac{\xi_{1,2}}{\kappa}\right)^2}-\frac{\cos\eta_{1,2}\frac{\lambda}{4}}{1-\left(\frac{\eta_{1,2}}{\kappa}\right)^2}\right]+\right.$$

$$\frac{\pi\cos\alpha_{1,2}}{\kappa a_{1,2}\beta_{1,2}}\left[\frac{\cos\xi_{1,2}\frac{\overline{}}{4}}{1-\left(\frac{\xi_{1,2}}{\kappa}\right)^2}+\frac{\cos\eta_{1,2}\frac{\overline{}}{4}}{1-\left(\frac{\eta_{1,2}}{\kappa}\right)^2}\right].$$

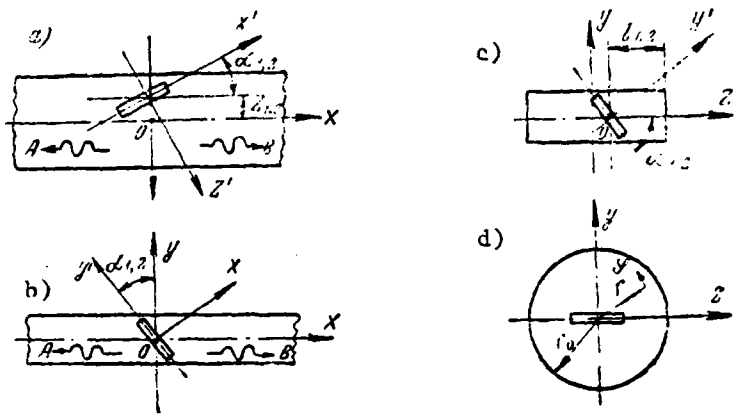

Fig. 3. Means of exciting waveguides by means of an aperture.

Here:

$$\beta_{1,2}=\sqrt{1-\left(\frac{\lambda}{2a_{1,2}}\right)^2};$$

$$\eta_{1,2}=\kappa\beta_{1,2}\cos\alpha_{1,2}+\frac{\pi}{a_{1,2}}\sin\alpha_{1,2};$$

$$\xi_{1,2}=\kappa\beta_{1,2}\cos\alpha_{1,2}-\frac{\pi}{a_{1,2}}\sin\alpha_{1,2};$$

the indices 1 and 2 relate to the first and second waveguides respectively (see Table 1).

The power $P_{1,2}$ being propagated in the rectangular waveguide is connected /1
with the effective voltage amplitude of the electric field by the formula:

$$P_{1,2}=\frac{|A_{1,2}|}{2Z_0}\beta_{1,2}a_{1,2}b_{1,2}. \qquad (12)$$

where Z_0 is the characteristic wave impedance of free space.

Consequently, for a rectangular waveguide:

$$S_{1,2}=\frac{\beta_{1,2}a_{1,2}b_{1,2}}{2Z_0}. \qquad (13)$$

As a result, from formulas (12), (1), and (2), we get:

$$R_{\text{вх}1,\,2} = \frac{Z_0}{\beta_{1,\,2} a_{1,\,2} b_{1,\,2} (p_{1,\,2}^2 + q_{1,\,2}^2)}. \qquad (14)$$

If the inclined aperture is cut on the narrow wall of the waveguide (Fig. 3b), from work [7] and formula (1), we get: $p_{1,\,2}=0$,

$$q_{1,\,2} = \frac{2\pi \sin \alpha_{1,\,2}}{\kappa^3 \beta_{1,\,2} a_{1,\,2}^2 b_{1,\,2}} \cdot \frac{\cos\left(\frac{\pi}{2} \beta_{1,\,2} \sin \alpha_{1,\,2}\right)}{1 - \beta_{1,\,2}^2 \sin^2 \alpha_{1,\,2}} \qquad (15)$$

and the radiation resistance is:

$$R_{\text{вх}1,\,2} = \frac{Z_0}{\beta_{1,\,2} a_{1,\,2} b_{1,\,2} q_{1,\,2}}. \qquad (16)$$

We shall derive formulas for determining the parameters $p_{1,2}$ and $q_{1,2}$ for the excitation of a rectangular waveguide by means of an aperture cut into the facing end (Fig. 3c). We shall use the method used in work [8] and applied in [4].

The components of the fundamental type wave in a rectangular waveguide are expressed thusly:

$$\left.\begin{aligned} E_y &= A_0 \cos\left(\frac{\pi}{a} z\right) e^{-i\kappa\beta x} \\ H_z &= \mp \frac{A_0 \beta}{Z_0} \cos\left(\frac{\pi}{a} z\right) e^{-i\kappa\beta x} \\ H_x &= -i A_0 \frac{\pi}{\kappa a Z_0} \sin\left(\frac{\pi}{a} z\right) e^{-i\kappa\beta x} \end{aligned}\right\}. \qquad (17)$$

The minus sign in these formulas relates to waves being propagated in the direction of the increase in x, and the plus sign in the direction of decrease.

We shall assume that the aperture is narrow and resonating, so that the voltage along it changes according to the law $e=U\cos\pi x$. The wave excited by the aperture in the waveguide is determined by expressions (17) (with a minus sign), if they are multiplied by the coefficient of excitation C. Using the method ana- /1
lyzed in work [4], we get the following formula for finding this coefficient:

$$C = -\frac{1}{2P_0} \int_{\text{щель}} [\mathbf{E}_1 \mathbf{H}_2] \, d\mathbf{S}. \qquad (18)$$

Here $\underline{E}_1$ is the field in the aperture and induced by the aperture in the waveguide. The field of the wave incident on the face end (without an aperture) and reflected off of it, that is, the sum of the space and reflected waves (17) are used as an auxiliary wave field, taking into account the fact that the reflection factor off the face end is equal to 1.

In this way, $\underline{H}_2$ in formula (18), with x=0:

$$\mathbf{H}_2 = \frac{2A_0 z_{1,2}}{Z_0} \cos\frac{\pi}{a_{1,2}} z. \qquad (19)$$

Taking into account that the aperture is narrow, after integrating expression (18), we get:

$$C = U \frac{A_0 \kappa 3}{P_0 Z_0} \frac{\cos\left(\frac{\pi}{a_{1,2}} \frac{l}{2} \cos z_{1,2}\right)}{\left(\frac{\pi}{a_{1,2}} \cos z_{1,2}\right)^2 - \kappa^2} \cos z_{1,2} \sin\frac{\pi}{a_{1,2}} l_{1,2}$$

The wave amplitude induced by the aperture in the waveguide is:

$$A = CA_0 = U \frac{2\kappa}{a_{1,2} b_{1,2}} \frac{\cos\left(\frac{\pi}{a_{1,2}} \frac{l}{2} \cos z_{1,2}\right)}{\left(\frac{\pi}{a_{1,2}} \cos z_{1,2}\right)^2 - \kappa^2} \cos z_{1,2} \cos\frac{\pi}{a_{1,2}} l_{1,2}$$

and consequently:

$$p_{1,2} = \left.\frac{2\kappa \cos z_{1,2}}{a_{1,2} b_{1,2}} \frac{\cos\left(\frac{\pi}{2} \frac{\lambda}{a_{1,2}} \cos z_{1,2} \sin\frac{\pi}{a_{1,2}} l_{1,2}\right)}{\left(\frac{\pi}{a_{1,2}} \cos z_{1,2}\right)^2 - \kappa^2}\right| \qquad (20)$$
$$q_{1,2} = 0$$

Taking into account that the aperture radiates only into one shoulder of the waveguide, the characteristic wave impedance is found from the expression:

$$R_{\text{в}1,2} = \frac{2Z_0}{\beta_{1,2}^2 a_{1,2}^2 b_{1,2}^2 p_{1,2}^2}. \qquad (21)$$

The problem of the excitation of a round waveguide by means of an aperture cut in the face end (Fig. 3d) may be solved in the same manner as for the case of a rectangular waveguide.

For the case of the disposition of the aperture symmetrically with respect to the radius of the cross sectional area, a wave is induced which is oriented in such a way that the vector $\underline{E}$ passing through the center of the cross section will be perpendicular to the aperture. Expressions for the components of the tangent and reflected waves in a round waveguide may be taken, for example, from work [9]. /1
Formula (18) for the coefficient of excitation is retained in this case. The auxiliary field on the facing end is determined by the expression:

$$H_z = -2A_0 \frac{\lambda_{\text{кр}}}{\lambda} \sqrt{1 - \left(\frac{\lambda}{\lambda_{\text{кр}}}\right)^2} J_1'(\kappa_c r).$$

An arbitrary Bessel function can be expressed [10] thusly:

$$2J_1'(x) = J_0(x) - J_2(x).$$

For calculating the integral (18), we take the Bessel function in the form of a series [10]:

$$J_n(\kappa_c r) = \sum_{m=0}^{\infty} (-1)^m \frac{\left(\frac{1}{2}\kappa_c r\right)^{n+2m}}{m!\,(n+m)!}.$$

After computing the integral, we get the amplitude of the field induced in the waveguide: $A = -U\frac{\sqrt{\left(\frac{\lambda}{\lambda_{кр}}\right)^2 - 1}}{S} Q,$

where:

$$S = \frac{\pi}{4} Z_0 \frac{\lambda_{кр}^2}{\lambda\lambda_в}\left(r^2 - \frac{1}{\kappa^2}\right) J_1^2(\kappa_c r_0), \qquad (22)$$

$$Q = \frac{1}{\kappa} + \sum_{m=1}^{\infty} (-1)^m \frac{\kappa_c^{2m}(2m+1)\pi^{2m}(2m)!}{2^{4m}(m!)^2(m+1)\kappa^{2m}} \times$$

$$\times \sum_{p=0}^{m} (-1)^p \frac{2^{2p}}{\pi^{2p}(2m-2p)}, \qquad (23)$$

where r_0 is the radius of the waveguide.

The power radiated into the round waveguide is:

$$P_{изл} = A^2 S = U_0^2 \frac{\left(\frac{\lambda}{\lambda_{кр}}\right)^2 - 1}{S} Q^2.$$

Consequently:

$$R_в = \frac{S}{Q^2\left[\left(\frac{\lambda}{\lambda_{кр}}\right)^2 - 1\right]}, \qquad (24)$$

$$p = -\frac{1}{S}\sqrt{\left(\frac{\lambda}{\lambda_{кр}}\right)^2 - 1}\, Q, \quad q = 0. \qquad (25)$$

Characteristics of Concrete Types of Junctions of Waveguides by Means of a Resonating Coupling Aperture /1

On the basis of the methodology and the expressions cited above, it is possible to generate computational formulas of the conductance and electrical lengths entering into the equivalent circuit for possible types of couplings or junctions of two rectangular waveguides and for couplings of a rectangular waveguide together

with a round waveguide (see the table). It should be noted that in coupling a rectangular waveguide together with a round waveguide (if the aperture is cut in the long wall of the rectangular waveguide), it is possible to assure radiation of all the power out of waveguide 2 into waveguide 1 at any orientation of an H_{11} type wave in waveguide 2. In this case, the field phase in the shoulder Q of the rectangular waveguide is equal to ψ, and in the shoulder $\delta-(-\psi)$, where ψ is the angle between the vector E passing through the center of the cross sectional area of the round waveguide and perpendicular to the center line of the rectangular waveguide.

For this, it is necessary to cut two perpendicular apertures in the waveguides whose conductances are equal to unity (in the figure in the table, the second aperture is shown by the broken line) with a concomitant fulfilling of the condition $p_1=q_1$, which follows from formulas (3) and (10).

Calculation Results and Results of Experiment

The formulas generated above were checked experimentally in a series of particular cases. The first case relates to the coupling of two rectangular waveguides by means of an aperture in the narrow wall of one and in the facing end of another (Fig. 4). This type of coupling is distinguished from the type examined above in

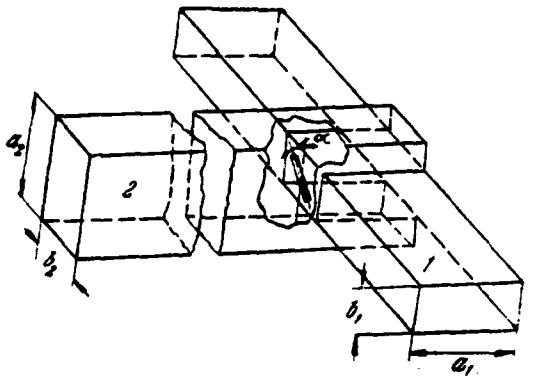

Fig. 4. Coupling of two rectangular waveguides by means of a resonating coupling aperture, experimental study.

that the cross section in which the aperture has been cut was not completely metallically coated, and the aperture goes through to the broad wall of the waveguide.

The computational and experimental relationships of conductance to the angle of incline of the aperture for waveguides of various cross sections are shown in Fig. 5. As may be seen from the figure, the experimental and computational curves differ from each other markedly. This is explained by the nonfulfillment of the /1

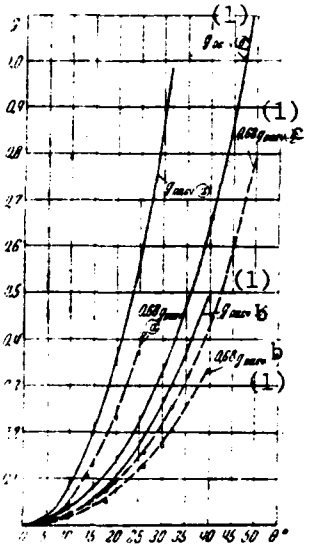

Fig. 5. Computational and experimental relationships of conductance g_1 of an aperture and the angle of incline of the junction (Fig. 4).
(.. experimental points) at:
a) $a_1<a_2$ & $b_1=b_2$;
b) $a_1=a_2$ & $b_1=b_2$;
c) $a_1=a_2$ & $b_1<b_2$

Key: (1) computational

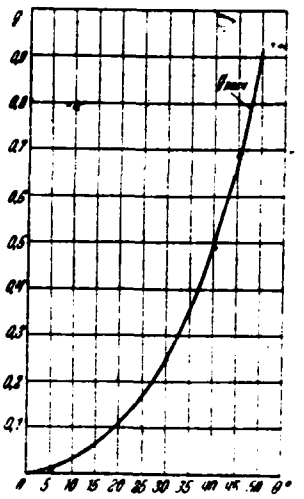

Fig. 6. Computational and experimental relationships of conductance and the angle of incline of an aperture disposed on the narrow wall of one waveguide and the facing end of the other (the figure in the table) with a coupling of rectangular waveguides (ϕ=90°; $\alpha_1=\alpha_2=\alpha$; $a_1=a_2$ and $b_1=b_2$).

.... are experimental points.

conditions of the theory (complete metallization of the cross section of the waveguide in which the aperture is cut, and the placement of the aperture completely on the narrow wall of the waveguide) in the experimental process. However, when the computational curve is multiplied by the constant coefficient 0.68, the curves derived from this practically overlap with the experimental curves. In the case of larger angles of inclination, when the aperture is completely disposed on the narrow wall, the experimental curve begins to approximate the computational curve without having to use the correction coefficient (curve b).

If the cross section of the waveguide in which the aperture is disposed has been completely metallized (the aperture is completely fitted on the narrow wall of the waveguide), the values for the computed and experimentally measured conductances

agree with an accuracy not less than 2%. The relationship between conductance and the angle of incline for this case is shown in Fig. 6.

A junction between a rectangular waveguide and a round waveguide was also studied experimentally. The coordinates of the aperture on the broad side of the waveguide and the size of the cross section of the narrow wall were computed for the conditions $g_2=1$ and $p_1=q_1$. The resonant length of the slot aperture, as in the foregoing case, was experimentally selected. For one aperture, the ksv [standing wave ratio] <1.1. In the case of a cross-shaped slot, the ksv was dependent on the orientation of the wave in the round waveguide; this is explained by the reciprocal influence of the slot apertures, which was not taken account of in the calculation. With decreases in the width of the aperture, the relationship of the ksv on the wave orientation decreased. For example, for apertures with a width of 1.5 mm, the ksv changed from 1.5 to 1.8. /1

Conclusions

The formulas for the calculation of the characteristics of the coupling between two waveguides by means of a resonant coupling aperture derived in the article give a computational accuracy sufficient for all practical purposes. In the experimentally confirmed cases, when the experimental conditions corresponded to the base presuppositions of the theory, the computational accuracy was not less than 2%.

The formulas derived in this way make it possible to compute the position and orientation of apertures on waveguides according to fixed coupling characteristics. However, the calculational methods for the resonant length of an aperture are lacking with sufficient accuracy in the cases considered here, and the resonant aperture length must be chosen experimentally.

BIBLIOGRAPHY

1. Watson, W. H. The Physical Principles of Waveguide Transmission and Antenna System. Oxford, 1947.

2. Levin, M. L. Journal of the Academy of Sciences of the USSR, Physics Series, Vol. 12, No. 3, 1948.

3. Matthael, G. L., Yaung, L., Jones, E. M. T. Microwave Filters, Impedance-Matching Networks and Coupling Structures. McGraw Hill Co., New York, 1964.

4. Veshnikova, I. Ye., Yevstropov, G. A. Radio Technology and Electronics, Vol. 10, No. 7, 1965, p. 1181.

5. Yevstropov, G. A., Tsarapkin, S. A. Radio Technology and Electronics, Vol. X, No. 9, 1965, p. 1663.

6. Yevstropov, G.A., Tsarapkin, S.A. Radio Technology and Electronics, Vol. XI, No. 5, 1966, p. 822.

7. Fradin, A. Z. Antenny sverkhvysokikh chastot [Antennas for Superhigh Frequencies]. Soviet Radio Publishing House, 1957.

8. Antenny santimetrovykh voln [Antennas for Centimetric Waves]. No. 1, Translated from English. Soviet Radio Publishing House, 1950.

9. Shirman, Ya. D. Radiovolnovody i ob'ëmnye rezonatory [Radio Waveguides and Cavity Resonators]. Svyaz'izdat [State Publishing House of Literature on Communications and Radio], 1959.

10. Gradshteyn, I. S., Ryzhik, I. M. Tablitsy integralov, summ, ryadov i proizvedeniy [Tables of Integrals, Sums, Series, and Derivatives]. Fizmatgiz [State Publishing House of Literature on Physics and Mathematics], 1962.

CALCULATING FOR A ROUND WAVEGUIDE WITH AN AZIMUTHALLY MAGNETIZED FERRITE ROD /1

R. R. Yurgenson, N. G. Teytel'baum

On the basis of calculations carried out with the help of a computer of the propagation constant of the principal wave type quasi-H_{11} in a round waveguide with an azimuthally magnetized ferrite, an analysis of the relationship between the differential phase shift and the various parameters of the ferrite and the waveguide in the frequency range is presented. Solutions for the field components of the electromagnetic waves are derived in the form of generalized power series. Series and particular cases are transformed into Bessel functions or into a Whittaker function. Recommendations on selecting parameters for equipment designed to generate optimal phase shifter characteristics are given. The quality factor and losses are assessed in an approximative fashion.

Introduction

Recently, a series of works have appeared in which a fast-acting, unilateral ferrite phase shifter using a ferrite with a rectangular hysteresis loop, a so-called "bistabile" phase shifter [1, 2], and results of experimental studies carried out are cited. Normally, this kind of phase shifter is a rectangular waveguide, along whose axis a ferrite tube is disposed, or a set of rings magnetized in the azimuth direction. It is controlled by current pulses passing along the conductor loop.

A phase shifter is distinguished by its very low level of controlling magnetic fields, insofar as the demagnetizing factor of the specimen is equal to zero. Despite the fact that a similar phase shifter has found wide application in practice, it has not been calculated theoretically, up to this point, due to the complexity inherent in this problem. In work [3], the possibility of creating a "bistabile" phase shifter in a round waveguide with the use of a symmetrical magnetic wave (H_{01}) is examined. This kind of wave is most favorable from the point of view of the interaction of the ferrite with the SVCh [superhigh frequency] field with azimuthal biasing. The authors present a method for solving the problem and for calculating the differential phase shift for a ferrite tube attached to the waveguide walls. Obviously, this disposition of the ferrite is far from being optimal, but even in this case, quite large phase shifts (on the order of 0.3 rad/cm) are derived. However, the difficulties connected with

exciting a symmetrical wave in a round waveguide significantly lower the merit of this phase shifter. In the present work, problems in the theory and calculations for a "bistabile" phase shifter in a round waveguide using the quasi-H_{11} principal wave mode are examined. /1

The Solution to Wave Equations

The theory of electromagnetic wave propagation in a ferrite medium magnetized by means of an azimuthal magnetic field, not depending on the radius, was considered in some of the works cited [4, 5]. The authors of these works restricted themselves to the cases when the field components do not change in the azimuthal direction. In work [5], it was noted that if the dependency of the field components on the coordinate angle is expressed in the form $e^{in\phi}$, then a system of second order differential equations is derived for the longitudinal field components.

In a cylindrical coordinate system (r,ϕ,z), the tensor μ has the following form for an azimuthally magnetized ferrite:

$$\|\mu\| = \mu_0 \begin{Vmatrix} \mu & 0 & j\mu_a \\ 0 & \mu_\varphi & 0 \\ -j\mu_a & 0 & \mu \end{Vmatrix},$$

where:

$$\mu_a \approx \frac{\tilde{\gamma} M}{\omega},$$

where $\tilde{\gamma}$ is the gyromagnetic ratio, ω is the angular frequency, and M is the residual magnetization,

$$\mu_0 = 4\pi \cdot 10^{-4}, \ \frac{H}{m}.$$

For the residual magnetization of a ferrite that is less than the saturation magnetization, it may be approximately assumed that:

$$\mu = \mu_\varphi. \tag{3}$$

From the Maxwell equations with the time dependency relationship $e^{i\omega t}$ and a relationship to the z-coordinate expressed in the form $e^{i\gamma z}$, and a relationship to the ϕ-coordinate expressed in the form $e^{in\phi}$, a system of equations for the longitudinal field components may be derived in the following manner:

$$\left.\begin{aligned} E_z'' + \frac{1}{\rho} E_z' + \left(1 - \frac{n^2}{\rho^2}\right) E_z - \frac{\beta}{\rho} H_z = 0 \\ H_z'' + \frac{1}{\rho} H_z' + \left(1 - c + \frac{\alpha}{\rho} - \frac{n^2}{\rho^2}\right) H_z - \frac{\eta}{\rho} E_z = 0 \end{aligned}\right\}, \quad (4)$$

/1

where:

$$\beta = \frac{i n \omega \varepsilon_a \mu_0}{\kappa}, \quad \eta = -\beta \frac{\varepsilon}{\mu \mu_0},$$

$\rho = \kappa r$ is the radius normalized for the wave number, $\kappa^2 = \omega^2 \varepsilon \mu \mu_0 - \gamma^2$, with γ being the propagation constant along the z-axis, and ε is the dielectric permittivity of the ferrite:

$$c = \frac{\omega^2 \varepsilon \mu \mu_0 \mu_a^2}{\kappa^2 \mu^2}, \quad \alpha = \frac{\gamma \mu_a}{\kappa \mu}, \quad (5)$$

c and α are dimensionless magnitudes, with the prime symbol denoting differentiation with respect to ρ.

The transverse field components are determined according to the longitudinal[1] components in the following manner:

$$\left.\begin{aligned} E_r &= -\frac{i}{\kappa}\left(\gamma \frac{dE_z}{d\rho} - \frac{i n \omega \mu \mu_0}{\rho} H_z\right) \\ H_\varphi &= -\frac{i}{\kappa}\left(\omega \varepsilon \frac{dE_z}{d\rho} - \frac{i n \gamma}{\rho} H_z\right) \\ E_\varphi &= \frac{i}{\kappa}\left(\frac{i n \gamma}{\rho} E_z + \omega \mu \mu_0 \frac{dH_z}{d\rho} + \frac{\omega \mu_a \gamma \mu_0}{\kappa} H_z\right) \\ H_r &= \frac{i}{\kappa}\left(-\frac{i n \omega \varepsilon}{\rho} E_z - \gamma \frac{dH_z}{d\rho} - \frac{\omega^2 \varepsilon \mu_a \mu_0}{\kappa}\right) H_z \end{aligned}\right\}. \quad (6)$$

Getting rid of H_z and E_z successively from system (4), we get differential equations of the fourth order for the longitudinal field components having variable coefficients and which may be written in the form:

$$\sum_{\nu=0}^{4} \rho^\nu g_\nu(\rho) y^{(\nu)} = 0, \quad (7)$$

where:

$$y = \frac{1}{\beta} E_z; \quad y^{(\nu)} = \frac{d^\nu y}{d\rho^\nu};$$

[1] Here and in what follows, the factor $e^{i(\omega t - \gamma z + n\phi)}$ is left out.

$$\left.\begin{aligned} g_0(\rho) &= n^2(n^2-1) - \alpha n^2 \rho - (2n^2-1)\rho^2 + \alpha\rho^3 + (1-c)\rho^4 \\ g_1(\rho) &= \alpha\rho + (4-c)\rho^2 \\ g_2(\rho) &= -2(n^2-1) + \alpha\rho + (2-c)\rho^2 \\ g_3(\rho) &= 4; \quad g_4(\rho) = 1 \end{aligned}\right\}. \tag{8}$$

$$\sum_{\nu=0}^{4} \rho^{\nu} q_{\nu}(\rho)\, x^{(\nu)} = 0, \tag{9}$$

where: /1

$$\left.\begin{aligned} x &= \frac{1}{\eta} H_z \\ q_0(\rho) &= g_0(\rho) - c\rho^2 \\ q_1(\rho) &= g_1(\rho) - 2c\rho^2 \\ q_\nu(\rho) &= g_\nu(\rho), \ (\nu = 2, 3, 4) \end{aligned}\right\}. \tag{10}$$

The solution of the homogeneous differential equation (7) may be expanded in the neighborhood of the regular singular point in the equation $\rho=0$ into the series:

$$y_i = \rho^{m_i} \sum_{l=0}^{\infty} A_l^{(i)} \rho^l. \tag{11}$$

The roots m_i and the coefficients of the series A_i^1 may be determined according to the Frobenius method [6, 7]. For $n=\pm(1,2,3\ldots)$, we get:

$$m_1 = |n| + 1; \quad m_2 = |n|; \quad m_3 = -|n| + 1; \quad m_4 = -|n|. \tag{12}$$

that is, the number of values of the root m_i is equal to the order of differential equation (7).

It is well known from [6] that if the difference in the roots m_i is a whole number, then series (11) is a partial solution for equation (7), only for the leading root $m_1=|n|+1$. The remaining three solutions to the differential equation are constructed in the form of a more general series containing ln ρ.

Insofar as in the present case we are interested in solutions that are regular at the point $\rho=0$, solutions containing ln ρ will not be further considered.

The first partial solution is expressed thusly:[1]

$$y_1 = \rho^{n+1} \sum_{l=0}^{\infty} A_l \rho^l, \tag{13}$$

[1]Here and in what follows, the sign of the module on n will be left out.

where the coefficients are determined according to the recurrent formulas:

$$\left.\begin{aligned} A_0 &= \frac{1}{(2n+1)\,2^n\,\Gamma(n+1)} \\ A_l &= -\frac{a\,F_1(n+l+1)A_{l-1}+F_2(n+l+1)A_{l-2}+z\,A_{l-3}+(1-c)A_{l-4}}{F(n+l+1)} \\ F(n+l+1) &= (n+l+1)(n+l)[(n+l+2)(n+l-1)-2(n^2-1)]+n^2(n^2-1) \\ F_1(n+l+1) &= (n+l)^2-n^2 \\ F_2(n+l+1) &= 2(n+l-1)(n+l)+(1-2n^2)-(n+l-1)^2c \\ A_i &= 0, \text{ if } i<0 \end{aligned}\right\} \quad (14)$$

here $\Gamma(n+1)$ is the gamma function. /1

Substituting the partial solution y_1 into equations (4), we get the first solution for the system, regular at zero:

$$\left.\begin{aligned} E_{z1} &= \beta C_1 U_{n,1}^{(a,c)}(\rho) \\ H_{z1} &= C_1 T_{n,1}^{(a,c)}(\rho) \end{aligned}\right\}. \quad (15)$$

Here:

$$U_{n,1}^{(a,c)}(\rho) = y_1, \quad T_{n,1}^{(a,c)}(\rho) = \rho^n \sum_{l=0}^{\infty} Q_l \rho^l, \quad (16)$$

where:

$$Q_l = [(n+l+1)^2-n^2]A_l + A_{l-2}.$$

The solution to equation (9) is built in the same way as the solution to equation (7). Substituting the solution x_1 found into equations (4), we get the second solution for the system, regular at zero:

$$\left.\begin{aligned} H_{z2} &= \eta C_3 T_{n,2}^{(a,c)}(\rho) \\ E_{z2} &= C_3 U_{n,2}^{(a,c)}(\rho) \end{aligned}\right\}. \quad (17)$$

Here:

$$T_{n,2}^{(a,c)}(\rho) = x_1 = \rho^{n+1} \sum_{l=0}^{\infty} B_l \rho^l; \quad (18)$$

C_1 and C_3 are arbitrary constants; the coefficients B_l are equal to:

$$\left.\begin{aligned} B_0 &= \frac{1}{(2n+1)\,2^n\,\Gamma(n+1)} \\ B_l &= -\frac{a\,F_1(n+l+1)B_{l-1}+F_2(n+l+1)B_{l-2}+a\,B_{l-3}+(1-c)B_{l-4}}{F(n+l+1)} \\ F_2(n+l+1) &= 2n+l+1)(n+l)+(1-2n^2)-[(n+l+1)(n+l-1)]c \end{aligned}\right\}. \quad (19)$$

F and F_1 are determined according to formulas (14):

$$B_\xi = 0, \quad \text{if} \quad \xi < 0; \tag{20}$$

$$U^{(\gamma,\ c)}_{n,\ 2}(\rho) = \rho^n \sum_{l=0}^{\infty} M_l \rho^l,$$

where:

$$M_l = [(n+l+1)^2 - n^2] B_l + \alpha B_{l-1} + (1-c) B_{l-2}.$$

The region of the convergence of the series representing solutions (15) and (17) of the system of equations is determined by the variable coefficients entering into equations (7) and (9) [6]. This region is an open plane.

The generalized power series entering into expressions (15) and (17) contain module n, and for this reason, they do not depend on variations in the sign on n.

In the particular cases ($\mu_a \to 0$; $n \to 0$), the solutions to the system must turn /1
into known solutions for an isotropic medium or for an azimuthally magnetized ferrite medium with radial symmetry. We shall investigate these cases.

1. In going to the limit $\mu_a \to 0$, system (4) decomposes into two independent Bessel equations for H_z and E_z. In this kind of medium, it is possible that there exist two kinds of waves, TE and TM waves. If $\mu_a \to 0$ ($c=\alpha=\beta \to 0$), the first solution (15) gives TE waves:

$$E_{z1} = 0, \quad H_{z1} = C_1 T^{(0,\ 0)}_{n,\ 1}(\rho). \tag{21}$$

where:

$$\lim_{\substack{c \to 0, \\ \alpha \to 0}} T^{(\gamma,\ c)}_{n,\ 1}(\rho) = T^{(0,\ 0)}_{n,\ 1}(\rho) = J_n(\rho).$$

$J_n(\rho)$ is a Bessel function.

The second solution (17), at $\mu_a \to 0$ ($c=\alpha=\eta \to 0$), it changes into TM waves:

$$H_{z2} = 0, \quad E_{z2} = C_3 U^{(0,\ 0)}_{n,\ 2}(\rho) \tag{22}$$

where:

$$\lim_{\substack{c \to 0, \\ \alpha \to 0}} U^{(\gamma,\ c)}_{n,\ 2}(\rho) = U^{(0,\ 0)}_{n,\ 2}(\rho) = J_n(\rho).$$

2. In going to the limit $n \to 0$, system (4) also decomposes into two independent equations: a Bessel equation for E_z and an equation for H_z reducible to a Whittaker equation. This is the case of radial symmetry considered in [4, 5].

Applying the limit $n \to 0$ ($\beta=\eta \to 0$) to solutions (15) and (17), we get for the first solution:

$$E_{z1} = 0, \quad H_{z1} = C_1 T_{0,1}^{(\alpha,c)}(\rho), \qquad (23)$$

where:

$$\lim_{n\to 0} T_{n,1}^{(\alpha,c)}(\rho) = T_{0,1}^{(\alpha,c)}(\rho) = \frac{M_{\varkappa,0}(u)}{\sqrt{u}},$$

$$u = 2i\rho\sqrt{1-c}, \quad \varkappa = \frac{\alpha}{2i\sqrt{1-c}}.$$

$M_{\varkappa,0}(u)$ is a Whittaker function.

For the second solution:

$$H_{z2} = 0, \quad E_{z2} = C_2 U_{0,2}^{(\alpha,c)}(\rho), \qquad (24)$$

where:

$$\lim_{n\to 0} U_{n,2}^{(\alpha,c)}(\rho) = U_{0,2}^{(\alpha,c)}(\rho) = J_0(\rho).$$

The transverse field components in both cases are determined according to formulas (6).

From what has been analyzed here, it follows that the solutions to system (4), regular at zero, include among themselves all types of waves propagated in an azimuthally magnetized ferrite medium. In this kind of medium, both components E_z and H_z are always distinct from zero (with the exception of the case when n=0). In Fig. 1 are shown graphs of the following functions:

$U_{1,1}^{(\alpha,c)}(\rho)$; $U_{1,2}^{(\alpha,c)}(\rho)$; $T_{1,1}^{(\alpha,c)}(\rho)$; $T_{1,2}^{(\alpha,c)}(\rho)$ at n=1, α=0.54, c=0.45.

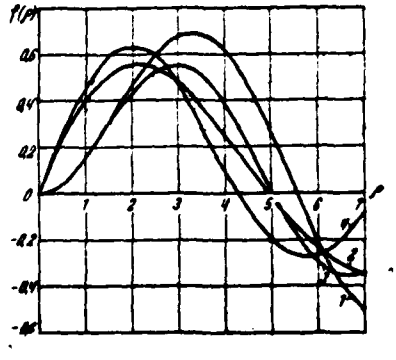

Fig. 1. Graphs of the following functions:
$T_{1,2}^{(\alpha,c)}(\rho)$ (curve 1);
$T_{1,1}^{(\alpha,c)}(\rho)$ (curve 2);
$U_{1,1}^{(\alpha,c)}(\rho)$ (curve 3);
$U_{1,2}^{(\alpha,c)}(\rho)$ (curve 4).

Deriving the Characteristic Equation

We shall examine a round waveguide of infinite length with radius a with an azimuthally magnetized ferrite rod with radius b. The electromagnetic field

components for the dielectric surrounding the ferrite can be written in the form:

$$\left.\begin{aligned}
E_{z1} &= [C_{2n}J_n(\rho_1) + C_{4n}N_n(\rho_1)]\\
H_{z1} &= [C_{5n}J_n(\rho_1) + C_{6n}N_n(\rho_1)]\\
E_{\varphi 1} &= \frac{i}{\kappa_1^2}\left[-\frac{in\bar{\gamma}}{2\pi\bar{r}}E_{z1} + \kappa_1\sqrt{\frac{\mu_0}{\varepsilon_0}}H'_{z1}\right]\\
H_{z1} &= -\frac{i}{\kappa_1^2}\left[\varepsilon_1\kappa_1\sqrt{\frac{\varepsilon_0}{\mu_0}}E'_{z1} + \frac{in\bar{\gamma}}{2\pi\bar{r}}H_{z1}\right]\\
E_{r1} &= -\frac{i}{\kappa_1^2}\left[\bar{\gamma}\kappa_1 E'_{z1} + \frac{in}{2\pi\bar{r}}\sqrt{\frac{\mu_0}{\varepsilon_0}}H_{z1}\right]\\
H_{r1} &= \frac{i}{\kappa_1^2}\left[\frac{in\varepsilon_1}{2\pi\bar{r}}\sqrt{\frac{\varepsilon_0}{\mu_0}}E_{z1} - \bar{\gamma}\kappa_1 H'_{z1}\right]
\end{aligned}\right\}, \qquad (25)$$

where:

$$\kappa_1 = \sqrt{\varepsilon_1 - \bar{\gamma}^2},\ \bar{\gamma} = \frac{\gamma}{\kappa_0},\ \bar{r} = \frac{r}{\lambda_0},\ \kappa_0 = \omega\sqrt{\varepsilon_0\mu_0} = \frac{2\pi}{\lambda_0},\ \rho_1 = 2\pi\kappa_1\bar{r},$$

ε_1 is the relative dielectric permittivity of the dielectric, $\varepsilon_0 = \frac{10^{-9}}{36\pi}$, F/m. The prime symbol denotes differentiation with respect to the argument of the function; C_{2n}, C_{4n}, C_{5n}, C_{6n} are arbitrary constants. The field components in the ferrite layer are determined according to formulas (6), (15), and (17).

Substituting the expressions for the field components from expressions (6), (15), (17), and (25) into the boundary conditions (when r=a and r=b) we get six equations for determining the arbitrary constants:

$$C_{2n}J_n(\rho_{a1}) + C_{4n}N_n(\rho_{a1}) = 0, \qquad (26)$$

$$C_{5n}J'_n(\rho_{a1}) + C_{6n}N'_n(\rho_{a1}) = 0, \qquad (27)$$

$$C_{1n}\left[\frac{n^2\bar{\gamma}\mu_a}{\rho_{b2}}U^{(a,\,c)}_{n,\,1}(\rho_{b2}) + \mu_a\bar{\gamma}T^{(a,\,c)}_{n,\,1}(\rho_{b2}) + \nu\kappa_2 T'^{(a,\,c)}_{n,\,1}(\rho_{b2})\right] +$$

$$+ C_{3n}\left[-\frac{\bar{\gamma}\kappa_2}{\rho_{b2}}U^{(a,\,c)}_{n,\,2}(\rho_{b2}) - \mu_1\varepsilon_2 T'^{(a,\,c)}_{n,\,2}(\rho_{b2}) + \frac{\kappa_2^2\bar{\gamma}\varepsilon_2}{\nu}T^{(a,\,c)}_{n,\,2}(\rho_{b2})\right]$$

$$\times in\sqrt{\frac{\varepsilon_0}{\mu_0}} + C_{3n}\frac{in\bar{\gamma}\kappa_2^2}{\rho_{b1}\kappa_1}\sqrt{\frac{\varepsilon_0}{\mu_0}}J_n(\rho_{b1}) - C_{6n}\frac{\kappa_2^2}{\kappa_1}N'_n(\rho_{b1}) +$$

$$+ C_{4n}\frac{i\kappa_2^2\bar{\gamma}}{\kappa_1\rho_{b1}}N_n(\rho_{b1})\sqrt{\frac{\varepsilon_0}{\mu_0}} - C_{5n}\frac{\kappa_2^2}{\kappa_1}J'_n(\rho_{b1}) = 0, \qquad (28)$$

$$C_{1n}\frac{in\mu_a}{\kappa_2}\sqrt{\frac{\mu_0}{\varepsilon_0}}U^{(a,\,c)}_{n,\,1}(\rho_{b2}) - C_{3n}J_n(\rho_{b1}) +$$

$$+ C_{3n}U^{(a,\,c)}_{n,\,2}(\rho_{b2}) - C_{4n}N_n(\rho_{b1}) = 0, \qquad (29)$$

$$-C_{1n}T^{(a,\,c)}_{n,\,1}(\rho_{b2}) + \frac{in\mu_a\varepsilon_2}{\kappa_2\mu}\sqrt{\frac{\varepsilon_0}{\mu_0}}T^{(a,\,c)}_{n,\,2}(\rho_{b2}) + C_{5n}J_n(\rho_{b1}) + C_{6n}N_n(\rho_{b1}) = 0. \qquad (30)$$

$$-C_{1n}\left[\mu_a\varepsilon_2 U_{n,1}^{(2,c)}(\rho_{b2})+\frac{\bar{\gamma}\kappa_2}{\rho_{b2}}T_{n,1}^{(2,c)}(\rho_{b2})\right]\frac{in\kappa_1}{\kappa_2^2}+$$

$$+C_{2n}\varepsilon_1\sqrt{\frac{\varepsilon_0}{\mu_0}}J_n'(\rho_{b1})-C_{3n}\left[\kappa_2 U_{n,2}^{(2,c)}(\rho_{b2})-\frac{n^2\bar{\gamma}^2\mu_a}{\rho_{b2}^2}T_{n,2}^{(2,c)}(\rho_{b2})\right]$$

$$\times\frac{\varepsilon_2\kappa_1}{\kappa_2^2}\sqrt{\frac{\varepsilon_0}{\mu_0}}+C_{4n}\varepsilon_1\sqrt{\frac{\varepsilon_0}{\mu_0}}N_n'(\rho_{b1})+C_{5n}\frac{in\bar{\gamma}}{\rho_{b1}}J_n(\rho_{b1})+$$

$$+C_{6n}\frac{in\bar{\gamma}}{\rho_{b1}}N_n(\rho_{b1})=0. \qquad (31)$$

In equations (26)-(31), the following notation has been introduced:

$$\rho_{b1}=2\pi\kappa_1\bar{b},\quad \rho_{a1}=2\pi\kappa_1\bar{a},\quad \bar{a}=\frac{a}{\lambda_0},\quad \bar{b}=\frac{b}{\lambda_0},$$

$$\rho_{b2}=2\pi\kappa_2\bar{b},\quad \rho_{a2}=2\pi\kappa_2\bar{a},\quad \kappa_2=\frac{\kappa}{\kappa_0}=\sqrt{\varepsilon_2\mu-\bar{\gamma}^2},$$

ε_2 is the relative dielectric permittivity of the ferrite.

The condition of the equality to zero of the determinant of systems (26)-(31) /1
determines the characteristic equation with respect to the propagation constant $\bar{\gamma}$. It should be noted that the magnitudes μ_a and $\bar{\gamma}$ enter into the characteristic equation only as cofactors, or as a ratio. For this reason, the value of the determinant does not change if the signs on μ_a and $\bar{\gamma}$ are exchanged.

At $\bar{\gamma}<1$ in the waveguide, waves of the waveguide type are propagated. If $\varepsilon_2\mu>\bar{\gamma}^2>1$, the coefficient κ_1 becomes imaginary, and in the characteristic equation it is necessary to exchange the Bessel and the Neumann function for a modified Bessel function and a Macdonald function. In this case, a surface type wave will be propagated in the dielectric.

Analysis of Calculation Results

The propagation constant was calculated by using a computer for the quasi-H_{11} principal wave type (n=1). Secondarily, the quasi-E_{11} wave mode, which is most easily excited within exterior type waves, was considered.

Functions represented by the generalized power series (15) and (17) were studied preliminarily. In the calculations, 24 initial members of the series for each function were taken. At the same time, the calculation error in the function was less than 10^{-7}. For calculations, values of the dielectric and magnetic parameters were chosen that are normally encountered in actual ferrites:

$$\varepsilon_2=6,\ 8,\ 10,\ 12;\quad \mu=1;\quad \mu_a=\pm(0{,}3;\ 0{,}4);\quad \varepsilon_1=1.$$

The geometrical dimensions of the waveguide and the ferrite varied across the limits: $\frac{a}{\lambda_0}$=0.2-0.3 with a step of 0.001, $\frac{b}{a}$=0.3-0.65, with a step of 0.05.

For the sake of generality in the derivations, all parameters and values of the propagation constant were normalized to the wavelength.

In Figs. 2, 3, 4, and 5, the relationships of the differential phase shift $\Delta\bar{\gamma}$ and $\frac{a}{\lambda_0}$ for various values of ε_2, μ_a, $\frac{b}{a}$ are presented. The curves fall off to the right for those values of $\frac{a}{\lambda_0}$ at which the quasi-E_{11} wave mode arises.

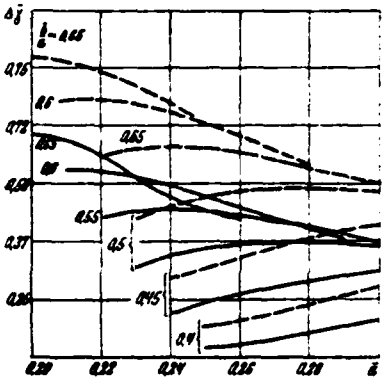

Fig. 2. Dispersion characteristics at ε_2=6;
——— μ_a=±0.3;
– – – – μ_a=±0.4.

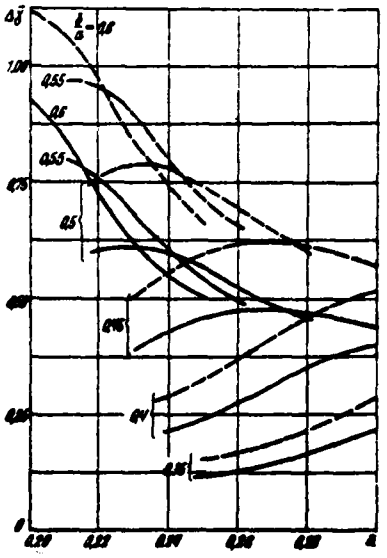

Fig. 3. Dispersion characteristics at ε_2=8;
——— μ_a=±0.3;
– – – μ_a=±0.4.

As may be seen from these figures, the character of the relationships between the differential phase shift and the frequency is not constant. Along some sections (with normal dispersion), with an increase in frequency the values of

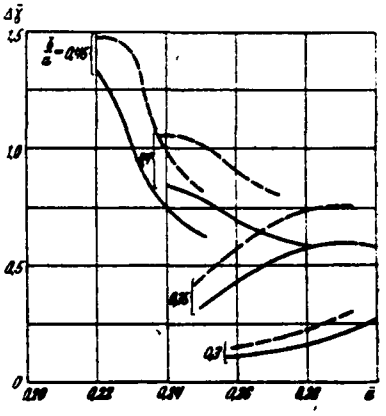

Fig. 4. Dispersion characteristics at $\varepsilon_2=10$;
——— $\mu_a=\pm 0.3$; — — — $\mu_a=\pm 0.4$.

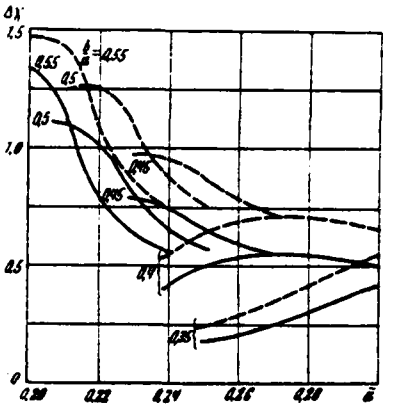

Fig. 5. Dispersion characteristics at $\varepsilon_2=12$;
——— $\mu_a=\pm 0.3$; — — — $\mu_a=\pm 0.4$.

$\Delta\bar{\gamma}=f(\frac{a}{\lambda_0})$ increase. These sections correspond to relatively "weak" fillings of the waveguide by means of the ferrite. On other sections, the characteristic runs almost parallel to the abscissas axis, and then in third sections, an increase in the normalized propagation constant decreases with an increase in frequency.

In this latter case, the phase shift to a unit length either does not vary /1
with an increase in frequency, or it varies only in relation to the slope of the characteristic. Propagation of waves on this section may occur only with a very strong filling of the waveguide by means of the ferrite or with large values of ε_2.

In this way, the character of the frequency relationships is determined basically by the degree of filling of the waveguide by the ferrite. With an increase in the filling of the waveguide by the ferrite, the concentration of the superhigh /1
frequency energy increases in the latter. At first, with a weak filling, the effect of the dielectric waveguide shows up strongly, and the concentration of superhigh frequency energy varies strongly with frequency variations. Beginning at a certain moment, when all the energy, even at the low frequency portion of the frequency range, is concentrated in the ferrite, this relationship becomes weak, and the characteristics become less dependent on frequency.

The form of the curves in the third section are connected with the excitation

of waves and their propagation in regions near the critical regions, with large $\frac{b}{a}$ or ε_2. It is possible to explain this beginning with the curves $\bar{\gamma}(+\mu_a)=f(\frac{a}{\lambda_0})$ shown in Fig. 6.

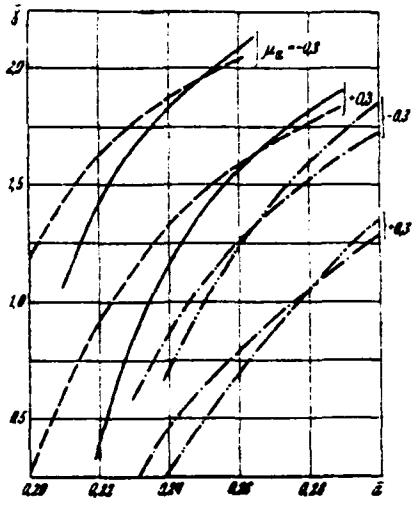

Fig. 6. Dispersion characteristics at
——— ε_2=10; $\frac{b}{a}$=0.5; — — — ε_2=8; $\frac{b}{a}$=0.6;
—·—·— ε_2=8; $\frac{b}{a}$=0.45; —··—··— ε_2=10; $\frac{b}{a}$=0.4.

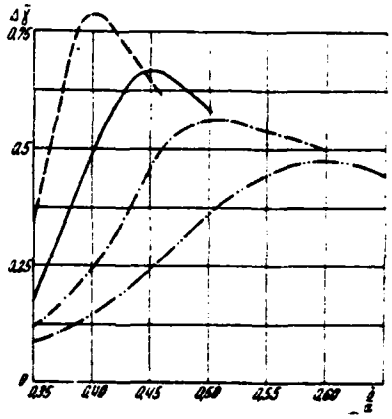

Fig. 7. Relationship of differential phase shift to ferrite radius at μ_a= =±0.3; $\frac{a}{\lambda_0}$=0.25;
——— ε_2=10; — — — ε_2=12;
—·—·— ε_2=8; —·—··— ε_2=6.

The relationships between the differential phase shift and the degree of filling of the waveguide by the ferrite $\bar{\Delta\gamma}=f(\frac{b}{a})$ are shown in Fig. 7.

From the figure, it may be seen that the activity of the phase shifter increases at first with an increase in b/a, while this relationship becomes less frequent the larger ε_2. With further increases in the filling, the increase in this characteristic slows down, and then it begins to drop. This nature of the curves can be explained by variation in the concentration and structure of the superhigh frequency field in the ferrite.

At determined diameters of the ferrite, different for each ε_2, a maximum concentration of the superhigh frequency field occurs in the area of the radial wave polarization in the ferrite. In this case, the phase shift reaches a maximum value. /1
Further on, the energy is redistributed across the cross section of the waveguide, as a result of which the interaction between the superhigh frequency field and the ferrite becomes weaker. As a consequence, there is no sense, from the point of view of enhancing the phase shifter activity, in increasing the value of b/a by /1

means of a more well-defined value.

On the other hand, from a comparison of the curves in Fig. 7 with the frequency characteristics, it follows that in order that the frequency characteristics not be dependent on the frequency, it is necessary to work with fillings that are smaller than those corresponding to the maximum activity for all values of ε_2 under consideration.

One of the more important parameters characterizing phase ferrite equipment is the level of losses, and connected with this, Q-factors. Under "Q-factor," it has become accepted to mean the ratio between a derived phase shift in degrees to losses expressed in decibels. A precise determination of the magnitude of losses requires substituting the tensor components μ and ε_2 into the base equation, taking into account their imaginary portions. For an approximate assessment of losses and the Q-factor in a region far from the ferromagnetic resonance, it is possible to use the well-known method cited in work [8], expanding the function $\bar{\gamma}(\varepsilon_2, \mu, \mu_a)$ into a Taylor series around a value corresponding to the case without losses. Thus we get:

$$\gamma'' = \varepsilon_2'' \frac{\partial \gamma'}{\partial \varepsilon_2'} + \mu'' \frac{\partial \gamma'}{\partial \mu'} + \mu_a'' \frac{\partial \gamma'}{\partial \mu_a'}. \qquad (32)$$

The values of the derivatives are determined graphically, and for this the equations $\bar{\gamma}'=f(\mu'_a)$, $\bar{\gamma}'=f(\mu')$, and $\bar{\gamma}=f(\varepsilon'_a)$ are constructed according to the computational data. The values for the imaginary components of the dielectric and magnetic permittivity are taken to be equal to $\varepsilon_2''=0.02$, $\mu''=0.003$, and $\mu''_a=0.002$.

Losses in the phase shifter with a phase shift of 360° (dB) are expressed thusly:

$$P = 54{,}7 \frac{\bar{\gamma}''}{\Delta \bar{\gamma}} \text{ [db]}, \qquad (33)$$

and the Q-factor thusly:

$$Q = 6{,}6 \frac{\Delta \bar{\gamma}}{\bar{\gamma}''} \left[\frac{\text{deg}}{\text{db}}\right]. \qquad (34)$$

A comparison of losses with the Q-factor of various phase shifters is carried out in the medium frequency range, in which there is observed a weak relationship between them and frequency. The calculation results are shown in Fig. 8.

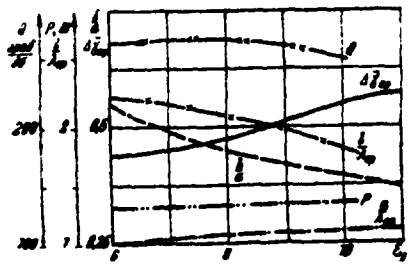

Fig. 8. Relationship between waveguide and ferrite parameters and the dielectric permittivity of the ferrite.

From a consideration of the curves, it is apparent that with an increase in the ferrite dielectric permittivity, the optimal diameter of the ferrite and a length necessary for deriving $\Delta\Phi=360°$ decrease. At the same time, the magnitude of the /1
differential phase shift to a unit length, overall losses, and the Q-factor, vary across a wide range.

Conclusions

The analysis carried out here of the functioning of a phase shifter with an azimuthal bias makes it possible to draw the following conclusions.

1. The character of the frequency relationships is determined basically by the degree of filling of the waveguide by the ferrite and by its dielectric permittivity.

2. The frequency deviation-duration product for a phase shifter is determined mainly by the magnitude ε_2. At $\varepsilon_2=6$, the value for the normalized differential phase shift is maintained as a constant with an accuracy to within 1% of the range of 16%, at $\varepsilon_2=8$, within the range of 12%, and at $\varepsilon_2=10$, within the range of 9%.

3. In creating phase shifters that work across wide bandwidths, it is possible to derive phase shifts on the order of 0.4 to 0.5 rad/cm with Q-factors around 270.

4. The theoretical studies carried out in this article may serve as the basis for designing phase shifters of a similar type.

* * *

The authors would like to express their gratitude to A. I. Potekhin for his valuable advice, and to G. L. Grayfer for carrying out the computer computations.

BIBLIOGRAPHY

1. Nourse, O. British Commmnications and Electronics, No. 6, 1964, pp. 398-402.

2. Woermbke, J. D., Myers, J. A. Microwaves, Vol. 3, No. 10, 1964, pp. 20-27.

3. Bolle, D. M., Heller, G. S. IEEE Transactions, Vol. MTT-13, No. 4, 1965, pp. 421-426.

4. Mikaelyan, A. L. "Volnovodnye i koaksial'nye ventil'nye sistemy dlya voln, obladayushchikh simmetriey vrashcheniya" [Waveguide and Coaxial Valve Systems for Waves Possessing Radial Symmetry], Articles from the Academy of Sciences of the USSR, Vol. 104, No. 2, 1955.

5. Sul, G., Walker, L. Voprosy volnovodnogo rasprostraneniya elektromagnitnykh voln v girotropnykh sredakh [Problems in Waveguide Electromagnetic Wave Propagation in Gyrotropic Media]. Foreign Literature Publishing House, 1955.

6. Kamke, E. Spravochnik po obyknovennym differentsial'nym uravneniyam [Handbook of Normal Differential Equations]. Publishing House of Literature on Physics and Mathematics, 1961.

7. Koddington, E. L., Levinson, N. Teoriya obyknovennykh differentsial'nykh uravneniy [The Theory of Normal Differential Equations]. Foreign Literature Publishing House, 1958.

8. Mikaelyan, A. L. Teoriya i primeneniye ferritov na SVCh [The Theory and Application of Ferrites for High Frequency Signals]. Gosenergoizdat [State Scientific and Technical Power-Engineering Publishing House], 1963.

A SPIRAL LINE WITH AN AZIMUTHALLY MAGNETIZED FERRITE CYLINDER /1

N. G. Motorin, B. C. Khmelevskiy, R. R. Yurgenson

A calculation is carried out for the propagation constant and the differential phase shift for the principal wave type in the following structure: a spiral line with an azimuthally magnetized ferrite, with the line disposed in an unbounded dielectric medium.

An assessment of the influence of the spiral parameters, the ferrite parameters, and the dielectric surrounding the spiral on the magnitude of the differential phase shift in the frequency range is given.

Introduction

Recently, a great amount of attention has been afforded the development of bistabile ferrite phase shifters. In the works [1, 2], experimental results on phase shifters using azimuthally magnetized ferrites in a rectangular waveguide have been described. In work [3], the theory of and calculations for a phase shifter in a round waveguide are presented.

It is of interest to examine a spiral line with an azimuthally magnetized ferrite cylinder on the inside and a dielectric material on the outside in contact with the spiral as a system representing a phase shifter. Several problems in the theory and calculation for the spiral line with an azimuthally magentized ferrite disposed on the outside of the spiral are given in [4]. The dispersion equation for the azimuthally magnetized ferrite cylinder within the spiral located in an unbounded space is presented in [5].

Deriving the Dispersion Equation

We shall examine a single-thread spiral with a radius a, pitch t, and helix angle θ, within which there is located an azimuthally magnetized ferrite cylinder, and outside of which there is an unbounded dielectric with dielectric permittivity ε_2.

In deriving the dispersion equation, we will assume that a thin conductor for

pulse reversal of magnetization is disposed along the axis of the ferrite cylinder and does not have any noticeable influence on the electromagnetic field. The /1
ferrite possesses a rectangular hysteresis loop, and current pulses act on it having such pulse heights that the residual magnetization does not depend on its radius.

The symmetrical case is taken into consideration, when the electric field components do not vary in azimuth.

In a cylindrical coordinate system (r,ϕ,z), the tensor of the ferrite permeability has the form:

$$\|\mu\| = \begin{Vmatrix} \mu & 0 & i\mu_a \\ 0 & \mu_\varphi & 0 \\ -i\mu_a & 0 & \mu \end{Vmatrix}. \qquad (1)$$

For residual magnetization $M \leq M_0$ (M_0 is magnetic saturation) in a SI [expansion unknown] system may be taken approximately according to [5] to be equal to:

$$\mu_a = \mu_0 \frac{\gamma M}{\omega}, \qquad (2)$$

where μ_0 is the permeability of a vacuum, γ is the gyromagnetic ratio, and ω is angular frequency.

The diagonal components for this are equal to:

$$\mu \approx \mu_\varphi \approx 1. \qquad (3)$$

Using [4], we may write expressions for the fields in the ferrite and the dielectric with great lag when the radial wave numbers in the ferrite and the dielectric are approximately equal:

in the ferrite:

$$
\left.
\begin{aligned}
H_{z1} &= \frac{C_2 M_{\varkappa,0}(2|\beta|r)}{\sqrt{2|\beta|r}} = S_{\varkappa,0}(2|\beta|r) \\
H_{r1} &= \mathrm{i}\frac{C_2}{\beta^2}\left[\omega^2\varepsilon_1\mu_a S_{\varkappa,0}(2|\beta|r) + 2\beta^2 S'_{\varkappa,0}(2|\beta|r)\right] \\
H_{\varphi 1} &= \mathrm{i}\frac{C_1\omega\varepsilon_1}{\beta} I_1(|\beta|r) \\
E_{z1} &= C_1 I_0(|\beta|r) \\
E_{r1} &= \mathrm{i}C_1 I_1(|\beta|r) \\
E_{\varphi} &= -\mathrm{i}\frac{C_2\omega\left(\mu^2-\mu_a^2\right)^2}{4\beta\mu} S_{\varkappa,1}(2|\beta|r)
\end{aligned}
\right\}, \qquad (4)
$$

Here, $M_{\varkappa,0}(2|\beta|r)$ is a Whittaker function,

$$
S_{\varkappa,1}(2|\beta|r) = \frac{2[\varkappa S_{\varkappa,0}(2|\beta|r) + S'_{\varkappa,0}(2|\beta|r)]}{\frac{1}{4} - \varkappa^2},
$$

β is the propagation constant, $\varkappa = \frac{\rho_a}{2\mu}\operatorname{sgn}\beta$, ε_1 is the dielectric permittivity of the ferrite, I_0, I_1 are modified Bessel functions, and the prime symbol denotes differentiation with respect to the independent variable:

in the dielectric:

$$
\left.
\begin{aligned}
H_{z2} &= D_1 K_0(|\beta|r) \\
H_{r2} &= -\mathrm{i}D_1 K_1(|\beta|r) \\
H_{\varphi 2} &= -\mathrm{i}D_2\frac{\omega\varepsilon_2}{\beta} K_1(|\beta|r) \\
E_{z2} &= D_2 K_0(|\beta|r) \\
E_{r2} &= -\mathrm{i}D_2 K_1(|\beta|r) \\
E_{\varphi 2} &= \mathrm{i}\frac{\omega\mu_2}{\beta} D_1 K_1(|\beta|r)
\end{aligned}
\right\}, \qquad (5)
$$

where K_0, K_1 are Macdonald functions, C_1, C_2, D_1, D_2 are unknown coefficients.

In expressions (4) and (5), the factor $\exp[\mathrm{i}(\omega t - \beta z)]$ has been left out. Substituting these formulas with r=a into the boundary conditions for an anisotropic cylinder:

$$
\begin{aligned}
&E_{z1} = E_{z2}, \quad E_{\varphi 1} = E_{\varphi 2}, \quad E_{z1}\operatorname{tg}\Theta + E_{\varphi 1} = 0, \\
&H_{z1}\operatorname{tg}\Theta + H_{\varphi 1} = H_{z2}\operatorname{tg}\Theta + H_{\varphi 2} \qquad (6)
\end{aligned}
$$

we get the dispersion equation, which holds good in the case of a small phase shift between current in neighboring windings of the spiral ($t\beta \ll 2\pi$) [7]:

$$\bar{\beta}^2 = \frac{\varepsilon_\Phi \frac{I_1(|\beta|a)}{I_0(|\beta|a)} + \varepsilon_\Delta \frac{K_1(|\beta|a)}{K_0(|\beta|a)}}{\frac{K_0(|\beta|a)}{K_1(|\beta|a)} + \frac{4\mu_0}{\mu(1-4\varkappa^2)} \frac{M_{\varkappa,0}(2|\beta|a)}{M_{\varkappa,1}(2|\beta|a}}, \qquad (7)$$

where:

$$\bar{\beta} = \frac{\beta}{\kappa_0 \operatorname{ctg}\theta}, \quad \kappa_0 = \omega\sqrt{\varepsilon_0\mu_0},$$

ε_Φ, ε_Δ are the relative dielectric permittivities of the ferrite and the dielectric.

At ε_Δ=1, equation (7) is in agreement with the equation derived in [5].[1]

Calculating the Propagation Constants and the Differential Phase Shift

The calculation of the propagation constant from equation (7) was carried out according to the methodology described in [4]. Graphs of the Kummer function were used [8], as well as the relationship between the Whittaker functions and the Kummer functions:

$$\frac{M_{\varkappa,0}(u)}{M_{\varkappa,1}(u)} = \frac{\Phi\left(\frac{1}{2}-\varkappa, 1; u\right)}{u\,\Phi\left(\frac{3}{2}-\varkappa, 3; u\right)}.$$

where Θ is the Kummer function, u=2|β|a.

With large independent variables, the asymptotic expansion of the Kummer function was used [8].

The calculation was carried out for a ferrite with ε_Φ=7,9,11 and with tensor components of its permeability $\frac{\mu}{\mu 0}$=1 and $\frac{\mu_a}{\mu 0}$=±(0.3; 0.5; and 0.8). These values correspond to the residual magnetization of the ferrites used in the superhigh frequency range.

If the tensor $\|\mu\|$ is expressed according to formula (1), the component μ_a<0 corresponds to the case when the propagation direction of the wave is in agreement with the positive value of the z-axis and opposite to the direction of magnetizing current. With this current direction, the propagation constant is strongly dependent

[1]The dispersion equation in [5] evidently contains typographical errors, because according to the sense of the text, the equation should contain modified Bessel functions.

on the residual magnetization (Fig. 1). The relationship of the normalized propagation constant $\bar{\beta}$ to the normalized radius of the spiral $\bar{a}=a\kappa_0 ctg\theta$ at various values of $\frac{\mu_a}{\mu_0}$ is shown in this figure. /1

The introduction of a dielectric on the outside of the spiral leads to an increase in the propagation constant, both for the negative value of μ_a, as well as for he positive value (Fig. 2). At the same time, the differential phase shift increases, and the region of the nondispersion characteristic $\overline{\Delta\beta}$ shifts to the side of the smaller values of $\bar{a}$ (Fig. 3).

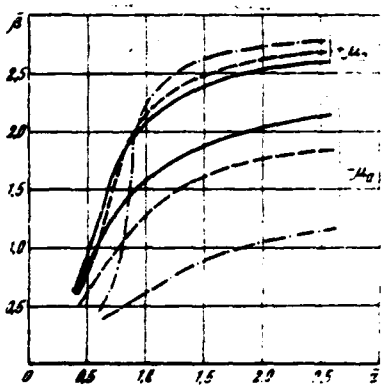

Fig. 1. Relationship between the normalized propagation constant $\bar{\beta}$ and the normalized spiral radius $\bar{a}$ for a ferrite with $\varepsilon_\Phi=11$, $\frac{\mu}{\mu_0}=1$, $\varepsilon_д=1$ at various values of $\frac{\mu_a}{\mu_0}$

—— $\frac{\mu_a}{\mu_0}=\pm0.3$; – – – $\frac{\mu_a}{\mu_0}=\pm0.5$; – – – $\frac{\mu_a}{\mu_0}=\pm0.8$.

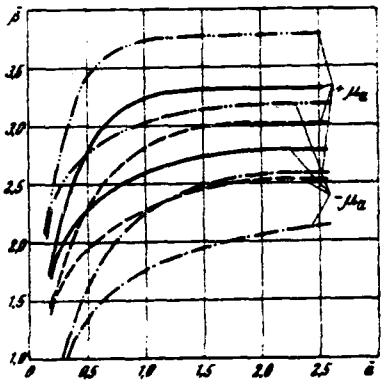

Fig. 2. Relationship between the normalized propagation constant $\bar{\beta}$ and the normalized spiral radius $\bar{a}$ for a ferrite with $\varepsilon_\Phi=9$, $\frac{\mu}{\mu_0}=1$, and $\frac{\mu_a}{\mu_0}=\pm0.3$ at various values of ε for the dielectric:

– – – $\varepsilon=3$; —·—·— $\varepsilon=7$;

—— $\varepsilon=10$; —·—··— $\varepsilon_д=15$.

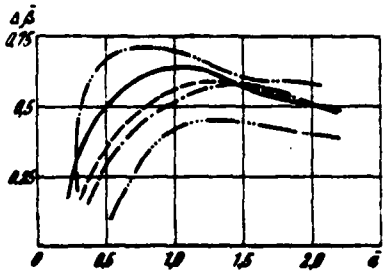

Fig. 3. Relationship between the region of the nondispersion characteristic $\overline{\Delta\beta}$ for a ferrite with:

$\varepsilon_\Phi=9$, $\frac{\mu}{\mu_0}=1$, and $\frac{\mu_a}{\mu_0}=\pm0.3$ at various values of ε for the dielectric:

—·—·— $\varepsilon_д=1$; —·—·— $\varepsilon_д=3$; – – – $\varepsilon_д=7$; —— $\varepsilon_д=10$; —·—·— $\varepsilon_д=15$.

The region of anamolous dispersion shows up clearly expressed; it can be used for creating phase shifters with differential phase shifts only weakly dependent on frequency.

The analysis of expression (4) for the magnetic components H_r and H_z makes it possible to explain the increase in $\overline{\Delta\beta}$ with increases in the dielectric permittivity of the surrounding space. A redistribution of the fields in the structure under consideration takes place in such a way that in the ferrite, the polarization region close to the radial region is extended for both bias orientations.

An increase in dielectric permittivity of the ferrite in the spiral system, just as in the case of the waveguide variant in [3], leads to an increase in the differential phase shift (Fig. 4). However, when there is no waveguide variant, the character of the variation in the differential phase shift in the frequency range is maintained.

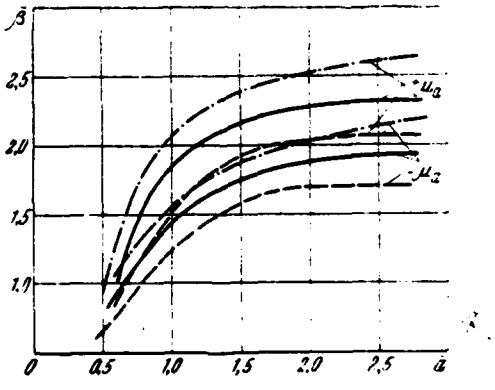

Fig. 4. Relationship of the normalized propagation constant $\bar{\beta}$ and the normalized spiral radius $\bar{a}$ for ferrites with:
$\frac{\mu}{\mu_0}=1$, $\frac{\mu_a}{\mu_0}=\pm 0.3$, $\varepsilon_д=1$ at various values of ε_Φ:

– – – $\varepsilon_\Phi=7$; —— $\varepsilon_\Phi=9$; –·–·– $\varepsilon_\Phi=11$.

It is of interest to compare the value of the differential phase shift to a unit length of the system for spiral and waveguide phase shifters. For a spiral phase shifter with parameters $\bar{a}=1.5$ mm, $\operatorname{ctg}\Theta=12$, $\varepsilon_\Phi=9$, $\varepsilon_д=1$, $\frac{\mu}{\mu_0}=1$, and $\frac{\mu_a}{\mu_0}=\pm 0.3$, /1
the value of the differential phase shift $\Delta\psi=155$ degrees/cm. If $\varepsilon_д=10$, then $\Delta\psi=195$ degrees/cm.

The value of $\Delta\psi$ derived in the cited work [3] for $\varepsilon_\Phi=9$, $\frac{\mu}{\mu_0}=1$, and $\frac{\mu_a}{\mu_0}=\pm 0.3$, and for a ratio of the ferrite radius to the waveguide radius equal to 0.47, is 21.5 degrees/cm, that is, the spiral phase shifter gives a differential phase shift per unit length several times greater than the waveguide phase shifter.

The small dimensions of a spiral phase shifter require significantly less power for phase switching.

The calculation presented here makes it possible to choose the geometrical dimensions and electric parameters of a system for designing a small-dimension phase shifter on a spiral line.

BIBLIOGRAPHY

1. Nourse, O. British Communications and Electronics, No. 6, 1964, pp. 398-402.

2. Woermbke, J. D., Myers, J. A. Microwaves, Vol. 3, No. 10, 1964, pp. 20-27.

3. Yurgenson, R. R., Teytel'baum, I. G. "Raschët kruglogo volnovoda s azimutal'no namagnichennym ferritovym sterzhnem" [Calculations for a Radial Waveguide with an Azimuthally Magnetized Ferrite Rod], In the present collection.

4. Sul, G., Walker, L. Voprosy volnovodnogo rasprostraneniya elektromagnitnykh voln v girotropnykh sredakh [Problems of Waveguide Electromagnetic Wave Propagation in Gyrotropic Media]. IIL [Publishing House of Foreign Literature], 1955.

5. Ivanov, K. P. Electronics Record, Vol. III, October 1964.

6. Mikaelyan, A. L. Teoriya i primeneniye ferritov na SVCh [The Theory of and Application of Ferrites for Superhigh Frequencies]. Gosenergoizdat [State Scientific and Technical Power-Engineering Publishing House], 1963.

7. Vaynshteyn, L. A. Elektromagnitnye volny [Electromagnetic Waves]. Soviet Radio Publishing House, 1957.

8. Yanke, E., Emde, F., Lesh, F. Spetsial'nye funktsii [Special Functions]. Nauka, 1964.

CALCULATION OF A Y-CIRCULATOR WAVEGUIDE WITH A FERRITE-DIELECTRIC ELEMENT /1

V. I. Vol'man

Results of calculations on and experimental studies of a Y-circulator waveguide with a ferrite-dielectric element are analyzed.

Introduction

As was demonstrated in work [1], the functional band of a Y-circulator waveguide increases in proportion to a decrease in the dielectric permittivity of the ferrite from which the ferrite cylinder is made. A similar effect may be expected, if a dielectric sleeve made of a material with $\varepsilon>1$ is placed on the ferrite cylinder. At the same time, the energy concentration in the ferrite cylinder decreases, and this is equivalent to a decrease in its dielectric permittivity. In this way, a Y-circulator with a ferrite-dielectric element is equivalent, according to its features at the first *approximation*, to a Y-circulator without a dielectric sleeve, but having a decrease in the value of the ferrite dielectric permittivity. This makes it possible to affirm that the principles of functioning in both variants of a Y-circulator are identical, and it yields the possibility of using all the ideas and methods for calculation analyzed in [1] for calculations involving a Y-circulator with a ferrite-dielectric element.

A standing wave of the first harmonic of an electric field is established at the central frequency of the working range of a Y-circulator with optimally selected values for the electrical parameters and the diameter of the ferrite cylinder on the Y-circulator surface (Fig. 1) [1]. One of the nodes of this kind of wave is disposed along the longitudinal axis of a side shoulder of the waveguide 2. At the same time, a type H_{20} wave is excited on shoulder 2; this wave is a higher type wave for a rectangular waveguide in shoulder 2, and consequently, it cannot be propagated in it.

By analogy with a Y-circulator without a dielectric sleeve, for determining /1
the optimal dimensions and parameters of the ferrite-dielectric element, it is necessary to study the electric field structure on the surface of the dielectric sleeve fitted onto the ferrite cylinder, and it is necessary to explain the

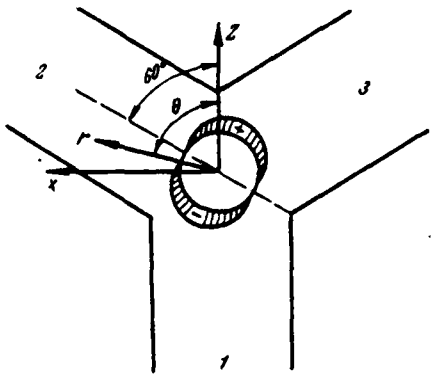

Fig. 1. Field structure on the surface of a ferrite cylinder.

conditions under which the electric field distribution takes the form shown in Fig. 1. At the same time, it is assumed that a Y-circulator with a ferrite-dielectric element will have optimal parameters, if the given field structure is established.

A very high dielectric permittivity of the ferrite and the presence of a dielectric sleeve causes a significant energy concentration in the ferrite-dielectric element and in the space immediately contiguous to it. At the same time, the distribution of pulse heights and phases of the propagating waves in the region of the junction of the waveguide shoulders of the circulator depends basically on the ferrite-dielectric element, and only to a small degree on the configuration and disposition of the metallic surfaces forming the Y-joint of the waveguide. For this reason, for studies on the field structure of a field on the surface of a dielectric sleeve, it is possible to disregard the effects of the Y-joint and to assume that the ferrite-dielectric element is disposed in an unbounded, isotropic medium with parameters ε_0 and μ_0.

Deriving the Basic Relationships

Assuming that the structure of the wave incident on the ferrite-dielectric element does not differ from the wave structure of the principal wave mode type in an H-plane horn, we may write the voltage vector components of its electrical and magnetic field in the following form [2]: /1

$$\left.\begin{aligned} E_{z\,\text{пад}} &= H^{(2)}_{3/2}(x_0\rho)\cos\frac{3}{2}\psi \\ H_{\rho\,\text{пад}} &= -\frac{i}{\eta_0}H^{(2)\prime}_{3/2}(x_0\rho)\cos\frac{3}{2}\psi \\ H_{\varphi\,\text{пад}} &= -\frac{i}{\eta_0}\frac{3}{2x_0\rho}H^{(2)}_{3/2}(x_0\rho)\sin\frac{3}{2}\psi \end{aligned}\right| , \qquad (1)$$

where $x_0^2 = \omega^2\varepsilon_0\mu_0$, $\gamma_\omega^2 = \frac{x_0}{\varepsilon_\theta}$, ω_0 is the frequency of the contiguous electromagnetic field.

The voltage vector component of the magnetic field of the incident wave tangential to the surface of the ferrite-dielectric element may be expressed thusly:

$$H_{\theta\,\text{пад}} = H_{\rho\,\text{пад}}\sin(\Theta-\psi) - H_{\varphi\,\text{пад}}\cos(\Theta-\psi). \qquad (2)$$

Using the addition theorem for cylindrical functions, after transforming from formulas (1) and (2), we get:

$$\left.\begin{aligned} E_{z\,\text{пад}} &= \frac{1}{2}\sum_{n=-\infty}^{\infty}\left[H^{(2)}_{3/2-n}(x_0R_1) - (-1)^n H^{(2)}_{3/2\ n}(x_0R_1)\right]J_n(x_0r)\,e^{in\Theta} = \\ &= \sum_{n=-\infty}^{\infty}A_n e^{in\Theta} \\ H_{\theta\,\text{пад}} &= -\frac{i}{4\gamma_0}\sum_{n=-\infty}^{\infty}\left\{\left[H^{(2)}_{n+7/2}(x_0R_1) + (-1)^n H^{(2)}_{-n-1/2}(x_0R_1)\right]J_{n-1}(x_0r) - \right. \\ &\left. - \left[H^{(2)}_{-n+7/2}(x_0R_1) + (-1)^n H^{(2)}_{n-1/2}(x_0R_1)\right]J_{n-1}(x_0r)\right\}e^{in\Theta} = \\ &= -\frac{i}{\eta_0}\sum_{n=-\infty}^{\infty}B_n e^{in\Theta} \end{aligned}\right| \qquad (3)$$

where R_1 is the distance between the center of the Y-joint and the upper horn. (Fig. 2).

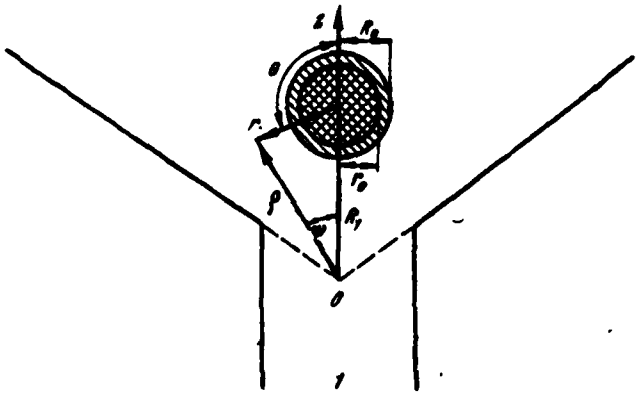

Fig. 2. Y-joint with a ferrite-dielectric element.

The tangential components of the field within the magnetized ferrite cylinder along the axis and in the dielectric may be written in the following form:

1. at $0 \le r \le r_0$:

$$\left.\begin{aligned} E_y^{(1)} &= \sum_{n=-\infty}^{\infty} a_n J_n(x_\perp r)\, e^{in\theta} \\ H_\theta^{(1)} &= -\frac{i}{\eta_\perp} \sum_{n=-\infty}^{\infty} a_n \left[J_n'(x_\perp r) - \frac{\kappa}{\mu} \frac{n}{x_\perp r} J_n(x_\perp r) \right] e^{in\theta} \end{aligned}\right\}, \quad (4)$$

where: /1

$$\eta_\perp^2 = \frac{\mu_\perp}{\varepsilon}, \quad x_\perp^2 = \omega^2 \varepsilon \frac{\mu^2 - \kappa^2}{\mu} = \omega^2 \varepsilon \mu_\perp,$$

ε is the dielectric permittivity of the ferrite, μ and κ are tensor elements of the ferrite permeability, r_0 is the radius of the ferrite cylinder.

2. at $r_0 \le r \le R_0$:

$$\left.\begin{aligned} E_y^{(2)} &= \sum_{n=-\infty}^{\infty} [b_n J_n(x_д r) + c_n Y_n(x_д r)]\, e^{in\theta} \\ H_\theta^{(2)} &= -\frac{i}{\eta_д} \sum_{n=-\infty}^{\infty} [b_n J_n'(x_д r) + c_n Y_n'(x_д r)] e^{in\theta} \end{aligned}\right\}, \quad (5)$$

where:

$$\eta_д^2 = \frac{\mu_д}{\varepsilon_д}, \quad x_д^2 = \omega^2 \varepsilon_д \mu_д$$

$\varepsilon_д$ and $\mu_д$ are respectively the dielectric permittivity and the permeability of the material from which the dielectric sleeve is made; R_0 is the dielectric sleeve radius.

If in accordance with the presumption stated above we disregard the effects of the metallic surfaces forming the Y-joint, then the tangential field components of the field dispersed spatially into the surrounding ferrite-dielectric element /1 are equal to (at $r \ge R_0$):

$$\left.\begin{aligned} E_y^{(3)} &= \sum_{n=-\infty}^{\infty} d_n H_n^{(2)}(x_0 r)\, e^{in\theta} \\ H_\theta^{(3)} &= -\frac{i}{\eta_0} \sum_{n=-\infty}^{\infty} d_n H_n^{(2)'}(x_0 r)\, e^{in\theta} \end{aligned}\right\}, \quad (6)$$

The coefficients entering into formulas (4)-(6) are determined after substituting these formulas into the following boundary conditions:

$$E_y^{(1)} = E_y^{(2)}, \quad H_\varphi^{(1)} = H_\varphi^{(2)} \quad \text{at } r = r_0; \tag{7}$$

$$E_y^{(2)} = E_y^{(3)} + E_{y\,\text{пад}}, \quad H_\varphi^{(2)} = H_\varphi^{(3)} + H_{\varphi\,\text{пад}} \quad \text{at } r = R_0, \tag{8}$$

as well as the solutions to the linear system of equations emerging with this.

As a result, we get:

$$\left.\begin{aligned} a_n &= \frac{b_n}{J_n(\varkappa_\perp r_0)}\left[J_n(\varkappa_\text{д} r_0) + \frac{c_n}{b_n} Y_n(\varkappa_\text{д} r_0)\right] \\ b_n &= \frac{\frac{\eta_\text{д}}{\eta_0}\frac{H_n^{(2)'}(\varkappa_0 R_0)}{H_n^{(2)}(\varkappa_0 R_0)} A_n - B_n}{D_n - \frac{c_n}{b_n} F_n} \\ c_n &= b_n\left(\frac{c_n}{b_n}\right) \\ d_n &= \frac{b_n}{H_n^{(2)}(\varkappa_0 R_0)}\left[J_n(\varkappa_\text{д} R_0) + \frac{c_n}{b_n} Y_n(\varkappa_\text{д} R_0)\right] - \frac{A_n}{H_n^{(2)}(\varkappa_0 R_0)} \end{aligned}\right\}, \tag{9}$$

where:

$$\frac{c_n}{b_n} = -\frac{J_n(\varkappa_\text{д} r_0)}{Y_n(\varkappa_\text{д} r_0)} \cdot \frac{\frac{\eta_\text{д}}{\eta_\perp}\left[\frac{J_n'(\varkappa_\perp r_0)}{J_n(\varkappa_\perp r_0)} - \frac{\kappa}{\mu}\frac{n}{\varkappa_\perp r_0}\right] - \frac{J_n'(\varkappa_\text{д} r_0)}{J_n(\varkappa_\text{д} r_0)}}{\frac{\eta_\text{д}}{\eta_\perp}\left[\frac{J_n'(\varkappa_\perp r_0)}{J_n(\varkappa_\perp r_0)} - \frac{\kappa}{\mu}\frac{n}{\varkappa_1 r_0}\right] - \frac{Y_n'(\varkappa_\text{д} r_0)}{Y_n(\varkappa_\text{д} r_0)}}, \tag{10}$$

$$D_n = \frac{\eta_\text{д}}{\eta_0}\frac{H_n^{(2)'}(\varkappa_0 R_0)}{H_n^{(2)}(\varkappa_0 R_0)} J_n(\varkappa_\text{д} R_0) - J_n'(\varkappa_\text{д} R_0), \tag{11}$$

$$F_n = \frac{\eta_\text{д}}{\eta_0}\frac{H_n^{(2)'}(\varkappa_0 R_0)}{H_n^{(2)}(\varkappa_0 R_0)} Y_n(\varkappa_\text{д} R_0) - Y_n'(\varkappa_\text{д} R_0). \tag{12}$$

The formation of the required structure of the electric field (see Fig. 1) on the surface of the dielectric sleeve is possible only in the case when, at $r=R_0$, the pulse heights of the harmonics with indices n=(1) and n=(-1) are: (1) equal to each other, (2) significantly exceed pulse heights of the harmonics with $|n| \neq 1$, and (3) are phase shifted with respect to one another by 60°. After simple transformations, it is possible to demonstrate that the first and third conditions are met, when the following equations are fulfilled: /1

$$\left[\frac{Y_1'(\varkappa_\text{д} R_0)}{Y_1(\varkappa_\text{д} R_0)} - \frac{\eta_\text{д}}{\eta_0}\frac{Y_1'(\varkappa_0 R_0)}{Y_1(\varkappa_0 R_0)} + \frac{2 J_1(\varkappa_0 R_0)}{\pi \varkappa_\text{д} R_0 Y_1(\varkappa_0 R_0)\left[J_1^2(\varkappa_0 R_0) + Y_1^2(\varkappa_0 R_0)\right]}\right] \times$$

$$\times\left[L_1^2 - \left(\frac{\kappa}{\mu}\frac{\eta_\text{д}}{\eta_\perp}\frac{1}{\varkappa_\perp r_0}\right)^2 M_1^2\right] = \frac{2}{\pi \varkappa_\text{д} R_0 Y_1(\varkappa_\text{д} R_0)}\left\{\left[\frac{\eta_\text{д}}{\eta_\perp}\frac{J_1'(\varkappa_\perp r_0)}{J_1(\varkappa_\perp r_0)} - \right.\right.$$

$$\left.\left. - \frac{Y_1'(\varkappa_\text{д} r_0)}{Y_1(\varkappa_\text{д} r_0)}\right] L_1 - \left(\frac{\kappa}{\mu}\frac{\eta_\text{д}}{\eta_\perp}\frac{1}{\varkappa_\perp r_0}\right)^2 M_1\right\}; \tag{13}$$

$$\frac{\kappa}{\mu}\frac{\varepsilon_{д}}{\varepsilon}\frac{1}{\varkappa_{-}r_0}=\frac{S_1-\sqrt{S_1^2+4L_1^2M_1^2}}{2M_1^2}. \tag{14}$$

where:

$$L_1=\left[\frac{\varepsilon_{д}}{\varepsilon}\frac{J_1'(\varkappa_{-}r_0)}{J_1(\varkappa_{-}r_0)}-\frac{Y_1'(\varkappa_{д}r_0)}{Y_1(\varkappa_{д}r_0)}\right]M_1-\frac{2Y_1(\varkappa_{д}R_0)}{\pi\varkappa_{д}r_0Y_1^2(\varkappa_{д}r_0)}; \tag{15}$$

$$M_1=J_1(\varkappa_{д}R_0)-\frac{J_1(\varkappa_{д}r_0)}{Y_1(\varkappa_{д}r_0)}Y_1(\varkappa_{д}R_0); \tag{16}$$

$$S_1=\frac{2\sqrt{3}}{\pi}\frac{J_1^2(\varkappa_0R_0)+Y_1^2(\varkappa_0R_0)}{\varkappa_{д}r_0Y_1^2(\varkappa_{д}r_0)}. \tag{17}$$

The simultaneous solution of equations (13) and (14) makes it possible to determine the necessary dimensions for the ferrite cylinder and the dielectric sleeve, that is, it yields a solution for the problem posed. However, because of the cumbersomeness of the equations derived, it is difficult to prove analytically that in this case the pulse height of the harmonics with $|n|=1$ significantly exceed the pulse heights of all the other harmonics. For this reason, the fulfillment of these equations was checked by a direct numerical calculation, whose results are examined below.

Results of Numerical Calculation

In comparison with a Y-circulator without a dielectric sleeve, in the circulator variant under consideration here, the parameters are significantly freer, that is, they have magnitudes which can be conveniently assigned arbitrarily within physically determined and applicable limits. Seven independent values are contained within the generally complex forms of equations (13) and (14): the dielectric permittivity of the ferrite ε; its effective permeability μ_1; the ratio of the permeability tensor elements $\frac{\kappa}{\mu}$; the radius of the ferrite cylinder multiplied by the wave number in free space $\varkappa_0r_0$; the dielectric permittivity of the sleeve material $\varepsilon_{д}$; the permeability of the sleeve material $\mu_{д}$; and the exterior diameter of the dielectric sleeve multiplied by the wave number in free space $\varkappa_0R_0$. A sleeve is usually made from a dielectric (fluoroplastic, polystyrene) with $\mu_{д}=1$ and $\varepsilon_{д}=2.2$-2.5; this reduces the number of free parameters to five. For the normal functioning of a Y-circulator, as emerges from the analysis carried out above, it is necessary that a system of two equations be satisfied. Consequently, of the remaining five arbitrary parameters, three may be assigned, and two may be determined from solutions to equations (13) and (14). As will be shown below, the selection of parameters is somewhat restricted by the demand that the discrimination

/1

between the shoulders of the Y-circulator be not less than 20 dB.

The calculation was carried out in the following order. The values for ε, μ_1, $\varepsilon_д$, $\mu_д$, and $\varkappa_0 r_0$, were assigned, and from equations (13) and (14), the values for $\varkappa_0 R_0$ and $\frac{\kappa}{\mu}$ were determined. The values of κ and μ may be found from the equation $\mu_1 = \mu\left[1-\left(\frac{\kappa}{\mu}\right)^2\right]$. In all calculations whose results are represented in the form of graphs in Figs. 3-4, it was taken that $\varepsilon_д = 2.4$ and $\mu_д = 1$.

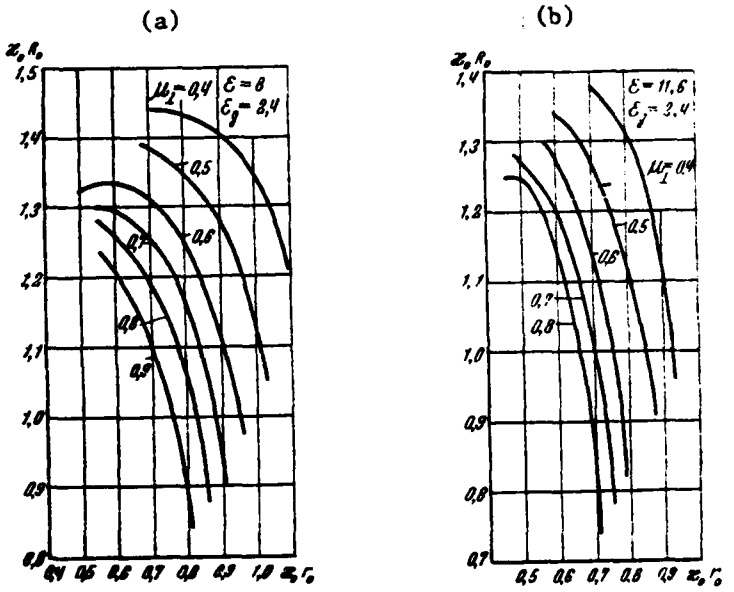

Fig. 3. Relationship between the optimal magnitude of the exterior radius of the dielectric sleeve and the ferrite cylinder radius.

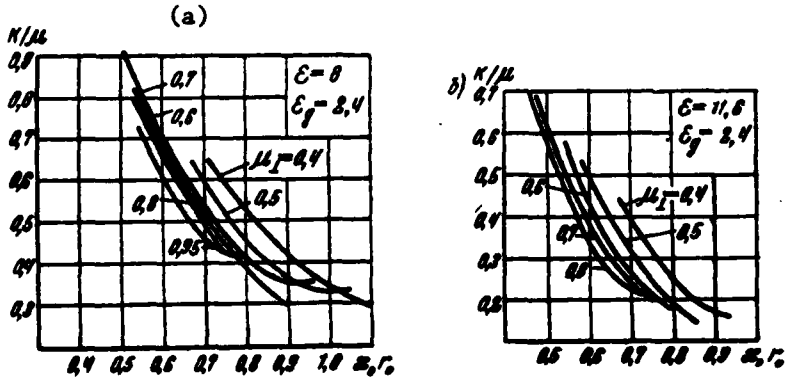

Fig. 4. Relationship between optimal values for the tensor parameters of the ferrite and the radius of the ferrite cylinder.

It is interesting to note that at some values of ε and $\mu_\perp$, the application of a thin dielectric sleeve leads to a decrease in the ratio $\frac{\kappa}{\mu}$, that is, it makes it possible to reduce somewhat the voltage of the exterior magnetic field. With an increase in the sleeve diameter, the ratio $\frac{\kappa}{\mu}$ begins to increase rapidly. This means that Y-circulators with thick dielectric sleeves function with large magnetizing fields, which is confirmed by experimental data. If for a Y-circulator without a dielectric sleeve, fields with intensities on the order of 50 to 200 oersteds are normal, then in broadband Y-circulators with a dielectric sleeve, the magnetizing field intensity increases to 800 to 1,000 oersteds.

We shall examine the influence of harmonics with an index $n \neq 1$ on the parameters of a Y-circulator. A uniform field distribution on the surface and around a ferrite cylinder corresponds to the zero harmonic (n=0) of the electric field. For this reason, under the influence of the field of this harmonic, all shoulders of the circulator are uniformly excited, that is, even at the central frequency of the Y-circulator's working range, a portion of the power enters the insulating shoulder, and the discrimination between the side shoulders of the circulator has a finite value. Thus, it turns out from the calculation that depending on the decrease in the dielectric sleeve diameter, the value of the maximum possible achievable discrimination decreases.

An analysis of the expressions for the pulse heights of harmonics with indices $n \geq 2$ and the results of the numerical calculations show that with real values for the parameters of the ferrite and parameters of the dielectric sleeve, the greatest amplitude (pulse height) of all the harmonics at $|n| \geq 2$ is possessed by the /1
second harmonic (on the order of 0.1-0.25). However, the distribution of the second harmonic of the electric field on the dielectric sleeve surface is such that it has practically no influence on the division of the power between the circulator side shoulders (see Fig. 3 and [1]).

Frequency Range Characteristics

The working frequency range for a Y-circulator is restricted by the minimal necessary value of discrimination between the circulator side shoulders (normally 20 dB) and by the maximum achievable reflection factor from its input (normally not greater than 0.05 to 0.12). As is well known [3], these parameters are

interlinked, and this makes it possible in an investigation of frequency range characteristics of a circulator to examine the relationships between the frequency and only the magnitude of discrimination.

If the frequency of electromagnetic oscillations entering as input into a Y-circulator is different from the resonant frequency of the circulator, then, as it follows from calculation, the amplitudes of the harmonics with indices n=1 and n=-1 cease to be equal. In addition, the optimal phase relationships between these harmonics [1] are disrupted. As a result, the formation of the pure standing wave of the first harmonic of the electric field on the surface of the ferrite cylinder, as shown in Fig. 1, becomes impossible. This leads to the excitation of a type H_{10} wave mode in the insolating shoulder of the circulator, and as a result, also to a decrease in the discrimination between the circulator side members.

In Fig. 5, the relationship between the relative width of the working frequency range of a Y-circulator and the diameter of a dielectric sleeve fitted onto the ferrite circulator is shown at various values of the ferrite parameters. The working frequency range of a Y-circulator is determined as a difference in frequencies, between which limits the discrimination between the side shoulders of the circulator is not less than 20 dB. The order of this computation does not

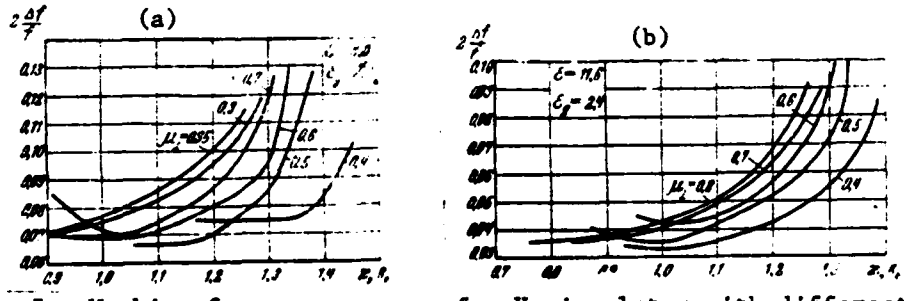

Fig. 5. Working frequency range of a Y-circulator with different values of μ_1.

differ from that analyzed in the article in work [1]. With the calculation, it is presumed that the zero harmonic of the electric field has no influence on the magnitude of discrimination. However, with sufficiently thick dielectric sleeves, the pulse height of the zero harmonic becomes so great that even at the Y-circulator's resonant frequency, the discrimination between the side shoulders is less than 20 dB. This imposes a restriction on the selection of the maximum dielectric /1

sleeve diameter and disallows the possibility of realizing a working frequency range greater than 8 to 10%. In Fig. 6, the relationship between the maximum achievable frequency range of a Y-circulator and the electric parameters of a ferrite with a discrimination not exceeding 20 db is presented. As may be seen

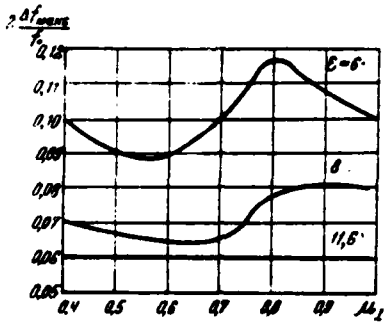

Fig. 6. Maximum achievable working frequency range for a Y-circulator with a dielectric sleeve.

from the graphs presented here, the use of a dielectric sleeve yields the possibility of extending the working frequency range of Y-circulators in comparison with Y-circulators without dielectric sleeves by several times.

Results of Experimental Study

As for the case of a Y-circulator without a dielectric sleeve as well [1], for confirming the correctness of the presumptions at the base of the calculations for a Y-circulator waveguide with a ferrite-dielectric element, the distribution of the module of electric field intensity on the surface of a dielectric sleeve in a tuned Y-circulator was experimentally measured. The measurements were carried out with the help of a rotating sonde [1]. In order to avoid substantial error during this, the ferrite-dielectric element was attached to a rotating plug with the sonde.

The results of the experiment, presented in Fig. 7, confirm the presupposition concerning the fact that the principle of functioning of a Y-circulator with a ferrite-dielectric element and the physical processes taking place in it are identical to the same in a Y-circulator without a dielectric sleeve.

Insofar as there are no data in the literature concerning parameters of Y-circulators with ferrite-dielectric elements, in order to check the calculation

results, the parameters of a Y-circulator waveguide with various ferrite-dielectric elements were measured. Ferrite cylinders were prepared from grade M-18 ferrite with $\varepsilon=8$.[1] The results of the experimental study and corresponding calculational data are presented in the following table. /1

H_0, э	$\mu_\perp$	$\frac{\kappa}{\mu}$	κ	μ	$\varkappa_0 r_0$	$\varkappa_0 R_0$
88	0,91	0,24 0,37	0,23 0,38	0,97 1,03	0,72	0,91 1,02
125	0,83	0,35 0,45	0,33 0,45	0,95 1,0	0,65	1,19 1,23
172	0,73	0,45 0,52	0,42 0,51	0,92 0,97	0,62	1,32 1,26
236	0,71	0,47 0,44	0,43 0,4	0,91 0,91	0,68	1,26 1,28
400	0,36	0,74 0,66	0,6 0,52	0,81 0,79	0,66	1,41 1,45

Note. In the denominators of the fractions, values derived by means of a calculational method are shown.

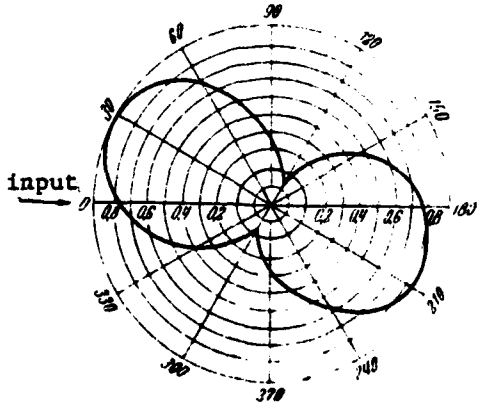

Fig. 7. The experimentally derived structure of an electric field on the surface of a dielectric sleeve.

Values for μ_1 and $\varkappa_0 r_0$ found experimentally were taken as baseline data for the calculation. All values entered into the table were derived at the central frequency of the working circulator frequency range.[2] /1

[1] In the work cited [4], an experimentally plotted curve of magnetization for this kind of ferrite is presented. This makes it possible according to a known external magnetic field intensity to determine the tensor parameters of the ferrite, taking into account the demagnetizing factors, and to compare them with the values generated from calculation.

As may be seen from the table, the agreement of calculational and experimental data is quite satisfactory.

[2]The measurements were carried out in the three-centimetric range.

BIBLIOGRAPHY

1. Vol'man, V. I. "Raschët volnovodnogo Y-tsirkulyatora" [The Calculation for a Y-Circulator Waveguide], Radio Technology, Vol. 20, No. 3, 1955, 21-30.

2. Levin, L. Sovremennaya teoriya volnovodov [Contemporary Theory of Waveguides]. Foreign Literature Publishing House, 1953.

3. Butterweck, H. J. "Der Y-Zirckulator"[Y-Circulators], Archives of Electronic Communications, Vol. 17, No. 4, 1963.

4. Mikaelyan, A. L. Teoriya i primeneniye ferritov na SVCh [The Theory and Application of Ferrites for Superhigh Frequencies]. Gosenergoizdat [State Scientific and Technical Power-Engineering Publishing House], 1963.